Chapter 9
Reed Instruments

Jean Kergomard

Abstract This chapter deals with self-sustained oscillations created by reed instruments. Single, double, and lip-reed instruments (lip reeds are encountered in brass instruments) are presented. A basic model is proposed, the reed being regarded as a single-degree-of-freedom oscillator. Single and double reeds are shown to be inward-striking reed, while for the simplest model of lips the reeds are striking outward. The consequences of this difference are analyzed at the end of the chapter, when the effects of the reed dynamics, especially the role of the reed damping, are investigated. Because these effects are complicated, focus is given to the oscillation threshold (frequency and mouth-pressure thresholds). However, for single and double reed instruments, many useful results can be obtained with a simpler model, by ignoring the reed dynamics, i.e., equating the reed with a spring without mass. A large part of the chapter is devoted to this model. This is relevant because the resonance frequency of the resonator, and therefore the playing frequency, is much smaller than that of the reed. The different regimes for cylindrical and conical resonators are analyzed, with the nature of bifurcations. Playing frequencies, amplitudes, and spectra are found to depend on the excitation parameters, which are mainly the mouth pressure, the reed opening at rest and the reed compliance. In order to obtain insights in the behaviors, cylindrical resonators with single reed can be simplified to archetypes of nonlinear systems, either iterated map systems or Van der Pol oscillators. Simple conclusions can be drawn. Unfortunately, this is not possible for a lip-reed instruments because, for outward-striking reeds, the playing frequency is slightly higher than the reed resonance frequency.

This chapter deals with reed instruments. Single, double, and lip-reed instruments (lip reeds are encountered in brass instruments) are presented. This chapter and the following chapter, dedicated to flutes, will therefore encompass most types of wind instruments.

J. Kergomard (✉)
CNRS Laboratoire de Mécanique et d'Acoustique (LMA), 4 impasse Nikola Tesla CS 40006, 13453 Marseille Cedex 13, France
e-mail: kergomard@lma.cnrs-mrs.fr

A. Chaigne, J. Kergomard, *Acoustics of Musical Instruments*, Modern Acoustics and Signal Processing, DOI 10.1007/978-1-4939-3679-3_9

9.1 Background on Self-Sustained Oscillations

The first study related to wind instruments was carried out by Mersenne [80] and Bernoulli [15] who focused on the resonance frequencies of the tube. This topic, which is still being investigated nowadays, led to a fundamental understanding of several manufacturing parameters related to the resonator: cross-section variations, location and diameter of the toneholes, height of the chimney, etc. This was developed in detail in Chap. 7. For bowed-string instruments, a seminal work was also carried out by Mersenne. Following Mersenne's work, the next step was to understand the excitation of the system. The first attempts appeared at the end of the nineteenth century (Helmholtz [68] and Rayleigh [93]) and were further investigated during the twentieth century. Today, many questions remain open concerning this complex subject.

Self-sustained oscillations were introduced in Chap. 8. They are encountered in three kinds of instruments: reed instruments (including brass instruments), flutes, and bowed-string instruments. It is noteworthy that the last family can also produce sound with free oscillations (pizzicati). The fundamental research question is the understanding of the sound production, and therefore the oscillation *regimes*, as well as the conditions at which they can be obtained. For wind instruments, it is well known that several regimes with different frequencies can be obtained for a given fingering.

The study of musical instruments does not deal only with the conditions for oscillations to emerge, but deal mainly with the kind of oscillation which can exist. This differs from problems of practical interest such as Larsen effect, or oscillations of piping systems: the problem is not to product these oscillations, but to prevent them. Self-sustained oscillations are produced by an energy source, which is continuous, or rather slowly varying, a linear resonator, such as a tube or a string, and a feedback mechanism (Fig. 9.1). The feedback is very rapid, because it happens at the playing frequency, which in general is related to the reflections in the resonator (if no reflections occur in the resonator, the playing frequency cannot be related to the resonator length). The feedback mechanism is therefore much more rapid than the control loop of the energy source by the instrumentalist, via the force feedback and the sound hearing.

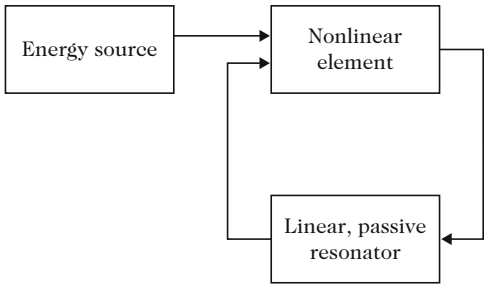

Fig. 9.1 Elementary block diagram of the loop of a self-sustained oscillation instrument

The simplest models assume that the nonlinearity, which is essential for the conversion of a continuous excitation into steady oscillations, is localized at the input of the resonator. This input is the entry of the tube for reed instruments, and the contact between the string and the bow for bowed-string instruments. This assumption markedly simplifies the analysis. In a well-known 1983 paper, Mc Intyre et al. [79] attempted to unify the three kinds of self-sustained instruments by using two elements only: the localized nonlinearity and the resonator. Obviously this assumption implies some simplifications (and is questionable for flute-like instruments), but provides initial elements of understanding. The authors demonstrated in particular the utility of the reflection function instead of the impulse response (which corresponds in the frequency domain to the input admittance or impedance of the resonator, see Chap. 4). However, for certain purposes, it is necessary to consider a non-localized nonlinearity. Moreover the models describing the transients can slightly differ from the models for the steady-state regime: this remark demonstrates the complexity of the phenomena. The following three chapters are of unequal length: a "preferential" treatment has been given to reed instruments, because today we have a model both simple and rather reliable. This allows presenting different approaches, in both time and frequency domains, for both transient and steady-state regimes. These methods help explain how the sound is produced, even if several problems remain open. Some analogies given by the table of Chap. 1 can sometimes be used, but obviously this is not always possible, because important differences exist between the nonlinearities.[1] The physics of reed instruments is based on the effect of a valve, which is a solid element (of the wall) modulating a flow, and the playing frequencies are close to the maxima of the input impedance. On the contrary the sound production of flute-like instruments is based on the instability of an air jet, without significant wall vibration, and the playing frequencies correspond to the maxima of the input admittance. In addition a significant broadband noise due to turbulence exists in flue instruments.

The outline of the present chapter is as follows: the models are first described in Sect. 9.2. Models without reed dynamics are then explored in Sects. 9.3 and 9.4 with a focus on emergence and stability of regimes. Finally the effect of the reed dynamics is investigated in Sect. 9.5.

[1]The bowed-string instruments can be compared to cylindrical reed instruments with an excitation at a certain distance of the extremities; it is well known that the harmonics whose number is multiple of n disappear in the spectrum when the string is excited at a distance equal to the nth part of the length. The clarinet is equivalent to the string bowed at its middle: the two parts of the string play the same role, and are equivalent to a unique string, with a double characteristic impedance. The excitation parameters can also be compared: the bow velocity is equivalent to the mouth pressure, while the bow force is equivalent to the reed-mouthpiece parameter defined hereafter. Nevertheless the nonlinearity of reed instruments and bowed strings is extremely different, and that of the bowed string poses very difficult problems concerning stability.

9.2 Reed Instruments Models

9.2.1 Introduction

A reed is a type of valve, capable of modulating the air flow rate produced by a pressure difference between the upstream (the instrumentalist mouth) and the downstream (the instrument mouthpiece). This principle is common to all kinds of reed instruments, either with a (single or double) cane reed, a metallic reed, or a lip reed. The main distinction between this different instruments is based on the shape of the resonator, and the ratio between the natural frequencies of the reed and those of the resonator. Similar types of sources can be found in an industrial setting, such as electro-pneumatic loudspeakers with an electrically controlled valve. Their main advantage lies in the capacity to produce very loud sounds. Converting a static (dc) pressure into an alternating (ac) one with the same energy can produce extremely loud sounds, which are difficult to generate with linear sources.

In the case of reed instruments, the energy source is the flow itself, and the measurement of acoustic pressures within the mouthpiece requires particular microphones (170 dB is rather usual!). Fortunately the radiation has a very low efficiency and cannot damage our ear. The external sound is much less loud, because of the strong reflection at the end of the tube (which allows the sound production). A reed can be modeled as a flexible structure, such as an elastic beam, with a pressure difference acting of the two faces. The real boundary conditions can be rather complicated. As a first approximation, the beam can be considered as a cantilever beam with one fixed end and one free end, but its displacement can be limited by another reed (for double reeds) or by the mouthpiece (for single reeds). This kind of boundary conditions exists also for stringed instruments: it is called "conditional" [111], and produces strong nonlinearities. When the reed closes the mouthpiece, it is called a "beating reed." When no obstacle stops the displacement, the reed is "free"; it is the case of the accordion and harmonica. For cane reed, the lips strongly damp the reed vibration, and limit the amplitude of the vibration between lip and the ligature (but this amplitude does not vanish). In Chap. 5 an example of localized damping has been studied; to produce an accurate model for the reed is not easy. In particular the lips have complex geometrical and mechanical characteristics. For organ reeds, the tuning wire plays the role of the lower lip of the clarinettist. Its position allows the tuning of the pipe, and this fact demonstrates the weak coupling between reed and pipe in reed organs.

Some instruments have (single or double) reeds which are encapsulated and this causes difficulties in playing: the damping and vibrating length of the reed cannot be controlled during playing. This is the case of crumhorns and bagpipes. The difficulty of creating a model is even greater for lip reeds. Often a simple, global model is used, based on an experimental modal expansion of the reed vibration. To take into account one vibration mode only gives very useful information, even if it is not sufficient at higher frequencies (some authors proposed more precise models [5, 40, 44]). In what follows, we consider a single mechanical reed oscillation mode.

In order to understand the fundamental physical features, which are essentially nonlinear, it is necessary to introduce major simplifications, even if details related to sound quality are lost. For single reed instruments, we therefore first assume that the reed is a spring without dynamics (without neither mass nor damping), and obtain first results concerning the sound production.

9.2.2 Mechanical Response of a Reed: Experimental Data

9.2.2.1 General Considerations

A major obstacle to the study of the characteristics of a reed instrument is the number of parameters that influence sound production. Moreover when carrying out a measurement involving an instrumentalist, it is not easy to be sure that he or she does not influence, either consciously or not, the result of a given task. For this reason, the artificial mouth is a very useful device: it acts as a good surrogate for an instrumentalist.[2] Using artificial blowing it is possible to measure the reed mechanics in the form of a mechanical response to a pressure excitation (see, e.g., [47]). If this pressure is assumed to be almost uniform on each of the two sides of the reed (see discussion hereafter), the frequency response is defined as follows:

$$H_{\mathrm{mr}}(\omega) = \frac{\mathscr{Y}(\omega)}{\Delta P(\omega)}, \tag{9.1}$$

where $\mathscr{Y}(\omega)$ is the reed displacement at low excitation level and $\Delta P(\omega)$ the pressure difference across the reed. The subscript m stands for mechanical, and the subscript r for reed. Obviously the reed displacement is not uniform, thus the response measurement should be completed by the measurement of the reed deformation. However, we assume that the displacement of the reed extremity represents the reed displacement, at least when the reed does not beat. Another difficulty of the measurement lies in the control of the pressure difference $\Delta P(\omega)$ (see [29]). Figures 9.2 and 9.3 show two examples of responses for a single reed and lips, respectively.

Concerning a single reed, the support of the lip plays a significant role for reducing the vibrating length of the reed, and mainly a role of reed damping. For the example shown in Fig. 9.2, it can be seen that the first reed resonance lies close to 2000 Hz. The response argument is $+\pi/2$ at the resonance; this is evident in particular for the reed without lip of Fig. 9.2. Consequences will be analyzed in Sect. 9.2.3.2. For the lips of a trombonist, a precise analysis of the figure shows the

[2]This kind of device is based upon an old idea. For instance during the eighteenth century the Kempelen machine imitated the voice. There are also numerous more recent works: we cite [6, 70, 109] for the clarinet, and [58, 114] for brass instruments. The organ obviously is a kind of artificial mouth!

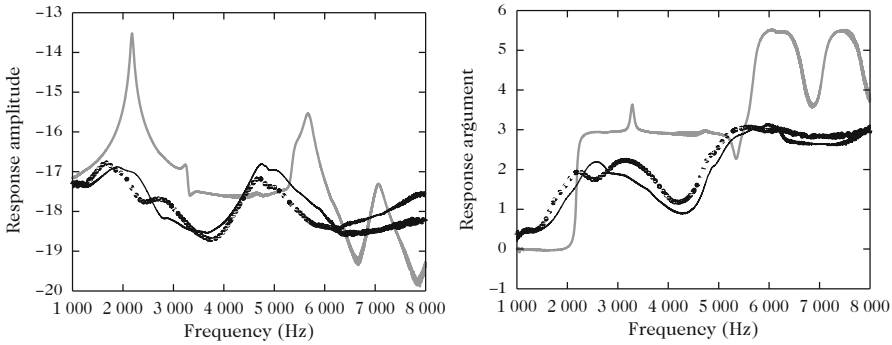

Fig. 9.2 Response of a single clarinet-like reed of to an oscillating pressure differences: without support of the lip (*gray* curve) and for two lip forces pressing on the reed (*black curves*). The amplitude scale is arbitrary, the argument is in radians (after [66])

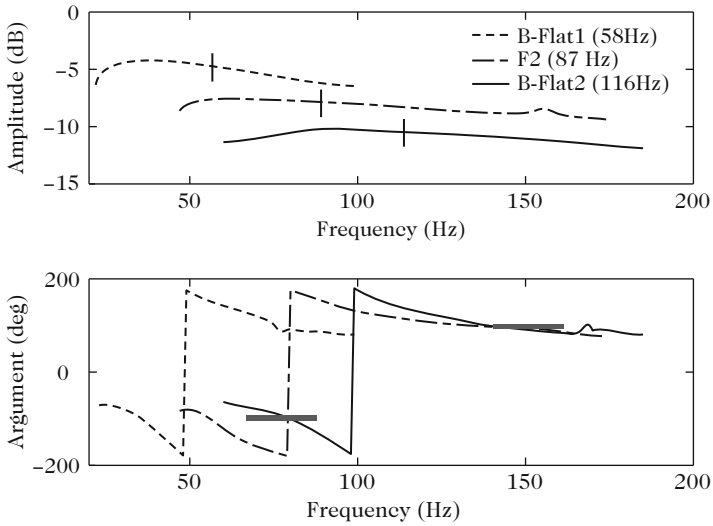

Fig. 9.3 Mechanical response of human lips (modulus and argument) to an oscillating pressure difference for three different notes of a tenor trombone: Bflat1 is the "pedal" tone. Its harmonics correspond to a series of impedance peaks, but the fundamental of the note does not correspond to a peak. The playing frequency is noted with a *small vertical dash* on the amplitude curve. For clarity the amplitude curves of the two highest pitches are shifted by 3 dB and 6 dB, respectively. The amplitude scale is arbitrary. The two *horizontal lines* on the argument curve at $\pm 90°$ indicate the resonances (after [88])

existence of two resonances which are close together. The argument is $-\pi/2$ for the first one while for the second, which is strongly damped, it is $+\pi/2$.

9.2.2.2 Single Reed of Clarinet–Reed Kind

The response shown in Fig. 9.2 corresponds to a given "embouchure" of the player. What we call embouchure corresponds to a particular setting of both the lip position and the force applied by the lips on the reed. Several resonances appear. Recent theoretical or experimental works analyzed these resonances, either without or with lip [92, 102, 106, 112]. From the first resonance of the response, it is possible to extract several parameters, which will be important for our simple model: (1) the static stiffness (per unit area), K_s, depending of the reed "hardness" (reeds are commonly classified using a single parameter, the "hardness," given by the reed makers); (2) the first resonance frequency, f_r, which allows deducing the modal mass (per unit area) of the first mode, $m_s = K_s/\omega_r^2$ (see Chap. 3, Sect. 3.3.1). So we obtain a single-degree-of-freedom model:

$$\frac{d^2y}{dt^2} + q_r\omega_r\frac{dy}{dt} + \omega_r^2 y = \frac{f_s}{m_s}, \tag{9.2}$$

where $y(t)$ is the tip displacement of the reed (at low excitation level), the origin being the value of y at rest (when $f_s = 0$), $q_r\omega_r$ is the damping coefficient, $q_r = 1/Q_r$ is the inverse of the quality factor of the reed, which depends on the positioning of the lips (q_r is equal to $2\zeta_0$, as defined in Chap. 2). ω_r is the resonance angular frequency and $f_s(t)$ is the force per unit area due to the acoustic pressure. For a clarinet reed, this force can be written as:

$$f_s = -\Delta p, \text{ where } \Delta p = p_m - p. \tag{9.3}$$

Δp is the difference of the pressure applied on the two faces (p_m is the mouth pressure, p is the pressure on the other face). The minus sign is explained as follows: if Δp increases, the reed will be closed (see Fig. 9.4).

The fundamental frequency of the played notes is assumed to be very close to the natural frequencies of the resonator and much lower than the resonance frequency of the reed, f_r. This is not true for very high notes and even wrong for the squeaks, but this assumption allows large simplifications for the study of this kind of instruments. Ignoring the reed dynamics leads to the simple equation:

$$K_s y = -\Delta p. \tag{9.4}$$

The quantity K_s can be measured, via the measurement of the ratio $\Delta p/y$. The "closure pressure" p_M, is the mouth pressure for which the reed remains closed in the static regime (then $y = -H$, and the mouthpiece pressure vanishes)[3]:

$$p_M = K_s H. \tag{9.5}$$

[3]The stiffness of the reed depends on the closure of the reed, and therefore varies with the pressure difference, because of the curvature of the mouthpiece lay. However, the closure pressure p_M varies very little [30].

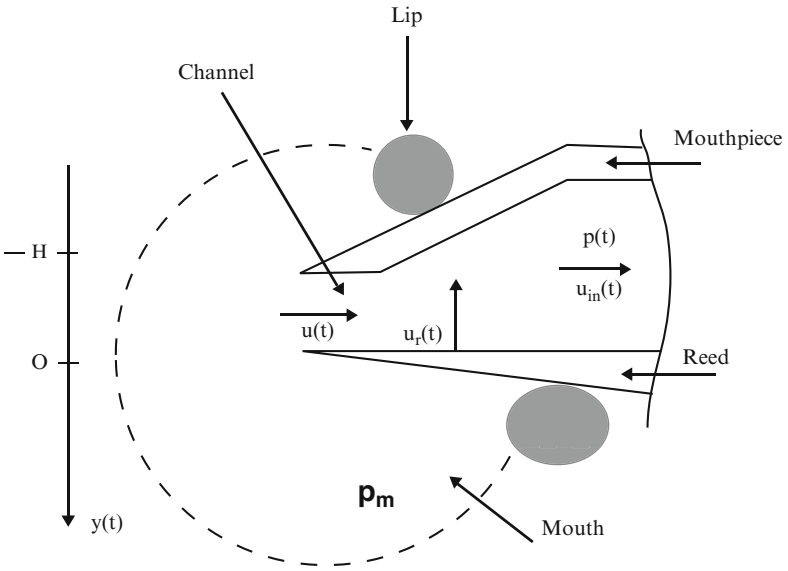

Fig. 9.4 Schematic representation of a clarinet mouthpiece with a single reed, and choice of orientations. The lower lip restricts the vibrating length and provides its damping. The model assumes a two-dimensional geometry, with a rectangular reed of width w. The definition of the flow rates is given in Sect. 9.2.4

Figure 9.5 shows simultaneous signals for the mouthpiece pressure and the reed displacement. On the left part, it is observed that the two signals are in phase and almost proportional: this justifies the assumption (9.4). Nevertheless an asymmetry is more noticeable for the displacement signal than for the pressure one. This indicates the presence of even harmonics. Here the spectra are not shown, but they exhibit a maximum of the response close to the harmonic 21, i.e., 2800 Hz: this frequency is the first resonance of the reed. On the right part of the figure, a limit of the displacement can be seen: it corresponds to the beating state of the reed. This is a nonlinear phenomenon. The linear frequency response (9.1) loses significance, because Eq. (9.2) needs to be completed by the following nonlinear condition:

$$y > -H. \tag{9.6}$$

9.2.2.3 Lip Reed

For instruments with a cane reed, the playing frequency is mainly controlled by one of the natural frequencies of the resonator, and the influence of the reed is small. This is different for lip-reed instruments. The lip resonances of a "brass" instrument player are crucial in order to obtain correct playing frequencies, which

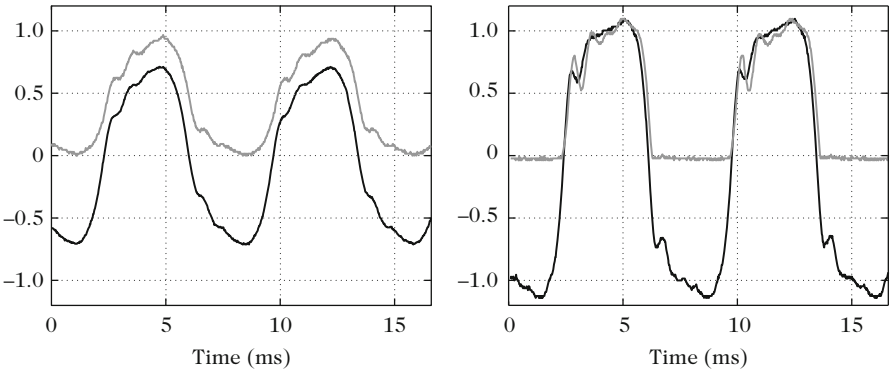

Fig. 9.5 Reed displacement (*gray curve*) and mouthpiece pressure (*black curve*) for a non-beating reed (on the *left*) and for a beating reed (on the *right*): for the latter case, a plateau of the displacement signal is visible, when the reed closes the mouthpiece. The scale is arbitrary. The instrument is a cylindrical tube with a clarinet mouthpiece (From [89])

are also related to the resonator natural frequencies. As a consequence, the coupling between reed and resonator is strong. The instrumentalist has to learn the control of his lips to get the correct mechanical resonance frequency which allows using a given resonance of the resonator. Thus the learning curve to obtain a "correct sound" is arduous. It requires a significant muscular training. Some instruments have a range of four octaves! In contrast to skilled players, the artificial mouths are similar to a beginner: it is difficult to dynamically control the artificial lip tension, and the compass is limited to two octaves.

It is therefore impossible to ignore the lip dynamic when trying to explain the brass instrument properties. Equation (9.2) with one reed mode is the simplest model and allows obtaining rather realistic synthesized sounds [64, 116]. Nevertheless it is sometimes better to take two modes into account, by using the so-called two-mass model. This is often done for the modeling of the vocal folds (the main difference between brass instruments and the voice lies in the degree of coupling between the "lips" and the resonator; the coupling between the folds and the vocal tract is weak).[4] Figure 9.3 shows that the two-mode model probably is more realistic for brass instruments, because two resonances appear: they are close together, with a strong attenuation for the second one. These twin resonances can be sharper with an artificial mouth, as reported in [88].

[4]In singing it is possible to continuously change in notes without changing the length and the shape of the vocal tract. The skilled brass instrument players can also play without instrument, but the timbre is strongly modified.

9.2.3 *Dynamic of the Fluid Passing the Reed*

9.2.3.1 Pressure Field, Flow Separation, Valve Effect (Single Reed)

Now we need to find a relationship between the pressure and velocity of the fluid, by investigating the properties of the flow which enters the resonator. Figure 9.4 shows a schematic representation of the mouthpiece of a single reed instrument. We remark the localized constriction at the extremity of the reed. Its length has an order of magnitude of 1 mm. The constriction can be regarded as a channel located between a "pressure reservoir" (i.e., the player mouth) and the entry of the clarinet mouthpiece (for lip-reed instruments, the channel consists of the space between the lips of the musician). The cross section of the channel is time-varying, and it is controlled by the reed (or lips) position during an oscillation. The flow at the entry of the instrument has the form of a jet at the channel exit: for a detailed description of the jet and the underlying hypotheses, the reader is referred to the Chap. 10 about flute-like instruments (see Sect. 10.3.1). The main result is that for $\Delta p > 0$ the velocity v_j at the end of the constriction (i.e., of the channel) is given by:

$$v_j = \sqrt{2\Delta p/\rho}. \tag{9.7}$$

Δp is defined by Eq. (9.3). The pressure at the instrument inlet is assumed to be equal to that in the channel. The above result is based upon a very simplified description of the flow separation, which is assumed to be localized at the channel exit. However, the precise determination of the separation point is not easy. It depends on the detail of geometry of the channel exit, i.e., on the channel flare and on the flow rate. The higher are the flare and the flow rate, the more upwards is the separation point (see [43, 69], pp. 311 and the following). An air jet is intrinsically unstable (see Sect. 10.3.2 in Chap. 10 on flutes), and becomes turbulent. Turbulence implies a fast mixing of the jet with the surrounding air, and consequently an abrupt deceleration happens without pressure recovery at the mouthpiece inlet. Without dissipation, it could be possible to apply the Bernoulli law, and a pressure increase would result from the velocity decrease. Actually dissipation "compensates" for the non-recovery of pressure in the mixing zone. When the turbulent mixing is over, the decelerated flow is assumed to be spread over the complete cross section of the mouthpiece (typically 15 mm in diameter) and to be almost uniform. Finally the nature of the acoustic source in reed instruments can be summarized as follows: it is a flow source using the valve effect. The fluctuating volume flow entering the instrument is the product of a velocity and a fluctuating cross-section area. The flow rate is mainly controlled by the pressure difference Δp, and the cross-section area by that of the channel exit.

Each quantity is the sum of an average part (over time) and a fluctuating part. The mouth pressure is assumed to be constant, i.e., the input impedance of the vocal tract at non-zero frequencies is negligible compared to that of the instrument. This will be discussed in Sect. 9.4.7 of this chapter. Conversely, the time-average static

pressure at the inlet of the instrument is assumed to be negligible compared to the mouth pressure. In other words the input impedance of the resonator is very small at zero frequency. Indeed an order of magnitude of the time-average flow resistance of the pipe can be estimated by ignoring the inflow effect and assuming a Poiseuille flow [Eq. (5.115)]. It is found to be less than 1 % of the characteristic impedance of the clarinet tube at the playing frequency [73, p. 251]. Concerning the estimation of the flow velocity at the inlet of the tube, the use of the previous model leads to a Mach number (the ratio of the velocity to the sound speed) significantly lower than 1 %. Such a value for the Mach number allows neglecting convective effects on wave propagation. This is valid as long as nonlinear propagation is not considered (see Chap. 8).

9.2.3.2 Inward- and Outward-Striking Reeds

For the last two centuries many authors have tried to characterize the reeds according to the effect of the pressure difference across the reed. For inward-striking reeds an increase in the pressure difference Δp tends to close the reed channel, while for outward-striking reeds, it tends to open the reed channel. The behavior of the two kinds of reeds is very different, as demonstrated by the differences in playing frequencies. This will be explained in Sect. 9.5 of this chapter. Figure 9.6 gives a schematic representation of this difference [50]. The clarinet reed therefore is an inward-striking reed, and is described by Eq. (9.3): for a positive pressure difference, the force is exerted upward[5] (see Fig. 9.4). Fletcher [49] proposed a finer distinction for the reeds, by distinguishing the mean pressure on the two faces of the reed. We do not go further on this difficult subject.

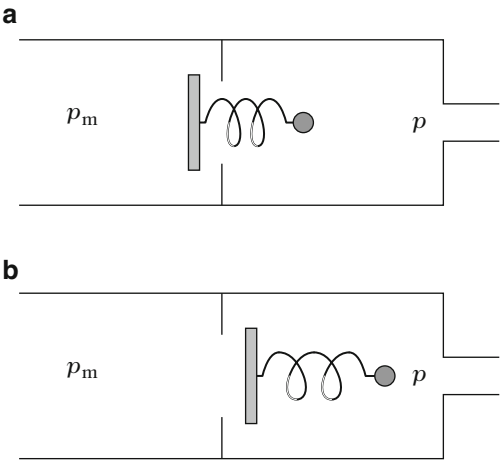

Fig. 9.6 Principle of an inward-striking reed (**a**) and an outward-striking reed; (**b**) after Fletcher [50]. A positive pressure difference $\Delta p = p_m - p$ tends to close the reed for the case (**a**) and to open the reed for the case (**b**)

[5]This is consistent with the value of the response argument $H_{mr}(\omega)$ around the resonance, as given by Eq. (9.1). We saw that it is equal to $+\pi/2$: using Eq. (9.2), the argument of the ratio $\mathscr{Y}(\omega)/F(\omega)$ is $-\pi/2$, thus that of the ratio $\mathscr{Y}(\omega)/\Delta p(\omega)$ is $+\pi/2$.

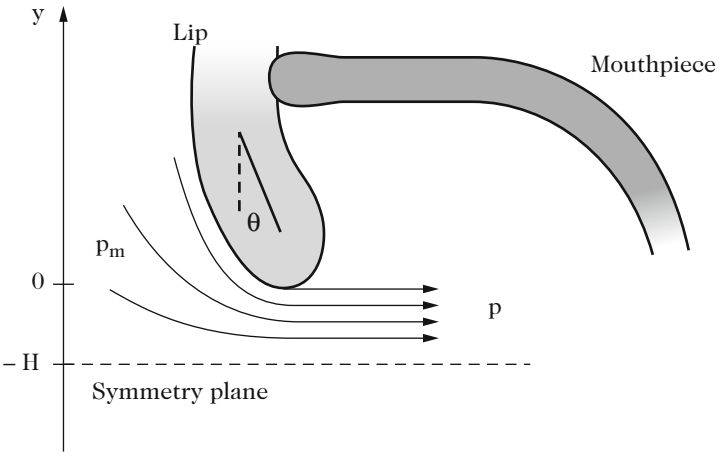

Fig. 9.7 Lip reed seen as a swinging door. The two lips are assumed to be symmetrical. The point $y = -H$ corresponds to the closure of the lips

9.2.3.3 The Case of the Lip Reed

The case of the lip reed is more complicated than that of the single reed with a mouthpiece. The geometry and the mechanical structure of the lips and their surrounding (the "embouchure") are complex. A drastically simplified geometry is often considered in order to describe the valve effect. It is possible to use a model of a "swinging door" (see Fig. 9.7), for each lip, assuming a perfect symmetry between the two lips.

The lips are again approximated by a one-degree-of-freedom oscillator: a rotation abound an equilibrium position defined by an angle θ, with respect to the vertical axis [1]. For this simplified geometry, there is a localized constriction at the end of the lip, and it is possible to apply the air flow description used for cane reeds. We assume rather arbitrarily that flow separation occurs at the neck of the channel formed between the lips, with a jet velocity given by Eq. (9.7). After a certain distance into the mouthpiece, the jet rapidly expands and produces a zone of turbulent mixing. After this zone, the velocity field is supposed to be uniform over a cross section of the mouthpiece, and the pressure in the lip channel is equal to the pressure in the mouthpiece. For a trombone, the diameter of the mouthpiece is around 30 mm, and it is much larger than the lip opening.

Therefore at the extremity of the lip, the upstream pressure is the mouth pressure, p_m, and the downstream pressure is the mouthpiece pressure. Thus it is reasonable to consider that the force exerted on the lip is proportional to the pressure difference, Δp. With this model, the lip enters the mouthpiece for an increasing pressure difference, and this corresponds to an outward-striking reed. With an orientation convention similar to that used for the clarinet reed, the force projection on the axis can now be written as:

$$f_s = +\Delta p. \tag{9.8}$$

There is a great similarity with the model of a clarinet reed, but the force is given by the previous equation. Figure 9.7 depicts a very simplified schematic representation. A static closure pressure can again be defined, but *it is now negative*, because we should inhale to close the lips. For the sake of simplicity, the closure pressure will be denoted $-p_M$, where p_M is given again by Eq. (9.5).

Other models can be found in the literature. Some of them take into account both the vertical and the horizontal movements of the lips. A review is given in [24], with a discussion of the link to the models of singing voice and speech. Some models can also consider an inward-striking behavior under certain conditions.

Figure 9.8 shows an example of lip movement [22, 23]. We will not go further in the discussion of the model. We conclude that it is difficult to develop an accurate and reliable model. In fact the first resonance probably corresponds to a mode of an outward-striking reed. In this chapter, we limit our study to the latter case.

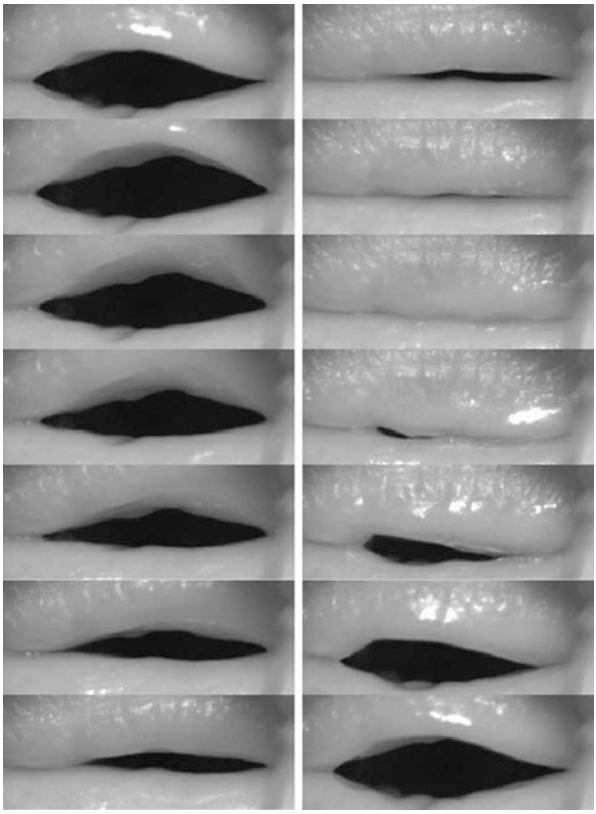

Fig. 9.8 Movement of the upper lip during one period [21]

9.2.4 Reed Opening Area and Flow Rate

9.2.4.1 Outgoing Channel Flow Rate

Let us first estimate the flow rate u entering the resonator. The jet velocity is assumed to be equal to that at the output of the reed channel. The flow rate can therefore be simply expressed with respect to the cross-section area of the jet S_j, i.e., that of the reed channel:

$$u = v_j S_j. \tag{9.9}$$

S_j plays a major role for the control of the flow valve effect. In a two-dimensional flow, we get a very simple linear relation between the opening area and the channel height:

$$S_j = (y + H)w, \tag{9.10}$$

where w is the effective width (see Fig. 9.4 for the definition of y and H). This linearity was experimentally verified by Dalmont et al. [34]. However, Backus [7] experimentally found an area depending on the height with a power q, $S_j \propto (y+H)^q$, where $q = 4/3$, and this dependence has been used by many authors. For reasons that will be explained soon, we keep the linear dependence for the single reed.

A similar debate exists for the double reed. If the shape to the reed end is seen as two circle arcs, it should be found a power $q = 1.5$ or more (see [8]), but authors found [117] a linear dependence on the reed opening. For lip reeds, many authors investigated this issue, and they found a power between 1 and 2, for instance, by graphical inspection (see, e.g., Fig. 9.8).

9.2.4.2 Flow Rate Due to the Reed and Total Flow

Equation (9.9) gives the flow rate passing through the reed channel. However, another source of flow, of secondary importance, exists: it is the flow produced by the reed vibration, which is similar to the flow produced by any vibrating surface, such as a loudspeaker membrane. The reed pushes and pulls out air inducing a flow rate u_r equal to:

$$u_r = -S_r \frac{dy}{dt}, \tag{9.11}$$

where S_r is the effective area of the reed. The sign $-$ comes from the orientation choice in Fig. 9.4: the reed produces a flow entering the resonator when y decreases (in the figure it is not obvious that this displacement flow enters the resonator, however, it might be clearer that an equivalent flow induced by the top of the reed "leaves" the mouth, which surrounds the mouthpiece! There is actually no creation

of volume by the reed movement). The total flow rate entering the instrument is therefore:

$$u_{\text{in}} = u + u_r. \tag{9.12}$$

If plane waves are assumed at the instrument inlet, this flow rate is related to the input impedance, or, in time domain, to the impulse response $h(t)$, which is the inverse Fourier Transform of the input admittance (this has been largely studied in Part II):

$$u_{\text{in}}(t) = [h * p](t).$$

It is often convenient to choose the flow passing through the channel as the unknown u, which is related to the impulse response $h(t)$ by the following equation:

$$u = [h * p](t) + S_r \frac{dy}{dt}. \tag{9.13}$$

The flow created by the reed movement is responsible for the added term. The effect of this term was studied in [86]. For frequencies much lower than the reed resonance, there is a simple interpretation to this term. The reed stiffness K_s is equivalent to a small volume V_{eq} added at the input of the instrument. For a constant mouth pressure p_m and a non-beating reed:

$$\frac{dy}{dt} = -\frac{1}{K_s}\frac{d(\Delta p)}{dt} = \frac{1}{K_s}\frac{dp}{dt} = \frac{H}{p_M}\frac{dp}{dt}. \tag{9.14}$$

Combining Eqs. (9.11) and (9.14):

$$u_r = -\frac{V_{\text{eq}}}{\rho c^2}\frac{dp}{dt} \quad \text{where} \quad V_{\text{eq}} = \frac{\rho c^2}{p_M} S_r H; \tag{9.15}$$

$$u = u_{\text{in}} + \frac{V_{\text{eq}}}{\rho c^2}\frac{dp}{dt}. \tag{9.16}$$

Thus the flow due to the reed is equivalent to adding a compliance in parallel to the pipe input impedance, V_{eq}. It is that of an air volume localized at the instrument input if the frequency is sufficiently low [see Chap. 1 Sect. 1.5, Eq. (1.154)].[6] In general it is easy to correct the mouthpiece volume by the volume V_{eq}. This correction is independent of the fingering, and can be measured.

[6] V_{eq} differs from the air volume displaced by the reed, $S_r H$. Furthermore this description assumes that the stiffness by unit area K_s does not vary with the pressure level. In practice when the reed progressively closes the mouthpiece, the stiffness varies, as well as V_{eq}, and consequently the playing frequency.

If the mouthpiece is almost cylindrical, the addition of a closed volume in parallel with the pipe input impedance implies a shift of the impedance maxima which corresponds to an extension of the cylinder by a length $\Delta\ell$. This length is defined such as $V_{\text{eq}} = S\Delta\ell$, where S is the cross-section area of the tube, therefore:

$$\Delta\ell = \frac{\rho c^2}{p_M}\frac{S_r}{S}H. \tag{9.17}$$

Measurement results give a length of about 10 mm added to that of a clarinet mouthpiece [32].

9.2.5 Basic Model (Clarinet-Like Reed)

9.2.5.1 Three-Equation Model

By gathering the different equations discussed above one obtains a basic model. We use the length correction defined by Eq. (9.17).[7] in the general Eq. (9.13):

$$u = [h * p](t) + \frac{S\Delta\ell}{H}\frac{p_M}{\rho c^2}\frac{dy}{dt}. \tag{9.18}$$

When using the closure pressure p_M, Eq. (9.2) becomes

$$\frac{d^2y}{dt^2} + q_r\omega_r\frac{dy}{dt} + \omega_r^2 y = -H\omega_r^2\frac{\Delta p}{p_M}. \tag{9.19}$$

Now we can suppose that the flow separation situation is reversible when the pressure difference is inverted,[8] and that the area of the reed channel depends linearly on its height. Equations (9.7) and (9.10) yield

$$u = u_A\left(1 + \frac{y}{H}\right)\sqrt{\frac{|\Delta p|}{p_M}}\text{sign}(\Delta p) \quad \text{if} \quad y > -H \tag{9.20}$$

$$\text{and} \quad u = 0 \quad \text{if} \quad y < -H \quad \text{(beating reed)}, \tag{9.21}$$

[7]Here it is a notation only, because the interpretation as a length correction is limited to low frequencies and cylindrical mouthpieces.

[8]All above-mentioned hypotheses are satisfied again, but in the reverse sense: the cross section of the tube is much larger than that of the reed channel, then there is a jet formation at the output of the channel (in the mouth), and there is no pressure recovery. This is somewhat arbitrary, but the situation with a flow entering the mouth seems to be quite extreme, and was never observed experimentally.

where the flow rate u_A is given by:

$$u_A = wH\sqrt{\frac{2}{\rho}p_M} = wH^{3/2}\sqrt{\frac{2}{\rho}K_s}. \tag{9.22}$$

Equations (9.18)–(9.20) form a system of three equations with three unknowns, u, the flow rate going out to the channel into the resonator p, the pressure at the input of the resonator and y the vertical displacement of the reed. The two first equations are linear, and can be described in the frequency domain, while the third is nonlinear (remember that a necessary condition for the production of steady self-sustained oscillations is the existence of a nonlinearity which limits the amplitude).

9.2.5.2 Simplified Two-Equation Model

A useful approximation consists in approximating the reed with a simple static spring. This is a good approximation when the natural angular frequency ω_r is much higher than the (angular) playing frequency. In this case $y = -H\Delta p/p_M$, and Eq. (9.19) can be eliminated together with the unknown y:

$$u = u_A\left[1 - \frac{\Delta p}{p_M}\right]\sqrt{\frac{|\Delta p|}{p_M}}\text{sign}(\Delta p). \tag{9.23}$$

For a non-beating reed, the condition (9.6) needs to be added. This condition can be also written as: $\Delta p < p_M$. For a beating reed, when the channel is closed, the flow rate vanishes

$$u = 0 \text{ if } \Delta p > p_M. \tag{9.24}$$

Such a model is not completely satisfactory because it implies a discontinuity of the flow rate derivative. It should be completed by a transition with a very narrow channel and, for instance, a Poiseuille flow [115]. The curvature of the mouthpiece lay should be also taken into account. These subtle phenomena are not investigated in this book. Furthermore the discontinuity in derivative yields difficulties in the numerical treatment [16, 72].

These simplifications lead to a characteristic function $u(\Delta p)$, which has been measured for a stationary flow [34], with positive pressure differences only. Figure 9.9 shows the result, which is perfectly in accordance with the law (9.23), except for the highest pressures. For these pressures, there is no abrupt transition to a beating reed, and the flow does not vanish completely, because the reed does

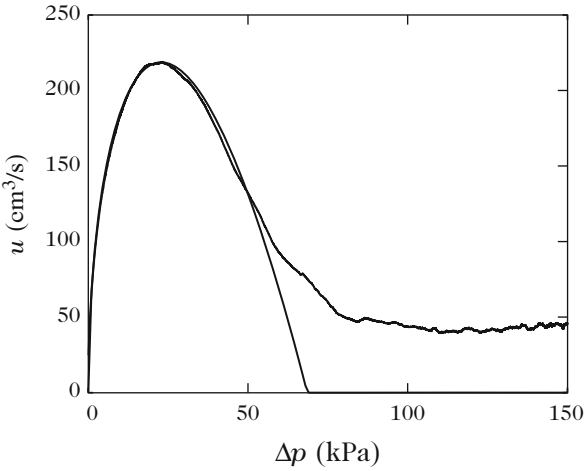

Fig. 9.9 Nonlinear characteristic measured (*thick line*) and calculated (*thin line*) based on (9.23) and (9.51). The increasing portion of the curve is close to a square root of the pressure difference, because the displacement of the reed is very small. In the decreasing portion the progressive closure of the reed becomes dominant. The experiments do not exhibit any beating of the reed, because the flow does non vanish for large pressure differences

not entirely closes the mouthpiece.[9] The measurement of the characteristic function leads to the values of two essential excitation parameters, p_M and u_A: however, their values obviously cannot satisfy all our hypotheses. As an example, if the jet cross section is not strictly equal to that of the reed channel, the formula (9.23) remains identical, but the value of u_A can be changed based on experiments.[10]

The global shape of the curve is rather intuitive: the flow rate first increases when the pressure difference increases, but it is expected to almost vanish for high pressure differences. Hence a saturation occurs, then a decrease. If the mouth pressure p_m does not depend on time, it is possible to write a function $u = F(p)$ which does not depend on the parameter p_m, deduced from the function

[9]In the two-dimensional model we ignored that the air can pass through the sides of the reed, because the mouthpiece lay is curved, and the reed does not perfectly wrap the lay. Moreover the extremity of the mouthpiece is not planar. The air can also flow between the reed and the mouthpiece; the reed does not remain perfectly planar, and twisting can occur. For a double reed, such as a bassoon reed, the way the reed is pressed by the fingers at its extremity is a quality criterion for instrumentalists, which are sanding their reed. When the reed closes linearly (the sides are closed simultaneously with the center), the closure is rather sudden, and the spectrum is rich in harmonics; on the contrary if the sides are closed before the center, the closure is more progressive, and the spectrum is poorer [67].

[10]A validation of the dynamic model can be obtained from a simultaneous measurement of the flow rate and the pressure. For instance it has not been proved that taking into account an unsteady term in the Bernoulli equation would improve the model; however, because of the effect of the reed dynamic, such a simultaneous measurement cannot give a quasi-static curve, as shown by Meynial [81]. He compared experiment and theory by measuring the velocity with a hot wire anemometer at several places in order to deduce the flow rate, and by measuring the pressure with a microphone. Another method could consist in measuring the pressure at several places in the tube, then deducing the input quantities from the knowledge of theoretical transfer functions. Similar ideas have been utilized for bowed strings [123], but it is tedious for a reed instrument, because the input impedance for the even harmonics is highly sensitive to the mouthpiece shape.

$u(\Delta p)$ (9.23): the modification of p_m leads to a simple translation of the curve. The other parameter of the function, u_A, which is a composite parameter, characterizes the amplitude of the curve. It depends on both the reed opening, that the musician can adjust when playing, and the reed stiffness, which is chosen a priori by the musician. This parameter is related to the maximum flow rate that can enter the tube: the maximum of the function $u(\Delta p)$, obtained for $\Delta p = p_M/3$, is

$$u_{\max} = u_A \frac{2}{3\sqrt{3}}. \tag{9.25}$$

Experiments compare very well with the model for the non-beating reed of a clarinet [30]. For an oboe reed, there is a significant difference between measurement and model, because the increase of the curve at low Δp is steeper. This observation was related to the jet behavior in the conical part which is the channel output of the double reed [3, 34, 61].

9.2.5.3 Dimensionless Equations

In order to draw general conclusions, it is convenient to make the three basic equations dimensionless. It is logical to divide the reed displacement by the height of the opening at rest, H, and the pressures by the closure pressure p_M. The flow rates are divided by p_M/Z_c, where $Z_c = \rho c/S$ is the characteristic impedance of the tube. Thus the following definitions are chosen for the unknowns and the parameters:

$$\tilde{y} = y/H;\ \ \tilde{p} = p/p_M;\ \ \tilde{u} = uZ_C/p_M; x = \tilde{y} + \gamma$$

$$\gamma = \frac{p_m}{p_M}\ ;\quad \zeta = Z_c \frac{u_A}{p_M} = Z_c w H \sqrt{\frac{2}{\rho p_M}} = \frac{wH}{S}\sqrt{2\frac{C_p}{C_v}\frac{p_0}{p_M}}.$$

In the last expression of ζ, the compressibility $1/\rho c^2$ has been replaced by its value with respect to the atmospheric pressure p_0 [see Eq. (1.98)]. Typical values of the reed parameter ζ are of the order of 0.3–0.4 [52, 89]: it will be seen that this parameter has a strong influence on the attack transients, while the mouth pressure dictates the amplitude and the spectrum of the sound. The input admittance, and therefore the function $h(t)$, is multiplied by Z_c. Introducing dimensionless variables and removing the superscripts (for the sake of simplicity), Eqs. (9.18)–(9.20) become

$$u = [h * p] + \frac{\Delta \ell}{c}\frac{dx}{dt}; \tag{9.26}$$

$$\frac{1}{\omega_r^2}\frac{d^2x}{dt^2} + \frac{q_r}{\omega_r}\frac{dx}{dt} + x = p; \tag{9.27}$$

$$u = \zeta(1 + x - \gamma)\sqrt{\gamma - p} \text{ if } 1 + x - \gamma \geq 0\,, \text{ or} \tag{9.28}$$

$$u = 0 \text{ if } 1 + x - \gamma \leq 0. \tag{9.29}$$

(One can assume that Δp is positive, because in practice the mouth pressure is almost always higher than the mouthpiece pressure, at least for quasi-cylindrical instruments). Using this hypothesis the two-equation model (9.23) is given by:

$$u = F(p), \text{ where} \tag{9.30}$$

$$F(p) = \zeta(1 - \gamma + p)\sqrt{\gamma - p} \text{ if } \gamma - p \leq 1; \tag{9.31}$$

$$F(p) = 0 \text{ if } \gamma - p \geq 1. \tag{9.32}$$

9.2.6 Basic Model (Lip Reed)

9.2.6.1 Three-Equation Model

The basic model for a lip reed (or more precisely for an outward-striking reed) is now given. Obviously we cannot reduce the 3-equation model to 2-equation model, because the reed dynamics play an essential role.

$$u = [h * p](t) + \frac{S\Delta\ell}{H}\frac{p_M}{\rho c^2}\frac{dy}{dt}; \tag{9.33}$$

$$\frac{d^2y}{dt^2} + q_r\omega_r\frac{dy}{dt} + \omega_r^2 y = H\omega_r^2\frac{\Delta p}{p_M}; \tag{9.34}$$

$$u = u_A\left(1 + \frac{y}{H}\right)\sqrt{\frac{|\Delta p|}{p_M}}\text{sign}(\Delta p), \tag{9.35}$$

where the coefficient u_A is given by:

$$u_A = wH\sqrt{\frac{2}{\rho}p_M} = wH^{3/2}\sqrt{\frac{2}{\rho}K_s}. \tag{9.36}$$

9.2.6.2 Dimensionless Equations

All dimensionless parameters are defined in the same way. Nonetheless here the closure pressure is negative, equal to $-p_M$, and we write

$$x = y - \gamma.$$

This yields

$$u = [h * p](t) + \frac{\Delta\ell}{c}\frac{dx}{dt}; \tag{9.37}$$

$$\frac{1}{\omega_r^2}\frac{d^2x}{dt^2} + \frac{q_r}{\omega_r}\frac{dx}{dt} + x = -p; \tag{9.38}$$

$$u = \zeta(1 + x + \gamma)\sqrt{\gamma - p}. \tag{9.39}$$

Here the flow rate is assumed to always enter the resonator. Moreover, the reed is assumed to be not beating, because this would imply that the mouth pressure γ should be negative (more exactly $\gamma + x < -1$). Brass instruments are played by blowing and not by inhaling!

9.3 Behavior of the Two-Equation Model (Regimes, Existence and Stability, Transients) Without Reed Dynamics

9.3.1 Introduction

For a reed instrument such as a clarinet or a saxophone, the playing frequencies and their first harmonics are lower than the first reed resonance frequency, except for the highest notes. This allows using the two-equation model. This approximation is considered to be valid in Sects. 9.3 and 9.4, and its limitations will be discussed in Sect. 9.5. Moreover, we assume that the reed displacement yields a simple correction to the length of the resonator, included in the total length, as well as the radiation length correction. The equation to be solved is Eq. (9.26) with $\Delta\ell = 0$:

$$u = [h * p](t) \quad \text{or} \tag{9.40}$$

$$U(\omega) = Y(\omega)P(\omega). \tag{9.41}$$

With Eq. (9.30), this is the two-equation model. Figure 9.10 shows the nonlinear function (9.30) for several values of the mouth pressure γ. For some approaches, we will further simplify this function. Several versions of the model of resonator can exhibit different aspects of the main phenomena. In some calculations, it will be assumed to be purely cylindrical, for other purposes it will be sufficient that it is quasi-cylindrical; for certain calculations, losses will be taken into account, but not always. Starting from the two-equation model, we first solve a system for the input variables only, then investigate the transfer functions, which allow deducing all quantities in the tube and outside. In the present analysis the control parameters are supposed to be time-independent: this obviously is far form real playing conditions, when the player modify these parameters at every time for expression purposes.

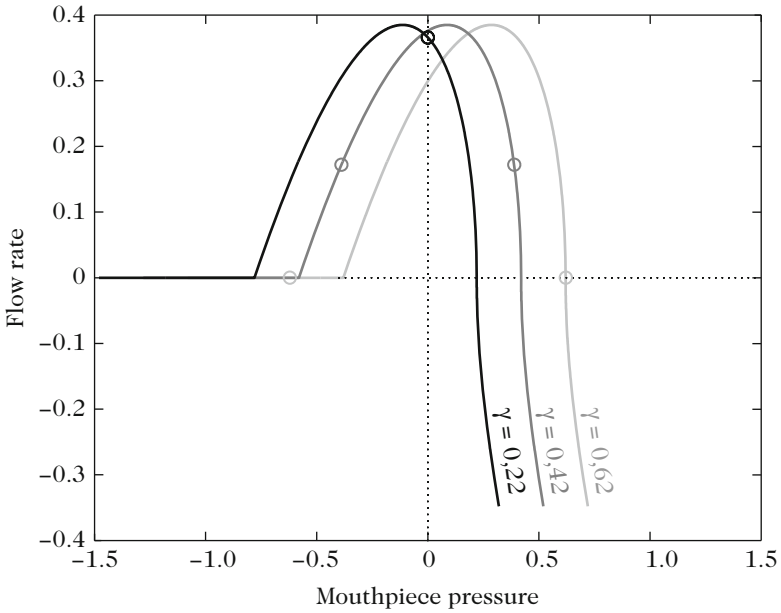

Fig. 9.10 Examples of flow curves [Eq. (9.30)] with respect to the pressure p in the mouthpiece for three values of the static pressure in the mouth. The variables are dimensionless: *from left to right* γ=0.22; 0.42; 0.62. When the pressure p is very low (and negative), the reed closes the mouthpiece. The limit points of the lossless approximation correspond to the two states of the square signal (see Sect. 9.3.3); they are denoted by *circles*. For the static regime, they coincide. The regime is static for $\gamma = 0.22$, while it is oscillating and non-beating for $\gamma = 0.42$, and oscillating and beating for $\gamma = 0.62$, with a zero flow rate. Here the flow rate has been divided by ζ, and the maximum value is $2/(3\sqrt{3})$

9.3.2 Static Regime and "Ab Initio" Method

9.3.2.1 Static Regime

A trivial solution for the system of Eqs. (9.40) and (9.30) can be found for the static regime, when the unknowns do not depend on time. If the pipe input impedance is assumed to be zero at zero frequency, the input pressure is zero as well at every time t, and the flow rate is $F_0 = F(0) = \zeta(1-\gamma)\sqrt{\gamma}$. For this situation, no sound is produced (when the reed closes the mouthpiece, if $\gamma > 1$, $F_0 = 0$). However, even for this regime, a transient exists if the mouthpiece pressure is not zero when the musician blows. Moreover the excitation pressure γ does not change instantaneously from 0 to a finite, stable value. After the transient, if the input pressure converges to 0, the regime is stable. In order to study the stability, one can imagine a deviation from the equilibrium, which yields a variation of the acoustic quantities. The outline of the study is as follows: if we are searching for a periodic steady-state regime, which is called "limit cycle" for dynamical systems (for the static regime the limit

cycle is a fixed point), the problem can be greatly simplified, e.g., by the use of the Fourier series. However, if we are searching for either the shape of a transient or the stability of the regime, the problem is much more complicated. In what follows, we present the most general method for solving the problem, including the transient; the solution is called "ab initio" and depends on known initial conditions.

9.3.2.2 "Ab Initio" General Method of Calculation

The system of Eqs. (9.30) and (9.40) can be solved by starting from the initial conditions. The impulse response $h(t)$ can be used, but its duration is very long, as explained in Chap. 4. It is better to modify the system, choosing as variables the outgoing and incoming pressure waves instead of the pressure and flow rate [99]. Using dimensionless variables, in the case of a perfect cylinder we have

$$p = p^+ + p^- \; ; u = p^+ - p^- \;\text{ with} \tag{9.42}$$

$$p^+ = \frac{1}{2}(p+u) \; ; p^- = \frac{1}{2}(p-u). \tag{9.43}$$

One can relate p^+ and p^- through a nonlinear function G:

$$p^+ = G\left[-p^-\right]. \tag{9.44}$$

It is obtained by a rotation of the function F by 45° (see [78] and Fig. 9.11). Equations (9.40) and (9.41) become, respectively:

$$\begin{aligned} p^-(t) &= \left[r * p^+\right](t) \\ P^-(\omega) &= R(\omega)P^+(\omega), \end{aligned} \tag{9.45}$$

where $R(\omega)$ is the classical reflection coefficient and $r(t)$ is the reflection function defined in Chap. 4. This formulation is possible whatever the shape of the resonator: the reflection function $r(t)$ is in general much shorter than the impulse response $h(t)$, and it can be used also for a numerical computation. Starting from Eqs. (9.43) and (9.45), the following useful equation is obtained

$$p(t) = u(t) + \left[r * (p+u)\right](t) = u(t) + \int_0^t r(t')\left[p(t-t') + u(t-t')\right]dt'. \tag{9.46}$$

The integral corresponds to the past time, which is known, and the use of the nonlinear equation (9.30) leads to the variables $p(t)$ and $u(t)$ when the initial conditions are defined. The integral is limited to 0 and t because the functions $r(t)$, $p(t)$, and $u(t)$ are causal. In general, in order to solve Eq. (9.46), time needs to be discretized.

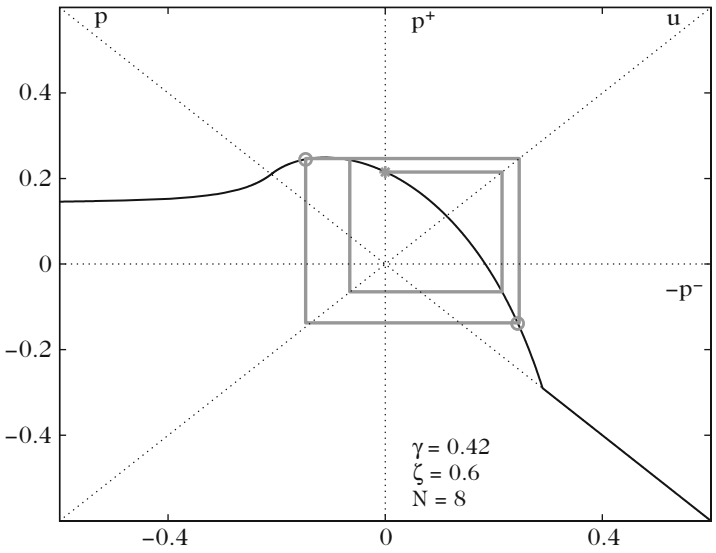

Fig. 9.11 The function G [see Eq. (9.44)] links the outgoing and incoming waves. The figure shows the principle of the iterative calculation of an ab initio solution when no losses are taken into account. *Circles* are the limit points. The values of the parameters are: $\zeta = 0.6$; $\gamma = 0.42$. Signals of pressure and flow rate are shown in Fig. 9.13a

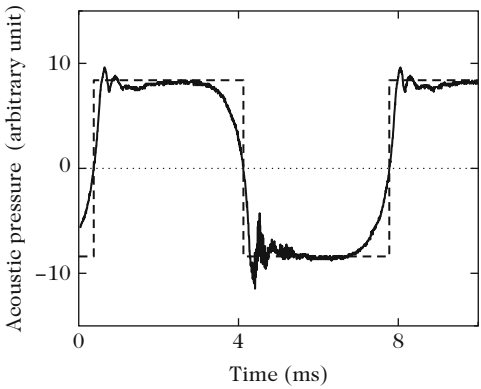

Fig. 9.12 Periodic signal for the internal pressure of a clarinet note, and its approximation by a square signal

The problem can be simplified, considering two types of approximations for the resonator: (1) the lossless approximation, (see Sect. 9.3.3), which leads to square signals for a cylinder (the pressure oscillates between two values, called "states"), and (2) the one-mode approximation for the resonator (Sect. 9.3.4), which leads to a Van der Pol equation. These approximations do not give all useful information: for instance, the spectrum of a square signal is not realistic compared to a real spectrum (Fig. 9.12). Nevertheless, essential conclusions related to sound production are reached.

9.3.3 *Lossless Approximation for a Cylinder: Helmholtz Motion*

9.3.3.1 Ab Initio Solution

For a perfect cylinder, the reflection function has a very short duration, because it corresponds to a simple delay of one round trip in the tube, with a convolution due to the visco-thermal losses and radiation effect. As a first approximation the latter is reduced to a change in sign and losses are ignored:

$$r(t) = -\delta(t - \tau), \tag{9.47}$$

where $\tau = 2\ell/c$ is the time of a round trip in the tube. Therefore:

$$p^-(t) = -p^+(t - \tau). \tag{9.48}$$

Equation (9.46) can now be written in the form:

$$p(t) = u(t) - p(t - \tau) - u(t - \tau). \tag{9.49}$$

If the pressure p^+ deviates from 0 at $t = 0$ and has the value $p^+(0) = p_0^+$, the problem is that of a sequence of unknowns when the time is discretized by intervals τ. Denoting for each variable $p(n\tau) = p_n$, the following system is obtained

$$p_n^- = -p_{n-1}^+; \tag{9.50}$$

$$p_n^+ = G(-p_n^-) = G(p_{n-1}^+). \tag{9.51}$$

This very simple sequence allows determining the solution at each time step $n\tau$. It corresponds to an elementary dynamical system called "iterated map." Each value of the sequence is obtained from the previous one by the iteration of a function. This implies that p^+ suddenly deviates from 0 at a point instant, because we consider a discrete time. This is not realistic, but allows finding basic solutions, with a steady-state regime having two states.[11] This shape is a particular case of the so-called Helmholtz motion, which was discovered experimentally by Helmholtz in the context of the bowed string, and will be discussed in Sect. 9.4.8.3. Notice that during the first round trip, from 0 to τ, the incoming wave is necessarily zero, because no wave comes back faster than the speed of sound. The solution of Eq. (9.51) can be found using a graphical method [78], as shown in Fig. 9.11. Starting from the

[11] In this section we implicitly assume that the mouth pressure suddenly goes from 0 to a non-zero value, then remains constant: $p = p_0^+$ until $\tau > t$. Thus the mouthpiece pressure is constant during the first round trip, and consequently, constant as well during every successive half-periods, resulting in a square signal shape, with two states. Other kind of initial conditions will be investigated further.

value $p_0^- = 0$, the value of p_0^+ corresponding to the imposed control parameters is deduced using Eq. (9.44). The next value $-p_1^- = p_0^+$ is determined, then the nonlinear function is applied, and so on. After a transient, the signal converges to two limit points, opposite in sign, which are the values of the two states of the square signal. Figure 9.13 shows the corresponding signals $p(t)$ and $u(t)$, as well as the result for other values of the parameters: the convergence can occur to the static regime (a unique limit point), or even to other regimes. This is studied in the following sections.

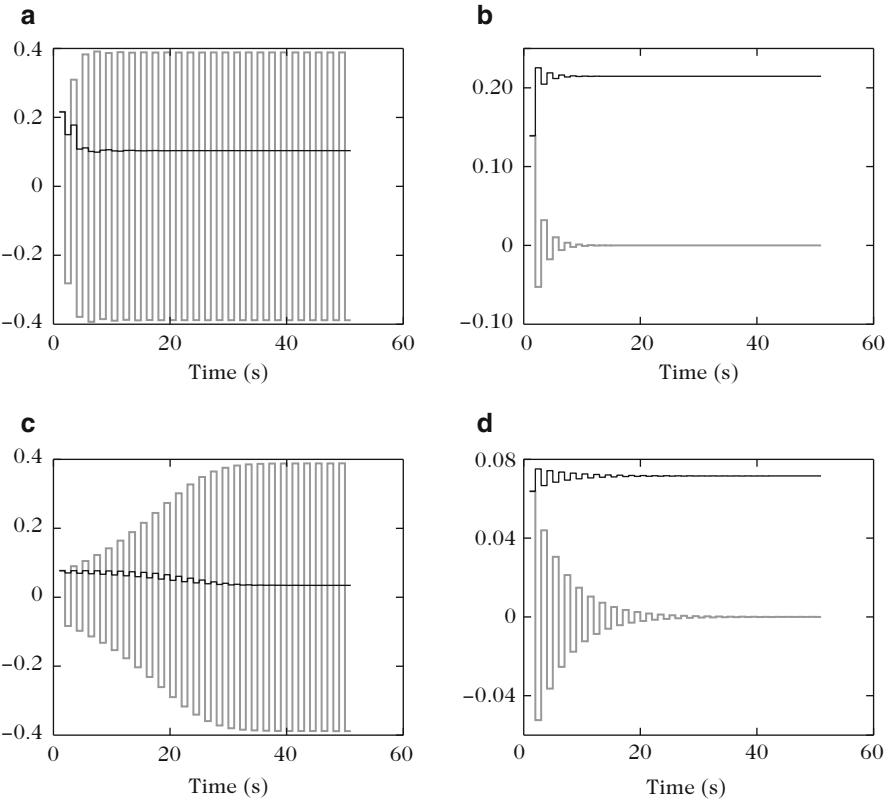

Fig. 9.13 Transients in square signals for two values of the reed parameter and the mouth pressure. In *gray*, the pressure; in *black*, the flow rate. (**a**) $\zeta = 0.6$, $\gamma = 0.42$; (**b**) $\zeta = 0.6$, $\gamma = 0.2$; (**c**) $\zeta = 0.2$, $\gamma = 0.42$; (**d**) $\zeta = 0.2$, $\gamma = 0.2$. The larger is the parameter ζ, the shorter is the transient. When γ is small, the signal converges to the static regime

9.3.3.2 Stability of the Static Regime; Start of the Transient

We continue the analysis of the solutions, and examine the stability of the regimes, the transients and the steady-state regime. Consider first an idealized attack, when the mouth pressure suddenly jumps from zero to a finite value, γ. Starting from the static regime, the pressure $p(t)$ remains small for the first time intervals and it is possible to linearize [Eq. (9.30)]:

$$u_n = F_0 + Ap_n \text{ ; with } F_0 = \zeta(1-\gamma)\sqrt{\gamma},\ \ A = \zeta\frac{3\gamma-1}{2\sqrt{\gamma}}. \tag{9.52}$$

where $F_0 = F(0)$ and $A = dF/dp$ at $p = 0$. Equation (9.49) gives

$$p_n - u_n = -(p_{n-1} + u_{n-1}). \tag{9.53}$$

It is the equation of the resonator, and it yields:

$$p_n = -p_{n-1}\frac{1+A}{1-A}\ ;\ p_n = p_0(-1)^n\left(\frac{1+A}{1-A}\right)^n, \tag{9.54}$$

where $p_0 = p_0^+ = F_0/(1-A)$. Expression (9.54) is obtained from Eq. (9.52) because $p_0^- = 0$.

If the factor raised to the power n is smaller than unity, the pressure p_n tends to 0 when n increases, otherwise it increases exponentially. The two cases correspond to a coefficient A which is negative or positive, respectively. If A is negative, the pressure converges to the static regime, which is stable; otherwise the static regime is unstable, see Fig. 9.13, and the pressure grows exponentially. Maybe the nonlinear terms of the function will produce a saturation to a stable oscillating solution. Given the expression of A, the threshold corresponds to a mouth pressure $\gamma = 1/3$. The larger is the reed parameter ζ (i.e., the wider is the reed opening at rest, or the smaller is the reed stiffness), the faster is the transient. From the perception point of view, this is an important characteristic of the sound.[12] Considering variables with dimensions, it can be shown that this linear problem up to a factor F_0/c stated corresponds for the tube to the calculation of the Green's function with an input admittance boundary condition: $Y = -AS/\rho c$, which is real. If the admittance Y is positive (negative A), the boundary is absorbing and the signal decreases, while if it is negative, the boundary is active and acts as a source, and the oscillation can start. Thus the problem involves a resistive termination, added to dissipation during propagation. The modal expansion shows that the complex natural frequencies are such that their real part, which is the instantaneous frequency during the transient, is higher than the frequency of the steady-state regime, which will be further studied. Thus there is a shift of the instantaneous frequency during the transient [36].

[12]For large values of ζ, and therefore for large pressure p_0, the validity of the expansion to the first order (9.52) is limited to the first values of the pressure, see, e.g., Fig. 9.13a

9.3.3.3 Simplified Model for the Non-beating Reed

For the sake of simplicity, we assume again that the pressure p does not deviate too much from the zero value (and we still assume $Z(0) = 0$; the more general case was investigated in [73]). We assume a non-beating reed which is typically obtained for a mouth pressure γ that is lower than 0.5, (see Sect. 9.4.6). A third order approximation of the flow rate gives (see [60, 124]):

$$u = F(p) \simeq F_0 + Ap + Bp^2 + Cp^3, \text{ where} \tag{9.55}$$

$$F_0 = \zeta(1-\gamma)\sqrt{\gamma},\ \ A = \zeta\frac{3\gamma-1}{2\sqrt{\gamma}},\quad B = -\zeta\frac{3\gamma+1}{8\gamma^{3/2}}\quad C = -\zeta\frac{\gamma+1}{16\gamma^{5/2}}\,. \tag{9.56}$$

In the normal range of variation for the parameter γ, the variation of the coefficient A is mainly due to the numerator, which varies almost linearly, while the parameters B and C only slightly vary. The parameters B and C are negative; this property will be shown to be essential in order for the oscillation to be saturated after the initial grow. All coefficients are proportional to the "reed opening" ζ; we conclude that A varies almost linearly with the mouth pressure; the other parameters are almost constant and negative. The series expansion allows simplifying calculations, but limits the validity of the results. However, the polynomial model can be used for a wide class of physical problems.

9.3.3.4 Existence of the Periodic Steady-State Regime

The steady-state can now be investigated if we assume a periodic behavior. The period is unknown, therefore it will be empirically determined (more straightforward methods will be further explained). It is first assumed to be equal to the round trip duration, $\tau = 2\ell/c$. Thus the variables are equal at times t and $t-\tau$:

$$p(t) = p^+(t) + p^-(t) = p^+(t) - p^+(t-\tau) = 0.$$

With this assumption, there is no non-zero periodic solution. This can be easily interpreted as follows: if a flow rate at the input of the instrument produces a positive pressure in the mouthpiece, this pressure travels to the end, then changes in sign and cannot recover the initial value after a single round trip.[13] It is easy to imagine that

[13]This kind of reasoning requires some care. For instance, why can't the same reasoning be valid for a flute-like instrument (see Chap. 10)? The reason lies in the nature of the source: for a flute, pressure and flow rate have to be inverted at the open end, and the flow-rate wave is reflected without change in sign at the end: thus the period $2\ell/c$ is possible. On the contrary a closed flute is similar to a clarinet.

with two round trips, a periodic regime is possible: if we search for a period equal to 2τ, the variables are equal at times $t+\tau$ and $t-\tau$, thus:

$$p(t+\tau) = p^+(t+\tau) - p^+(t)\ ; p(t) = p^+(t) - p^+(t-\tau). \quad (9.57)$$

$$\text{Therefore} \quad p(t) = -p(t+\tau). \quad (9.58)$$

A two-state signal is obtained, and the two values are opposite in sign. Thus the period 2τ is a solution. In order to find the two values, it is noticed that the flow rate is periodic with the period τ, because:

$$u(t+\tau) = p^+(t+\tau) + p^+(t) = p^+(t-\tau) + p^+(t) = u(t). \quad (9.59)$$

In steady-state regime, the flow rate is constant, as shown in Fig. 9.13. The limit points $\pm p_\infty$ are solutions of:

$$F(p_\infty) = F(-p_\infty), \text{ thus } A + Cp_\infty^2 = 0, \text{ and:} \quad (9.60)$$

$$p_\infty = \pm\sqrt{-\frac{A}{C}}. \quad (9.61)$$

If C is negative, this oscillating solution exists for positive A, when the static regime becomes unstable. If C were positive (it is not the case of the present model), solutions would exist when A is negative, i.e., when the static regime is stable. It is possible to theoretically show that in general the oscillating regime would be unstable, using either a perturbation method [71] or the theory of the topological degree [96]. A proof will be provided for our case in the following section. Concerning the square shape of the pressure signal and the constant value of the flow rate, it is possible to link these results to a reasoning in terms of input impedance. For a lossless cylindrical resonator open at the end, the input impedance has infinite maxima for frequencies which are odd multiple of the frequency $c/4\ell$, which corresponds to the period 2τ, and zero minima for frequencies which are even harmonics of this frequency. Consequently the pressure involves odd harmonics only, while the flow rate involves even harmonics only. Moreover the studied signals are constant during one half-period (see Sect. 9.3.3.1). Therefore during the steady-state regime, the flow rate can involve odd harmonics only, and a continuous component; finally it is constant, with neither odd nor even harmonics! These calculations can be easily generalized to the nonlinear function (9.30) [73, 76]; the two values of the pressure remain opposite, and the flow rate is constant. Figure 9.10 shows the limit(s) point(s) for three values of the pressure γ. The result is written as:

$$p_\infty = \pm\left[(3\gamma-1)(1-\gamma)\right]^{1/2} \text{ if } \gamma < 1/2;$$
$$p_\infty = \pm\gamma \text{ if } \gamma > 1/2. \quad (9.62)$$

9.3.3.5 Stability of the Periodic Oscillation Regime

How can be investigated the stability of the periodic oscillation regime? Similarly to what we did for the static regime [see Eq. (9.54)], the function F is linearized around the limit points. This time there are two limit points:

$$u_n = F(p_\infty) + (p_n - p_\infty)F'^{+}$$
$$u_{n+1} = F(-p_\infty) + (p_{n+1} + p_\infty)F'^{-},$$

where $F'^{\pm}$ is the derivative of F at $\pm p_\infty$. Using the equation of the resonator (9.53), we deduce

$$(1 - F'^{-})(p_{n+1} + p_\infty) = -(p_n - p_\infty)(1 + F'^{+}), \text{ and}$$
$$(1 - F'^{+})(p_{n+2} - p_\infty) = -(p_{n+1} + p_\infty)(1 + F'^{-}),$$

then

$$(p_{n+2} - p_\infty) = (p_n - p_\infty)\frac{(1 + F'^{-})(1 + F'^{+})}{(1 - F'^{-})(1 - F'^{+})}. \tag{9.63}$$

Stability is ensured if the factor multiplying $(p_n - p_\infty)$ has an absolute value smaller than unity. Squaring this factor, we obtain

$$(F'^{+} + F'^{-})(1 + F'^{+}F'^{-}) < 0. \tag{9.64}$$

And using Eq. (9.61):

$$A\left[1 + 4A(B^2/C + A)\right] > 0. \tag{9.65}$$

When A is small, *the stability condition* $A > 0$ *is opposite to that of the static regime*, QED. If A increases, considering the first order term in A in the bracket, it can be seen that:

– either C is negative, and the sign of the bracket can change for a non-zero, positive value of A. Beyond this threshold, it can be shown that a periodic regime exists with a double period. This kind of regimes is discussed hereafter. The most important result is that the *bifurcation* is *direct*. As a consequence the clarinet can play pianissimo. We already considered bifurcations for free oscillations (see Sect. 8.5 of Chap. 8); "direct"[14] means that after a threshold, $A = 0$, there

[14] In the literature the adjectives "normal" or "overcritical" or "supercritical" can be found instead of "direct." The contrary is "inverse," or "undercritical," and implies a discontinuity between two regimes, with a hysteresis, as it will be seen hereafter.

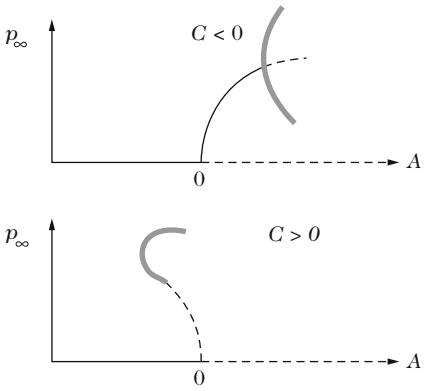

Fig. 9.14 Schematic bifurcation diagram in A $=$ 0 for the two cases positive C (inverse bifurcation) or negative C (direct bifurcation). *Solid, black line*: limit values of stable regimes, either static ($p_{\infty} = 0$), or oscillating (the positive value only is indicated). *Dotted, black line*: unstable regimes. Beyond the cases of calculation that are presented by the inequality (9.65), the hypotheses are as follows: for $C > O$, the unstable oscillation regime becomes stable, and for $C < 0$, there is a new bifurcation to a stable regime with four values (*lower octave*)

is continuity from a stable regime (here the static one) to another (here the oscillating one), when the control parameter (here A, or more precisely the mouth pressure) increases.

– or C is positive (this is not the case of the present model), and the solution of Eq. (9.61) exists for negative A only. It is unstable for small values of A. For a non-zero, negative value of A, it is possible to find a new periodic, stable regime, and the bifurcation is said "inverse." Figure 9.14 shows the two cases. No investigation concerning phenomena far from $A = 0$ is presented yet.

9.3.3.6 Period Doubling and Chaos: Discussion

What happens when the condition (9.65) is not fulfilled? It is possible to investigate the case when the bracket in Eq. (9.65) is negative: (1) either by computing the solution ab initio (*stable* regimes are obtained, but it is not sure that they are *all possible regimes*, because they depend on initial conditions, which are certainly not unique); (2) or by calculating the periodic steady-state regimes with a pre-supposed frequency, as above explained (but it is not possible to know whether *these regimes are stable*!). It is possible to try a period double, 4τ, and to confirm that the threshold of existence for the solutions is $A\left[1 + 4A(B^2/C + A)\right] = 0$, but the calculation is tedious. For the model (9.30), without series expansion around the static solution, the ab initio study, which corresponds to the graphical solution of Fig. 9.11, was done in [73, 105]. Frequency divisions by 2, 4, 6, 12,... are obtained, and the thresholds appearing for the mouth pressure (γ) depend of the reed parameter ζ. The weaker is the reed (large ζ), the earlier these regimes appear. When γ continues

to raise, the solution comes back to the "normal" frequency for $\gamma = 1/2$. This will be studied when looking at the beating reed behavior. For a fixed value of γ, it was possible to obtain with the same model, a complete scheme of period doubling toward a chaotic signal [77]. This scheme is called "subharmonic cascade," and was already studied for the case of a clarinet [20, 70, 78, 104, 105]. The chaos is a non-periodic regime (we could say with an infinite period), and it is called "deterministic chaos" because it is solution of a deterministic equation, while it is extremely sensitive to the initial conditions and for this reason it is unpredictable. This concept was presented in Chap. 8.

The reader can be surprised by this result of a frequency division, because this phenomenon is not common, while the frequency multiplication by a factor 3 is. This issue is treated hereafter. Actually, if realistic losses are taken into account in the model, the period doubling can disappear [35]. However, period doubling can be encountered for other reed instruments, such as the crumhorn or the bassoon [55]: the notes of a contrabassoon can be played with a bassoon.[15]

9.3.3.7 Other Types of Regimes: Twelfths

This section investigates regimes with triple frequency, also known as twelfth regimes. Equations (9.50) and (9.51) do not make any assumption concerning the variation of the signals during the time $\tau = 2\ell/c$. If the frequency is an odd multiple of $f_1 = c/4\ell$, which corresponds to the period 2τ (see the previous paragraphs), it is easy to find Helmholtz regimes (two-state signals) which satisfy Eqs. (9.58)–(9.61). It is sufficient to choose different initial conditions in order to initiate the triple frequency: we impose a non-zero value to the outgoing wave p^+ not only at $t = 0$, but also at $t = 2\tau/3$, and a zero-value at $t = \tau/3$. Therefore this regime has the same threshold than the "fundamental" regime. When it is reached it is not more difficult to sustain than the fundamental regime. A practical solution for imposing these initial conditions is easy: a small "register hole," located at the third of the length is opened, and allows emitting the twelfth. If we ignore the losses, after initialization, when closing this hole, the twelfth regime should remain stable.[16]

[15] In practice the frequency division is possible for very narrow ranges of parameters (γ or ζ), especially when approaching the chaotic regime. Consequently it is easy for an instrument maker to avoid these phenomena.

[16] In practice this is not always possible when playing a clarinet, because when closing the register hole, it is also possible to retrieve the fundamental regime. The reason is not simple. We will see that when losses are taken into account, the threshold pressure for the triple frequency is higher than that for f_1. This is not a sufficient reason, because beyond the threshold for the triple frequency, both regimes should be reachable by choosing the appropriate initial conditions. Notice that for other instruments, such as a flute or a bassoon, it is often easy to play the higher registers even without the opening of a register hole. Moreover baroque oboes have no register holes for overblowing.

9.3.4 One-Mode Approximation

The Helmholtz motion is an interesting approximation for the study of the transients, the regime stability, their frequency and their amplitude, but do not give insights into the real shape of the signal, i.e., of the spectrum: fortunately the signal is not perfectly square. In the next section (Sect. 9.4) the steady-state regime will be examined, taking losses into account. But beforehand it is interesting to make a study similar to the previous one for another approximation of the resonator, when this response is reduced to that of a single mode. This is also a rough approximation of the resonator, but it allows considering realistic losses and their frequency dependence.[17] In contrast, the previous model, "lossless model," took into account an infinity of modes with harmonically related frequencies.

9.3.4.1 Differential Equation for the Mouthpiece Pressure

In the second part of the book, the modal expansion of the dimensionless input impedance was obtained [see in particular Eq. (7.19)]:

$$Z(\omega) = j\omega \sum_n \frac{F_n}{\omega_n^2 - \omega^2 + j\omega\omega_n/Q_n}, \tag{9.66}$$

where ω_n is the frequency of the nth resonance, Q_n is the quality factor, and F_n the modal factor. The value of the (real) maximum of the impedance modulus is $Z_{Mn} = F_n Q_n/\omega_n$.[18] For a cylinder $F_n = 2c/\ell$ and $Z_{Mn} = 2cQ_n/(\ell\omega_n) = k_n/2\alpha$ (in dimensionless quantities) when radiation losses are ignored and α is given by Eq. (5.147). A great simplification is obtained by truncating the series after the first mode. For a cylinder, using a first order approximation of the losses, this is allowable near the resonance ω_1: starting from expression $Z(\omega) = j\tan(k - j\alpha)\ell$, the following equation is exact: $Z(\omega_1) = (\alpha\ell)^{-1} = 2Q_1/k_1\ell$ (for the study of a resonance peak, see Chap. 2). However, far from the resonances, the truncation strongly modifies the predicted response of the resonator. For the first register of the clarinet, the truncation is not as consequential as for conical instruments, because the second resonance frequency is far from the first one, and the first peak is dominant. Nevertheless one should not expect correct results for the spectrum.

[17] Meynial [81] studied a "monochromatic" resonator, by considering a tube with axial chimney, so that all the resonances, but the first, are strongly attenuated. Also the frequencies of the higher order modes are not multiple of the frequency of the first mode. The present model is close to this experimental realization, which produced a spectrum dominated by a single frequency, even at higher levels.

[18] We used Eq. (5.183) in dimensionless quantities, simplifying it by including the radiation length correction into the length ℓ.

Using Eq. (9.66), and truncating it to the first mode, we obtain

$$(\omega_1^2 - \omega^2 + j\omega\omega_1/Q_1)P(\omega) = j\omega F_1 U(\omega).$$

Its inverse Fourier Transform is written as:

$$\frac{d^2}{dt^2}p(t) + \frac{\omega_1}{Q_1}\frac{d}{dt}p(t) + \omega_1^2 p(t) = F_1\frac{d}{dt}u(t), \tag{9.67}$$

or, after the attack, if Eq. (9.55) is used

$$\frac{d^2}{dt^2}p(t) + F_1\frac{d}{dt}\left[(Y_{m1} - A)p(t) - Bp^2(t) - Cp^3(t)\right] + \omega_1^2 p(t) = 0. \tag{9.68}$$

$Y_{m1} = 1/Z_{M1}$ is the value of the (real) minimum of the admittance. This equation is a Van der Pol equation. It is now possible to consider the successive steps of the study of the Helmholtz motion (see Sect. 9.3.3). For the transient, approximate solutions of the Van der Pol equation can be found in the literature (see, e.g., [36]), but are not simple. We limit this section to the stability of the static regime, the early transient, and the existence of the periodic regime.

The solution of Eq. (9.68) is not sinusoidal, because of the nonlinear terms. The modal method can be generalized to an arbitrary number of modes in order to solve the exact problem; a system of nonlinear, ordinary differential equations has to be solved, and numerical methods are available for this purpose. This method is an alternative solution to the ab initio method [9, 36].

9.3.4.2 Stability of the Static Regime, Early Transient

A trivial solution is the static regime $p(t) = 0$. In order to study its stability, we linearize Eq. (9.68), by ignoring the terms with B and C. This equation becomes the equation of a linear oscillator with one degree of freedom. The damping can be negative, if A is larger than Y_{m1}. For A smaller than Y_{m1}, the oscillation is exponentially damped, and the oscillator returns to the static regime. On the contrary, the oscillation can grow exponentially, and the nonlinear terms will allow the saturation of the amplitude. This study of stability is similar to the one that leads to Eq. (9.54). The instability threshold of the static regime is now given by: $A = Y_{m1}$, instead of $A = 0$. In order to produce a sound, it is necessary to blow sufficiently hard to compensating for the losses. Notice that radiation losses have been neglected compared to the visco-thermal losses: but if they are large, the threshold is high. Paradoxically the radiation of a self-sustained oscillation instrument should not to be too efficient in order for the sound to exist (see also Chap. 7, Sect. 7.5.1).

- In the case of a cylindrical tube, by using the value of A given by Eq. (9.56), a simple result can be obtained. We simply consider that the perturbation due to

the losses is small, and replace γ by $1/3$ in the denominator of A. This yields the pressure threshold:

$$\gamma_{\text{th}} = \frac{1}{3} + \frac{\alpha\ell}{\zeta}\frac{2}{3\sqrt{3}}. \tag{9.69}$$

A typical order of magnitude for this threshold is 0.38. It is possible to derive the solution of the linearized equation (9.67), by assuming[19] $p(t) = 0$ at $t \leq 0$, and $u(t) = F_0 H(t) + Ap(t)$:

$$p(t) = \frac{4}{\pi} F_0 H(t) e^{-\alpha_o t} \sin \omega_1 t \text{ where } \alpha_0 = (Y_{m1} - A)c/\ell. \tag{9.70}$$

in the classical hypothesis of an oscillator which is either weakly damped of weakly excited, satisfying $|Y_{m1} - A| << \omega_1 \ell/c$ (see Chap. 2). If losses are ignored, this solution can be compared to that in square signals (9.54), and the two agree in both amplitude and phase.

- For a tube with an arbitrary profile, two observations can be made when looking at Eq. (9.68):
- The general expression of the modal expansion obtained in Chap. 7 [Eq. (7.38)] shows that the modal factor F_1 satisfies

$$F_1 = cS(0)\frac{\Phi_1^2(0)}{\Lambda_1} \text{ where } \Lambda_1 = \int_0^\ell S(x)\Phi_1^2(x)dx.$$

It depends on the geometry only, and is independent of losses. As a consequence, for a non-cylindrical instrument, it can strongly vary with frequency. Beyond the threshold, the amplification factor is the product of the modal factor by A [see Eq. (9.68)], and does not depend on losses. On the contrary, for free oscillations, the duration of the transient is determined by the quality factor (see Chap. 2). Similarly it is possible to show that the extinction transient when the mouth pressure decreases is not primarily linked to losses.

- The relevant quantity for the determination of the threshold is the minimum Y_{m1}, which is inversely proportional to the quality factor, but is also proportional to the modal factor. Consequently if the geometry imposes a very large impedance, it is possible to diminish the minimum Y_{m1} and therefore to lower the threshold without reduction of losses, by using the reactive effects due to reflections at cross-section changes. Thus the threshold is not only linked to losses, but mainly to the height of the impedance peak. This explains why the mouthpiece of brass instruments makes the attacks easier without reducing losses (this sentence is a

[19] The solution satisfies $p(t) = p(t)H(t)$, and the flow rate $u = H(t)[F_0 + Ap(t)]$ hence $u = F_0 H(t) + Ap(t)$. Thus it exists a source term in Eq. (9.68), which is equal to $2c\ell^{-1}F_0\delta(t)$. The solution is proportional to the Green's function of this equation, which was studied in Chap. 2, see Eq. (2.14).

simplified explanation, because it ignores the reed dynamic, essential for these instruments). These remarks fully justifies the importance that Benade [10] gave to the height of the impedance peaks (see Chap. 7 of the present book for a detailed study of the role of the brass instrument mouthpiece).

9.3.4.3 Negative Resistance and Energy

The term $-A$ in Eq. (9.68) can be interpreted as the energy source of the self-oscillating system: it corresponds to a negative resistance when sound is produced, i.e., when its absolute value is large enough to overcome the positive resistance of term Y_{m1} (A is the first derivative of the nonlinear function du/dp near $p = 0$). Figure 9.10 shows that for values of γ larger than $1/3$, the slope of the curve is negative and an oscillation regime with two states exists, while for $\gamma = 0.22$, the slope is negative.[20]

Extending this idea to the nonlinear operation range, we can rewrite the time derivative term of Eq. (9.68), up to the factor $\omega_1 Z_{M1}/Q_1$:

$$\frac{dp}{dt}\left[Y_{m1} - A - 2Bp - 3Cp^2\right].$$

Thus the source resistance is $R = -(A + 2Bp + 3Cp^2)$. Its instantaneous value oscillates because of the term Bp, but its absolute value diminishes with increasing p because the coefficient C is negative. Intuitively we understand that the oscillation does not continue to grow exponentially, but saturates and converges to a stable amplitude in the steady-state regime.

9.3.4.4 Existence of the Periodic Regime

In order to obtain an analytical expression for the periodic regime, we can seek an approximated solution of the nonlinear equation. To assume that the solution is sinusoidal is not rigorous, but often gives very good results. This is the simplest application of the harmonic balance technique (see the next paragraph). The result is

$$p(t) = 2\sqrt{\frac{1}{3}\frac{Y_{m1} - A}{C}}\cos(\omega_1 t + \varphi). \tag{9.71}$$

[20] The previous comment comes from the study of the function $F(p)$, where p_m (γ) is a parameter. Another way of thinking [50] considers the function $F(\Delta p)$ (see Fig. 9.9), with the following property: $(du/dp)_{p=0} = -(du/d\Delta p)_{\Delta p = p_m}$. This curve demonstrates that the oscillation threshold is obtained at the maximum of the curve, and that the increasing and decreasing parts of the curve correspond to a stable and an unstable static regime, respectively.

The phase φ of the oscillating factor is unimportant in a periodic, steady-state regime. The existence of this solution is ensured under the same condition as the instability of the static regime, $A > Y_{m1}$, because the coefficient C is negative. This confirms the direct behavior of the bifurcation. This solution can be compared to that of the lossless model, when $Y_{m1} = 0$. Starting from the square signal solution (9.61), the amplitude of the first harmonic of a square signal is calculated and the same result is obtained, up to the factor $2\sqrt{3}/\pi$. This explanation will be detailed further.

Let us summarize the present section. We compared the robustness of two approximated models: the lossless resonator and the one-mode resonator. This was easy for several features of the behavior of reed instruments, but the calculation of the stability of the oscillation regime leads to an intricate computation for the latter model [113] and is not presented here.

9.4 Away from the Reed Resonance (Two-Equation Model): Steady-State Regimes

9.4.1 Principle of the Harmonic Balance Method: First Harmonic Approximation

In order to study the spectra, we need to take into account the losses, which depend on frequency. The ab initio method (see Sect. 9.3.2.2) allows solving the problem numerically. Nevertheless another method, called "harmonic balance," is possible, at least for the steady-state regime. It was already presented in Chap. 8. It can be used numerically, but very useful analytical approximations can also be obtained. It is based upon the periodicity of the signal, which implies that it can be written in the form of a Fourier series:

$$p(t) = \sum_{n=-\infty}^{n=+\infty} P_n e^{jn\omega_1 t}, \tag{9.72}$$

where $P_{-n} = P_n^*$ since the signal is real, and ω_1 is the fundamental frequency, which is a priori unknown. P_1 can be chosen for instance as a positive, real quantity, because the phase of the signal has no significance in the steady-state regime. As a matter of fact, the relative phases are to be determined for the harmonics only (a periodic signal is invariant with respect to a temporal translation). The d.c. component P_0 is real as well. With this choice, the square signal $\pm p_\infty$ has the following spectrum:

$$P_{2\nu+1} = \frac{2(-1)^\nu p_\infty}{(2\nu+1)\pi}; \; P_{2\nu} = 0. \tag{9.73}$$

The even harmonics are zero, while the phase of the odd harmonics is alternately 0 and π. For the Helmholtz motion, the spectrum of the mouthpiece pressure is that of a square signal, and therefore it decreases with increasing frequency. When losses are taken into account, this spectrum decreases as well, but more rapidly, especially near the oscillation threshold. This allows seeking simple approximations. The simplest one is the so-called first harmonic approximation (also called in textbooks on dynamical systems the "describing function" method), for which the series (9.72) is truncated to $n = \pm 1$. Using this, we can investigate the existence of solutions, their frequency and their amplitude, by solving Eqs. (9.41) and (9.55):

$$u = F_0 + Ap + Bp^2 + Cp^3; \tag{9.74}$$

$$U(\omega) = Y(\omega)P(\omega). \tag{9.75}$$

The reed is assumed not to beat. The flow rate is also expanded in harmonics, and their amplitudes are Y_nP_n, where the Y_n are the values of the input admittance $Y(\omega)$ for the frequencies which are multiple of the frequency ω_1 (remember that this frequency is unknown). In Eq. (9.55), we keep the terms of frequency ω_1 only. The term of order 0 (a constant) and the term of order 2 of the polynomial cannot involve terms with frequency ω_1. Notice that the calculation of the powers in the polynomial is much easier with complex exponential than with trigonometric functions. If we "balance" the terms of frequency ω_1 on the left and the right of the nonlinear equation, we get

$$Y_1P_1 = AP_1 + 3CP_1^2P_1^* = AP_1 + 3CP_1^3. \tag{9.76}$$

The balance for the frequency $-\omega_1$ would not give any supplementary information, because we would obtain the complex conjugate equation. A trivial solution is $P_1 = 0$; it is the static regime. The other solution is

$$P_1^2 = \frac{1}{3}\frac{Y_1 - A}{C}. \tag{9.77}$$

- P_1 is chosen as a real quantity, therefore the imaginary part of this equation yields: $\Im m(Y_1) = 0$. Solutions exist if Y_1 is real, therefore the oscillation frequency can be calculated from $\Im m(Y_1) = 0$. As a first approximation (if the influence of visco-thermal effects on the sound speed is ignored), the first possible playing frequency for an open cylinder is $f_1 = c/4\ell$. A result of great musical importance is that the playing frequency does not depend on the amplitude. If higher harmonics are taken into account, this result is marginally modified, as explained further.[21]

[21] The oscillation condition is not given by the maximum of the input impedance modulus, but by the zero value of the imaginary part of the admittance. In Chap. 2 the difference between these two conditions was shown to be very small.

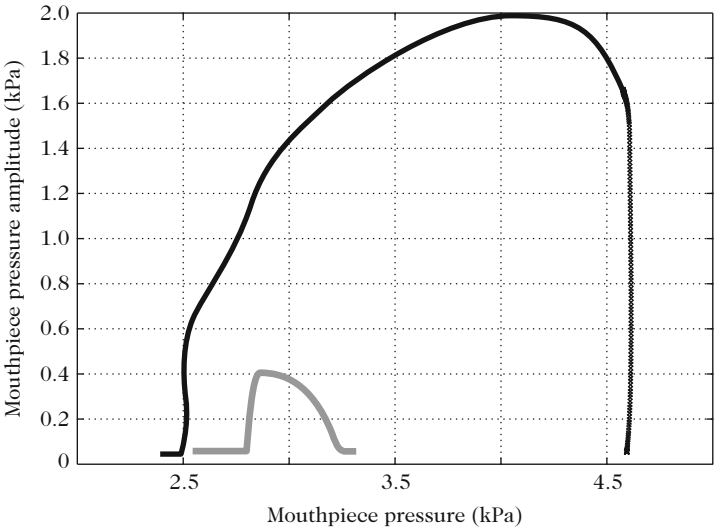

Fig. 9.15 Experimental bifurcation scheme (with artificial mouth) for a clarinet note, for two values of the reed parameter ζ. The ordinate is the root mean square (RMS) pressure. The bifurcation at the oscillation threshold is direct for both curves, while at the extinction threshold, it is inverse for the *black curve* (normal reed opening ζ), and direct for the *gray curve* (small ζ): beyond a certain value, which is called the "closure" pressure, there is no more oscillation, because the reed eventually closes the mouthpiece. This will be explained in Sect. 9.4.6, when studying the beating reed

- The real part of Eq. (9.77) gives the solution for the other unknown of the problem, i.e., the amplitude of the first harmonic. Replacing Y_1 by Y_{m1}, which is the real part of Y_1 at frequency ω_1, we found the result (9.71). Because C is negative, the solution exists only if A is larger than Y_{m1}. It is the same threshold as the instability threshold of the static regime. A diagram showing the measured amplitude for a clarinet-like instrument can be seen in Fig. 9.15: for rather weak amplitudes, the curve is similar to a square root curve. Notice that it is very delicate to measure small amplitudes near the threshold. At moderately high amplitudes, the reed begins to beat: this will be investigated in Sect. 9.4.6.

If we consider the case $Y_{m1} = 0$, we can compare the amplitude with that of a square signal [Eq. (9.61)]. The two values differ slightly. Indeed if the Eqs. (9.61) and (9.73) are combined, the following value is obtained for the Helmholtz motion: $P_1^2 = -\frac{A}{C}\frac{4}{\pi^2}$. The ratio between these two values is $2\sqrt{3}/\pi$, or 1.102 (i.e., less than 1 dB). The error is due to the truncation of the series of harmonics, and can be accepted for most applications.[22]

[22]This feature is related to the modulus of the input impedance for the different harmonics: for a cylinder, when losses are taken into account, the input impedance for the harmonic 2 is very small, and for the harmonic 3, it is approximately $\sqrt{3}$ times smaller than that of the fundamental.

9.4.2 Characteristic Equation and Instability Threshold of the Static Regime

For square signals, the instability threshold of the static regime and the threshold of the oscillation regime (stable or not) were distinguished. With the harmonic balance method, or more precisely with Eq. (9.77), the existence threshold of the oscillation regime was found. It is characterized by specific values of the frequency and of the excitation parameter A. More generally several oscillating solutions can be found: they cancel the imaginary part of $Y_1(\omega)$. For small amplitudes, Eq. (9.76) implies $Y_1 P_1 = A P_1$, thus:

$$Y(\omega) = A \text{ or } AZ(\omega) = 1. \tag{9.78}$$

This is the so-called characteristic equation, which is the equation of the linearized system. It is obtained when the nonlinear equation is linearized around the static solution. The solution of this equation is sinusoidal (but for degenerate cases, it can be a square signal [60]). This justifies the writing without the subscript 1, because there is no ambiguity. In the case of a one-mode truncation, the stability of the static regime (see Sect. 9.3.4.2) was deduced. The solution of the equation was sought in the form of a complex exponential (9.70), i.e., an exponentially increasing or decreasing sinusoid, according to the parameters of the problem. When the exponent has a zero real part, the (in)stability threshold of the static regime is found, but the existence threshold of the oscillation regime cannot be found by using the linearized equation. How is it possible to generalize this search for the instability threshold to Eq. (9.78)? We have to search for all (complex) zeros of the equation and to see if they correspond to growing exponentials or not. If all exponentials are decreasing, then the static regime is stable; if any exponential is growing, the static regime is unstable, and the solution of the nonlinear problem can be expected to be oscillating.[23] When a parameter varies and one decreasing solution switches to

This is very different for other types of instruments, such as conical instruments. This reasoning implies that losses are accounted for, because when losses are ignored, the impedance ratios are unknown (the impedance is infinite for the maxima and zero for the minima): the system is called "degenerate." In practice we have to consider losses, and make them tend to zero [60].

[23] For a more general system, the Nyquist criterion can be used: it is based on the location of the poles of the characteristic equation in the complex plane. Using the terminology of the control system theory [85], Eqs. (9.74) and (9.75) are typical of a (nonlinear) feedback loop system, functioning in free oscillations. For most industrial applications the aim is to push further the instability ranges of the feedback system, on the contrary the instrument maker and the player attempt to make the system unstable in order to produce self-sustained oscillations (see, e.g., [11, 41, 48]). The analysis of linear stability starts with the linearization of the nonlinear element of the feedback loop system (for us $u = F_0 + Ap$). In the linearized system this element is replaced by a quantity whose dimension is an admittance (the coefficient A in our equations, which is the derivative of the nonlinear function with respect to the acoustic pressure, when the latter is calculated at the operating point, i.e., at the equilibrium position of the system). Then the instability threshold is calculated by using an equation that is formally identical to Eq. (9.78).

an increasing solution, we get the instability threshold of the static regime. Exactly at the threshold, the exponent of the exponential is purely imaginary, because its real part vanishes. Therefore solving the characteristic equation for real frequencies provides the thresholds. As an example, using Eq. (9.68), it can be written as: $\omega_1^2 - \omega^2 + j\omega\omega_1 Z_{M1} Q_1^{-1}(Y_{m1} - A) = 0$. Because ω is real, this equation yields $\omega = \omega_1$, and $Y_{m1} = A$, i.e., the frequency and excitation pressure thresholds.

- Another, equivalent, formulation is often used for the study of dynamical system. Let us suppose that it is possible to write the equations of the linearized problem in the following form:

$$\frac{d}{dt}\mathbf{V} = \mathbb{M}\mathbf{V},$$

where $\mathbf{V}$ is a vector involving the physical variables of the problem, and $\mathbb{M}$ is a matrix involving the parameters of the problem.[24]

If all eigenvalues of the matrix $\mathbb{M}$ have a negative real part, the static regime is stable. If the real part of one of the eigenvalues becomes positive, this regime becomes unstable (notice that because $\mathbb{M}$ is real, the eigenvalue pairs are complex conjugate). The threshold value is given by the zero of the real part of an eigenvalue pair. This technique can be easily applied to Eq. (9.68), confirming the conclusions of Sect. 3.4.2. by writing the following relationship:

$$\mathbf{V} = \begin{pmatrix} p \\ dp/dt \end{pmatrix} \text{ and } \mathbb{M} = \begin{pmatrix} 0 & 1 \\ -\omega_1^2 & F_1(A - Y_{m1}) \end{pmatrix}.$$

9.4.3 *The Harmonic Balance Method: An Overview*

If we wish to go beyond the first harmonic approximation in order to solve Eqs. (9.55) and (9.41), we can truncate the series (9.72) to N harmonics, and increase N to infinity. When we fill the truncated series in Eq. (9.55), we obtain a set of equations corresponding to the first N harmonics. We obtain a system of nonlinear complex equations with N complex unknowns, P_n. Moreover a real equation has to be added for the d.c. component, with the real unknown P_0. Therefore the system of $2N + 1$ nonlinear real equations has $2N + 1$ real unknowns. The "balance" seems to be satisfactory. However, there is a supplementary unknown, the playing frequency,

[24] More generally, it can be written before the linearization:

$$\frac{d}{dt}\mathbf{V} = \mathbf{F}(\mathbf{V})$$

where the components of the vector function $\mathbf{F}(\mathbf{V})$ are nonlinear functions of the components of the vector $\mathbf{V}$. The matrix $\mathbb{M}$, already encountered in Chap. 8, is called "jacobian" of the function $\mathbf{F}$.

and it is solved by the possibility to impose a real P_1! In order to solve the problem numerically, the continuation method can be used: starting from a known solution, the parameters are slightly changed, and the equations linearized around the known solution. More specifically: Eq. (9.55) is treated in the time domain, while Eq. (9.41) is treated in the frequency domain, and the passage to one domain to the other is done alternately by summation and by Fourier Transform. In principle this method allows following all regimes when the parameters change, e.g., the mouth pressure γ, whatever stability of the regime is [46, 57, 98]. A free software, Harmbal, permits solving this type of problems, including the reed modes [45].

We will now investigate new simplifications, beyond the first harmonic approximation, yielding analytical results.

9.4.4 The Variable Truncation Method, and Its Application to Clarinet-Like Instruments

9.4.4.1 Odd Harmonics

Because the clarinet profile is mainly cylindrical, the even harmonics in the mouthpiece can be assumed to be much weaker than the odd ones. Thus it is interesting to split the pressure and the flow rate into a part involving even harmonics only (subscript s) and a part involving odd harmonics only (subscript a). The functions with subscript s satisfy: $f_s(t + T/4) = f_s(t - T/4)$ at every t, where $T = 2\pi/\omega_1$ is the period. The functions with subscript a satisfy: $f_a(t + T/4) = -f_a(t - T/4)$. For the product of two functions of one or another type, the following rules are applied: $f_s g_s$ and $f_a g_a$ are of type s, while $f_s g_a$ is of type a.[25] For the pressure, it can be assumed that $p_s << p_a$. Using a perturbation method, the calculation starts by ignoring the part p_s; the nonlinear equation is split into two equations:

$$u_s = F_0 + Bp_a^2; \tag{9.79}$$

$$u_a = Ap_a + Cp_a^3. \tag{9.80}$$

The second equation involves odd harmonics only, and is solved first, thanks to Eq. (9.75). The first equation gives the even harmonics of the flow rate from the odd harmonics of the pressure. Using Eq. (9.75), we finally deduce the even harmonics of the pressure, as explained hereafter. Here we solve Eq. (9.80) by truncating it to two harmonics, the first and the third. Bringing the series with terms -3, -1, 1, and 3 and equating the terms of frequency ω_1 (which is unknown) and $3\omega_1$, we obtain the equations:

[25] These rules are identical to the rules for even and odd functions. Notwithstanding the two types are not even and odd functions, in contradiction with what is written in [76]. It is possible to show that this could be true in the following case only: when the even harmonics have real coefficients P_n, and the odd harmonics have imaginary coefficients P_n. This can be checked by the reader.

$$\frac{Y_1 - A}{C} P_1 = 3(P_1^2 P_1^* + P_1^{*2} P_3 + 2P_3 P_3^* P_1); \tag{9.81}$$

$$\frac{Y_3 - A}{C} P_3 = P_1^3 + 3(P_3^2 P_3^* + 2P_1 P_1^* P_3). \tag{9.82}$$

Rejecting the solution $P_1 = 0$,[26] using the assumption that P_1 is real, Eq. (9.81) can be rewritten as:

$$\frac{Y_1 - A}{C} = 3P_1^2(1 + P_3/P_1 + 2\,|P_3/P_1|^2). \tag{9.83}$$

- Let us seek a solution to the equations, supposing that we are close to the threshold defined by Eq. (9.77). It is consistent to consider that P_1 is small, and following Eq. (9.82), P_3 is of order 3 in P_1. This solution is called "small oscillation solution." The harmonic n can be shown to be of order n in P_1. This power law for the harmonics near the threshold is very general (see [2]) and it is often called "Worman theorem" in musical acoustics (see [60, 94, 124]).[27]
- Another approximation is consistent with the previous one, but it is valid in a much wider range of pressures. It is called "Variable truncation method": the first harmonic is assumed not to be influenced by the third one, thus Eq. (9.83) is simplified into Eq. (9.77), and both the frequency and the amplitude can be determined. Consequently P_3 is deduced from Eq. (9.82) using the values of P_1 and ω_1. The higher harmonics can be successively found, and the approximation, whose accuracy decreases with the harmonic number, is very satisfactory for a clarinet-like instrument. For instance, for the lossless case, the error is 10 % for the harmonic 5 (0.8 dB) and 21 % the harmonic 11 (1.7 dB) [76]: this is due to the decrease of the spectrum of the lossless solution at high frequencies [see Eq.(9.73)] (the decrease is much more rapid when losses are introduced). For sake of simplicity, the cubic term $P_3^2 P_3^*$ is ignored, and the calculation yields

[26] What is this solution? Eq. (9.82) becomes: $(Y_3 - A)P_3/C = P_3^2 P_3^*$, and is nothing else than Eq. (9.76) written for the frequency $3\omega_1$. Two solutions are deduced: the static regime $P_3 = 0$, and the oscillating (sinusoidal) regime of frequency $3\omega_1$. The threshold for the latter is higher than that for the fundamental regime with frequency ω_1, because as a first approximation the admittances increase as the square root of frequency. As a consequence losses allow discriminating the threshold of the oscillation regimes: in order to reach the twelfth, it is required to blow harder. However, we had to avoid the fundamental regime during the attack, and this is possible thanks to the register hole, which strongly lowers the first resonance and shifts its frequency.

[27] This law also applies to the even harmonics: there is a minor difficulty, because according to the law, the second harmonic should be larger than the third, but this situation occurs for values of the mouth pressure which are extremely close to the oscillation threshold. Thus we consider that this result is not in contradiction with the ignoring of the even harmonics in Eq. (9.80) (see [76]).

$$\frac{P_3}{P_1} = -\frac{1}{3}\frac{A - Y_1}{(A - Y_1) + (Y_3 - Y_1)}. \tag{9.84}$$

- Several conclusions can be drawn:
- Because Eq. (9.77) is assumed to be valid, $Y_1 = Y_{m1}$ is real and the frequency does not depend on Y_3. When the second resonance is a perfect harmonic of the first, Y_3 also is real, but this is not the general case. For the different notes of a clarinet the inharmonicity of the resonances has been studied in detail (see, e.g., [32, 37, 86]). It is not large, because the various causes of inharmonicity are partially mutually compensating. As a reminder the following factors are influential: dispersion due to visco-thermal effects, temperature gradient, closed or open tone holes, non-uniformity of the cross section, etc. The effect of inharmonicity will be examined in Sect. 9.4.5.
- When the loss limit is approached, the admittances Y_1 and Y_3 vanish, and the Helmholtz motion is reached [see Eq. (9.73)]; this is true also when losses are independent of frequency ($Y_1 = Y_3$).
- When the amplitude becomes large (A becomes large compared to Y_1), the amplitude ratio converges to the result for the Helmholtz motion as well, because the admittances Y_1 and Y_3 have the same order of magnitude. As a consequence, the details of either the tube shape or the losses, i.e., the details of the pipe input admittance have a minor influence far from the threshold.
- Near the threshold, the denominator is almost equal to $Y_3 - Y_1$ (the reader can check that this is consistent with the power law, i.e., that P_3 is proportional to P_1^3), and all details have a significant influence. For instance, the visco-thermal dispersion leads to a complex Y_3, thus the phase of P_3/P_1 is not π, as for the Helmholtz motion.[28]
- The effective loss parameter is the ratio of the loss coefficient to the reed parameter ζ, because A is proportional to the latter. If ζ is small (small reed opening, stiff reed), the effect of losses, which increases with frequency, is significant. Therefore there are few higher harmonics, in contrast to the case of large ζ. This parameter has an effect on both the rapidity of the attacks (via the coefficient A), and the spectrum.

[28] When Y_3 is slightly larger than Y_1, the relative amplitude of the third harmonic is approximately:

$$\frac{P_3}{P_1} \simeq -\frac{1}{3}(A - Y_1)Z_3.$$

So it is nearly proportional to Z_3, which is small. For instance it is the case of a one-mode resonator: its spectrum remains close to that of a sinusoid even at high levels [82]. Nevertheless even if the conclusion were correct, the calculation would be inconsistent, because the even harmonics have been assumed to be small compared to the odd ones. Here this is not true, for example, for the second harmonic compared to the first one.

- Another important aspect of the result (9.84) is that it does not depend on the cubic coefficient of the nonlinearity. As a matter of fact it can be rigorously proved from Eq. (9.80) that the shape of the signal, which depends on ratios P_n/P_1 only, as well as the playing frequency, depend on the coefficient A and of admittances Y_n only. This relativizes the importance of the accuracy of the nonlinear model, except obviously for the amplitude, which crucially depends on the coefficient C. This simplicity stems from ignoring the terms of degree two (which are proportional to B) or higher in the polynomial $F(p)$. Yet this approximation is rather good for a clarinet, at least when the reed does not beat.

9.4.4.2 Even Harmonics

Even harmonics remain to be calculated. They are very weak in the mouthpiece, but relatively much stronger in the radiated sound field. After some calculation (details are not given here), the solution of Eq. (9.79) is obtained

$$P_2 = BZ_2(P_1^2 + 2P_1P_3 + \cdots). \tag{9.85}$$

Notice that at the threshold the power law is satisfied. As expected, the amplitude is proportional to the coefficient B of the quadratic term in the expansion (9.55) [76]. The nonlinearity plays an important role, as well as the input impedance near the dips, and therefore as the shape of the mouthpiece is also influential.

9.4.4.3 Application to a Perfectly Cylindrical Tube

In what follows we apply the previous formulas to a perfectly cylindrical tube. The coefficients A and C are written with respect to the excitation parameters γ and ζ [see Eq. (9.55)], and a model of losses is added. The threshold pressure γ_{th} is known, thanks to Eq. (9.69): because α is proportional to the square root of the frequency, which is inversely proportional to the pipe length, the correction factor in comparison to the lossless case $(1/3)$ is proportional to the square root of the length. This implies that if the tube length increases, the pressure threshold increases. We need to blow harder in order to obtain a sound. Another reasoning is the following: for a given mouth pressure γ, a length threshold exists, beyond which no oscillations are possible. Losses need to be diminished, by choosing a wider tube. This is one reason explaining why bass instruments require wider diameter. This issue was discussed in Chap. 5, Sect. 5.5.3.3. Concerning the amplitude of the first harmonic, a similar calculation can be made. Because $Y_{m1} = A_{\text{th}}$, it is found that $Y_{m1} - A = 3\sqrt{3}\zeta(\gamma_{\text{th}} - \gamma)/2$ and:

$$P_1^2 \simeq \frac{2}{3}(\gamma - \gamma_{\text{th}}). \tag{9.86}$$

For the third harmonic, by writing $Y_3 = Y_{m1}\sqrt{3}$, the following result is obtained.

$$\frac{P_3}{P_1} \simeq -\frac{1}{3}\frac{\gamma - \gamma_{\text{th}}}{\gamma - \gamma_{\text{th}} + 0.28\alpha\ell/\zeta}. \tag{9.87}$$

Finally, for the second harmonic, the impedance $Z_2 = \alpha(2\omega_1)\ell$ is very small, because it is at a minimum, and we get

$$\frac{P_2}{P_1} = -Z_2\zeta\frac{3}{2\sqrt{2}}\sqrt{\gamma - \gamma_{\text{th}}}\left(1 + 2\frac{P_3}{P_1} + \cdots\right). \tag{9.88}$$

Here the losses involve the product of α and ζ, and not their ratio as for the harmonic 3. Figure 9.16 shows experimental results in two forms, and exhibits the two ranges of amplitude for the odd harmonics. In the first range, their amplitude compared to that of the first harmonic grows according to the power law, while in the second range the amplitude is almost constant. For the harmonic 3, Eq. (9.87) is qualitatively verified. Many similar results can be found in [10]. Notice that at high level, the reed beats and the previous calculations are no longer valid.

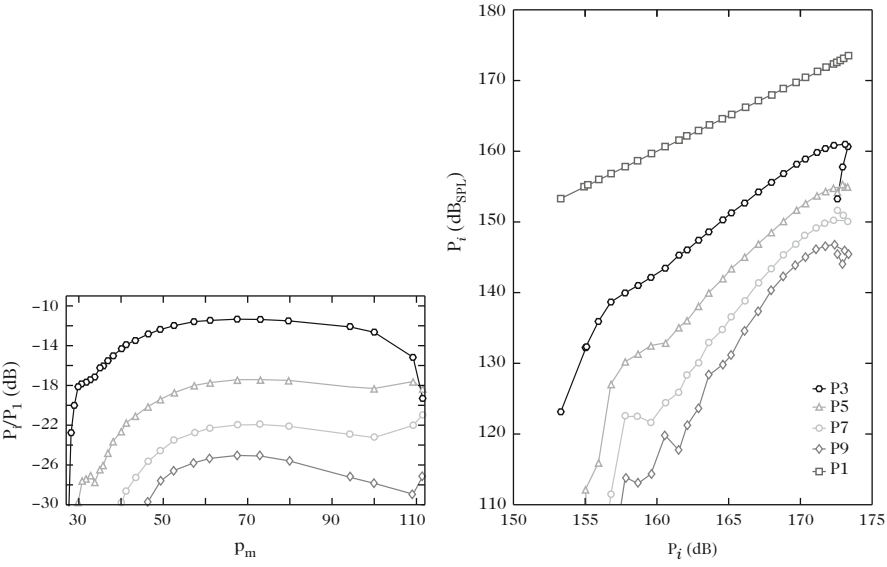

Fig. 9.16 Experimental results for a cylinder (four first odd harmonics) [89]. The *left plot* shows the amplitude ratios P_{2n+1}/P_1 as a function of the excitation pressure. The stabilization of the amplitude occurs at an amplitude level which is lower than that for a square signal, which would be $1/(2n+1)$ (i.e., in dB -9.5, -14, -17, -19, respectively). The scale for the mouth pressure p_m is in mbar. The *right plot* is an equivalent representation of the same results, which uses as an abscissa the amplitude (in dB) of the first harmonic. This representation is due to Benade [10], and provides a clear representation of the power law near the threshold

9.4.4.4 External Spectrum: Some Simple Consequences for a Cylinder at Low Frequencies

Lossless Model

At low frequencies the far-field radiated pressure p_{ext} is obtained by using a simple formula which will be detailed in the fourth part. We examine the case of a cylindrical open pipe without toneholes, which radiates in an omnidirectional way, i.e., as a monopole. The pressure p_{ext} is proportional to the time derivative of the flow rate at the output, with a delay of D/c, if D is the distance of the considered point to the tube output. According to the lossless model we used (square signals), the output pressure is zero, therefore $p_\ell^+ = -p_\ell^-$, and the output flow rate is $u_\ell = 2p_\ell^+$. Knowing how to calculate the outgoing wave at the input, we simply translate it by ℓ/c to obtain it at the output. Because the outgoing wave at the input is the half-sum of the pressure and the flow rate, the output flow rate is

$$u_\ell(t) = p(t - \ell/c) + u(t - \ell/c),$$

and, because in the lossless model the input flow rate is a constant, the external pressure is deduced as follows:

$$p_{\text{ext}} \propto \frac{du_\ell}{dt} = \frac{dp(t - \ell/c)}{dt}.$$

The interpretation of this result is easy, because for a plane wave the density of total acoustic energy in a slice of air does not depend on x: because there is no potential energy at the output and no kinetic (acoustic) energy at the input, the output flow rate is proportional to the pipe inlet pressure. Instead of a square signal, the far-field radiated pressure signal is a series of Dirac peaks which are alternately positive and negative. This is shown in Fig. 9.17. Concerning its spectrum, the ratio of the complex amplitude of the harmonics to that of the first one is $P_{\text{ext},2\nu+1}/P_{\text{ext},1} = 1$, instead of $(-1)^\nu/(2\,\nu + 1)$ [see Eq. (9.73)] for the internal spectrum.[29]

Model with Losses

When losses are taken into account (but not the dispersion), the transfer function is $U_\ell(\omega)/P(\omega) = 1/j\sin(k - j\alpha)\ell$ [see, e.g., the matrix given by Eq. (4.28)]. The external pressure is proportional to $\omega P(\omega)/\sin(k - j\alpha)\ell$, a delay function apart.

[29] This result is obtained for p_{ext} which is proportional to du_ℓ/dt. However, because of the delay due to the distance from the tube, the relative phase varies, and therefore the main conclusion concerns the real amplitude (i.e., the modulus of the complex amplitude): the ratio of the real amplitudes is 1 instead of $1/(2\nu + 1)$. Notice that the Fourier Transform of $\delta(t - \ell/c)$ is $\exp(-j\omega\ell/c)$, thus for $\omega = (2\nu + 1)\omega_1$, it is $(-1)^\nu$.

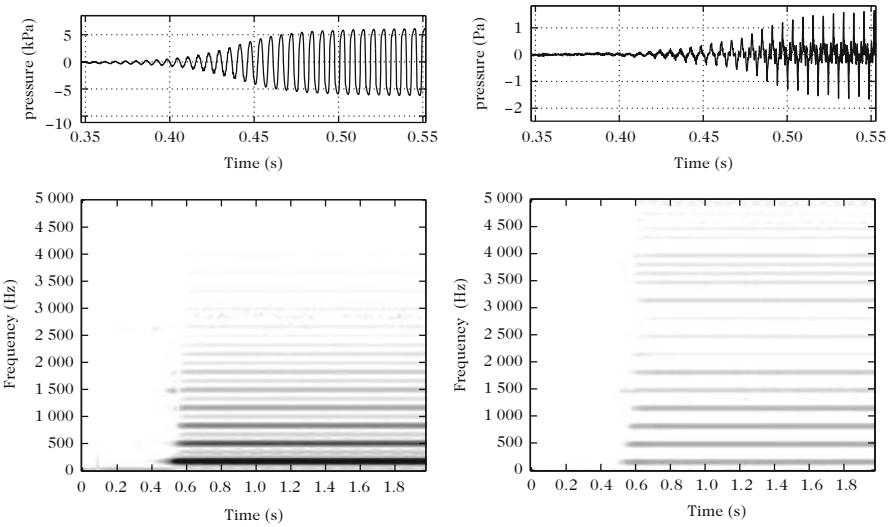

Fig. 9.17 Sound of a cylindrical tube with a clarinet mouthpiece: the internal pressure (on the *left*) is a rounded square signal (see also Fig. 9.12), the radiated pressure (on the *right*) is roughly the derivative of the previous one, because the monopole radiation at the end of the tube implies a derivative of the output flow rate, and because the latter signal is a square signal (in the lossless approximation). The time-frequency spectrograms (*bottom figures*) show that the first harmonic appears first, and confirm that the external sound is much richer in harmonics than the internal sound. The weakness of the even harmonics is also clear. Notice that the duration of the spectrogram is much longer than that of the signal

For odd harmonics $H_{2\nu+1}$, we write $\sin k\ell = (-1)^\nu$. Thus by neglecting the terms of order 2 in $\alpha\ell$, the complex amplitude with respect to that of the first harmonic is found to be equal to unity. Finally the expression (9.87) has to be multiplied by 3 and the modulus gives the result for the external pressure. For even harmonics, the situation is slightly more complicated (remind that their amplitudes are zero when losses are ignored). Limiting the calculation to the second harmonic:

$$\left|\frac{P_{\text{ext},2}}{P_{\text{ext},1}}\right| = \frac{3}{\sqrt{2}}\zeta\sqrt{\gamma-\gamma_{\text{th}}}\left[1+2\frac{P_3}{P_1}+\cdots\right]. \tag{9.89}$$

Compared to the internal spectrum, the value given by Eq. (9.88) is divided by $Z_2/2$. Curiously the harmonics 2 seems not to vanish with vanishing losses! In fact the factor in bracket is an infinite series depending on the odd harmonics of the internal spectrum, and we need to consider more and more terms when going far from the threshold... or when losses tend to zero. The Helmholtz motion in square signal does not produce even harmonics, but inversely if a signal is poor in harmonics, the even harmonics are relatively strong, as shown in Fig. 9.18.

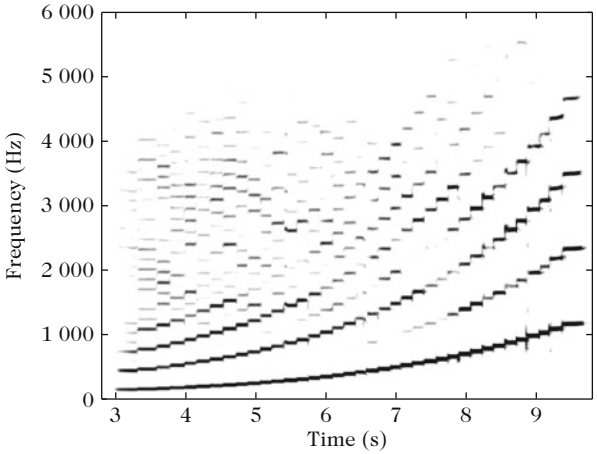

Fig. 9.18 Spectrogram of a clarinet chromatic scale (external pressure). The quasi absence of even harmonics is observed for lower notes. For higher notes their appearance is linked to the fact that the signal becomes less rich in harmonics, therefore differs from a square signal [see Eq. (9.89)]. One observes that frequencies below 1800 Hz are globally stronger than above this frequency. This corresponds to what Benade [10] called the cutoff frequency, due to the tonehole lattice (see Chap. 7)

9.4.5 *Variation of the Playing Frequency with the Excitation Level*

With the lossless model, the frequency is independent of the excitation level. In practice, it slightly varies. There are several causes, such as the reed dynamic, the flow rate due to the reed displacement, the effect of the vocal tract. This allows the player adapting the tuning with respect to what he hears, in a more or less efficient way. In this section a single cause is treated, the inharmonicity of the resonance frequencies. We limit the study to the steady-state regime. For this purpose we use the relationship obtained by Boutillon [18], which is related to the reactive power. It assumes that a nonlinear, quasi-static relationship exists between the input pressure and flow rate. Thus the reed is assumed to be without dynamic, like a massless spring, according to the model used since Sect. 9.3. In the steady-state regime, with a period T, it can be written as:

$$\int_t^{t+T} u dp = \int_t^{t+T} F(p) \frac{dp}{dt} dt = \left[F^{(-1)}(p) \right]_{p(t)}^{p(t+T)} = 0, \tag{9.90}$$

where $F^{(-1)}(p)$ is the integral of $F(p)$. If ω_p is the playing frequency, by using the expansion (9.72) and calculating the average of the product of two complex quantities (see Sect. 1.3 of Chap. 1), the following result is found:

$$\int u dp = 4\pi \sum_{n>0} n \, |P_n|^2 \, \Im m(Y_n). \tag{9.91}$$

This quantity is related to the reactive power [see Eq. (1.129)], i.e., to the derivative of the fluctuating power with respect to frequency. Therefore:

$$\Im m(Y_1) + 3\left|\frac{P_3}{P_1}\right|^2 \Im m(Y_3) + 5\left|\frac{P_5}{P_1}\right|^2 \Im m(Y_5) + \cdots = 0. \tag{9.92}$$

The advantage of this equation[30] is to provide a relation between frequency variation and the spectrum.

Denoting ω_1 the frequency of the first impedance peak, the other peaks are assumed to be at frequency $\omega_n = n\omega_1(1+\eta_n)$, where η_n measures the inharmonicity. The playing frequency is sought in the form: $\omega_p = \omega_1(1+\varepsilon)$. The input admittance is given by Eq. (9.66). We assume that for a frequency ω_n close to a resonance a single peak intervenes, thus for ω close to ω_n [see Eq. (2.39)]:

$$\Im m(Y) = 2\frac{\omega - \omega_n}{F_n}, \text{ with } F_n = \omega_n Z_{Mn}/Q_n. \tag{9.93}$$

For the frequencies ω_p and $n\omega_p$, at the first order in ε and η_n, we obtain

$$\Im m(Y_1) = 2\varepsilon\omega_1/F_1 \; ; \; \Im m(Y_n) = 2n\omega_1(\varepsilon - \eta_n)/F_n. \tag{9.94}$$

For a perfect cylinder, the modal coefficients $F_n = 2c/\ell$ are independent of n. If the cylinder is not perfect, the coefficients are assumed to remain independent of n at the first order of the perturbation. Using Eq. (9.92), we obtain

$$\varepsilon = \frac{\sigma}{1+\sigma'} \text{ where } \sigma = \sum_{n\geq 3} n^2\eta_n \left|\frac{P_n}{P_1}\right|^2 \text{ and } \sigma' = \sum_{n\geq 3} n^2 \left|\frac{P_n}{P_1}\right|^2. \tag{9.95}$$

Near the threshold, P_n/P_1 is very small, and ε vanishes. On the other hand, when we move away from the threshold, the influence of inharmonicity becomes significant. Let us consider the harmonics 1 and 3 only. In the extreme case where $|P_3/P_1| = 1/3$, the result would be the following:

$$\varepsilon = \eta/2. \tag{9.96}$$

This result provides an order of magnitude of the effect of inharmonicity, but obviously it is an approximation, because the harmonics of order higher than 3 are ignored. This is correct near the threshold only. Moreover the ratio $1/3$ was not observed for a cylindrical pipe. For $|P_3/P_1| = 0.2$, (this value seems to be encountered in practice), the result is $\varepsilon = 0.26\eta_3$. As a conclusion, if the second

[30] This equation is not an extra equation in addition to the equations harmonic balancing. The reader can check that, when limited to harmonics 1 and 3, it directly comes from Eqs. (9.81) and (9.82).

resonance frequency is 20 cents[31] too high (resp. too low) with respect to the first one, the frequency increases (resp. decreases) by around 10 cents during a crescendo. This order of magnitude is roughly confirmed by experiment, especially for a perfect cylinder, where inharmonicity is due to visco-thermal dispersion: the playing frequency increases with the excitation level. However, very close to the threshold the reed damping plays a predominant role and the frequency starts by decreasing, then increases [75, 89].

- Inharmonicity influences the playing frequency and more generally the self-sustained oscillation [87]. Benade [10] cited Bouasse [17, p. 91], who correctly felt the nonlinear character of the oscillation: *"the sustaining of the wave is made easier by the coincidence of the harmonic q of the pressure system due to the puffs with the partial $N = qn$ of the tube. Correlatively the puffs become more intense and regular: the reed is stabilized for the frequency n."* Harmonicity ensures the stability of the frequency when the level is changed, and if the peaks are of similar height, a too strong inharmonicity can lead to quasi periodic regimes (see, e.g., [56]). This phenomenon is a cause of the "wolf note" for the cellos (see Chap. 11). For the instrumentalist the quality of the different notes appear to be unequal. It is furthermore probable that harmonicity is an important element of the ease of playing.

In particular a periodic sound can be produced with a very low input impedance at the playing frequency, when the harmonics correspond to impedance peaks. Some specific cases are particularly interesting: the "pedal" sounds of brass instruments (their first harmonic is shifted with respect to the other harmonics, see Chap. 7). It is possible to produce a sound the frequency of which is the half of that of the second peak, because the resonance frequencies 3, 4, 5, etc., are harmonics of this frequency. More generally periodic "multiphonic" sounds can be produced: their frequency is generally very low, because it is the highest common factor when it exists [25]. For the point of view of perception, some sounds can have an almost vanishing at the fundamental frequency and many harmonics, and the perceived pitch corresponds to the inverse of the period. Furthermore various multiphonic regimes can be obtained on wind instruments, such as quasi-periodic, or chaotic regimes (as already mentioned) [38, 39, 107].

9.4.6 Beating Reed and Sound Extinction

9.4.6.1 Lossless Model (Steady-State Regime)

Up to now we considered that the reed does not beat, thus we supposed that the nonlinear function (9.30) is limited to low pressures. We used Eq. (9.31), or its simplified version (9.55). If the reed is allowed to beat, Eq. (9.32) needs to be used as

[31] The cent is the hundredth of a semi-tone. The latter corresponds to a frequency ratio of $2^{1/12} = 1.05946$, therefore the cent is a difference of 0.06 % in frequency.

well. This beating-reed model (see Sect. 9.2.5.2) is a rough approximation because in practice the closure is not sudden and the non-beating range becomes larger. Nevertheless it gives interesting results when they are compared to experiments. If it is assumed that a clarinettist plays as often with a non-beating reed as with a beating reed (see for a discussion [12]), the reader may be surprised by the treatment imbalance for these two types of functioning. A lot of work remains to do in order to understand the beating reed oscillation. It is actually the main operating mode of conical reed instruments (this will be seen hereafter). For a beating reed, all the analysis of small oscillations becomes useless.

We limit the analysis to the two-state approach for the steady-state regime, considering first a lossless resonator, then discussing a more general model with frequency-independent losses. We consider first the static regime: it occurs for $p = 0$ because the input impedance at zero frequency is assumed to be zero, and this implies $\gamma > 1$ for the dimensionless mouth pressure. For a mouth pressure higher than the closure pressure, the reed closes the mouthpiece: it is our definition of the closure pressure p_M. The stability of this regime is not discussed here, because the discussion should be rather long and the stability is intuitively understood. Now we search for the oscillation regime in the same way as in Sect. 9.3.3.4: because the mean pressure is zero, we search again for two opposite values of the two states: $\pm p_\infty$, with constant flow rate. If the reed beats for $p = -p_\infty$, the flow rate vanishes and, following Eq. (9.32), this implies

$$p_\infty \geq 1 - \gamma. \tag{9.97}$$

Equation (9.60) shows that the flow rate is constant, thus it also vanishes while the reed is open. If the reed was beating for both $p = p_\infty$ and $p = -p_\infty$, the regime would be the static regime). Thus, after Eq. (9.31):

$$p_\infty = \gamma. \tag{9.98}$$

So the reed does not close for the positive mouthpiece pressure and beats for the negative one, because of the large pressure difference $p_m - p$ between the mouth and the mouthpiece. The condition for this regime is given by Eq. (9.97):

$$\gamma > 1/2.$$

This solution[32] is illustrated in Fig. 9.19. This extremely simplified functioning can be described as follows: during one half-period, the mouthpiece pressure is opposite to the mouth pressure and the reed is closed, while during the other half-

[32]This solution can be easily shown to be stable whatever the value of γ is [91]. So, if the pressure increases with a non-beating reed, yielding several frequency divisions (see Sect. 9.3.3.6), then frequency multiplications occur in order to retrieve the normal frequency when the reed starts to beat (see [73]).

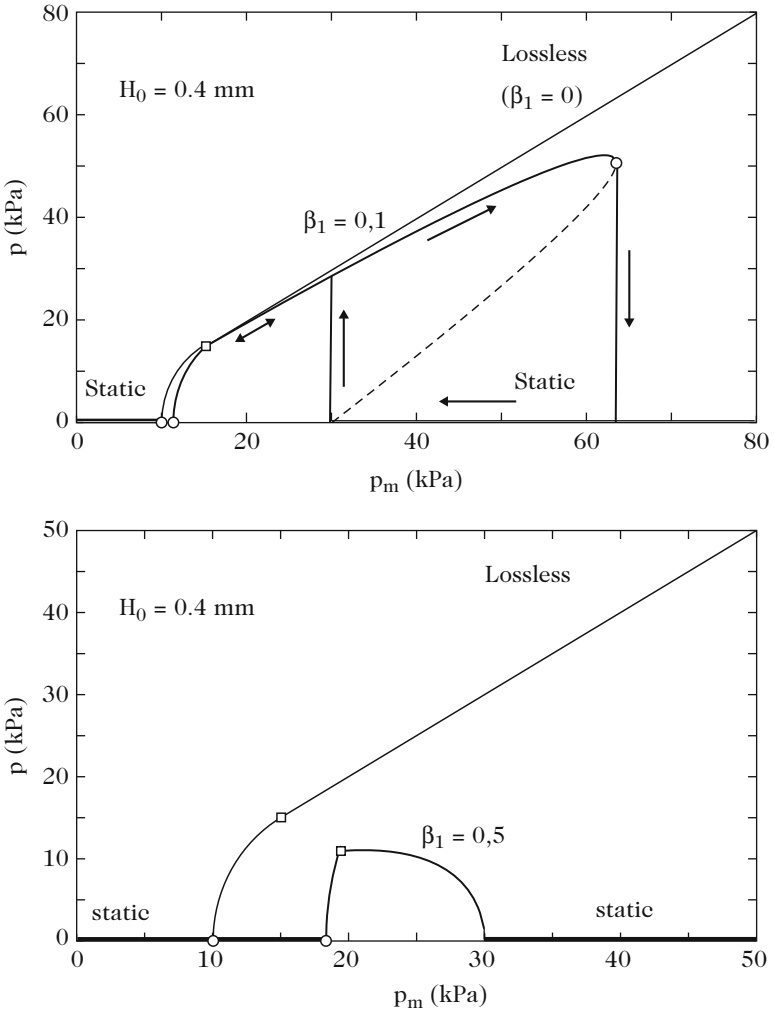

Fig. 9.19 Bifurcation schemes for the Raman model. *Top*: $\beta_1 = 0.1$, inverse bifurcation at the extinction; *bottom*: $\beta_1 = 0.5$ (very small reed opening), direct bifurcation. The reader can compare with Fig. 9.15 (experimental result)

period, it is equal to the mouth pressure and the flow rate vanishes (no pressure difference). This behavior can produce large sound levels in the mouthpiece, as explained in the introduction (Sect. 9.2.1).

9.4.6.2 "Raman Model" with Losses

A major drawback of the lossless model lies in the infinite increase of the acoustic pressure when the blowing pressure increases [see Eq. (9.98)]. A simple model can remedy this difficulty [35]: considering frequency-independent losses keeps square signals but allows finding a good agreement between experiment and model for the bifurcation schemes. This model is called "Raman model" by analogy with the model of bowed strings which was studied by the great Indian physicist at the beginning of the twentieth century. Writing the solution of the wave equation with damping in the form:

$$P = P^+ e^{-\alpha x} e^{-jk\ell} + P^- e^{\alpha x} e^{jk\ell},$$

and assuming a zero pressure at the output, it is found that the reflection coefficient at the input is $R = P^-/P^+ = -e^{-2\alpha x} e^{-2jk\ell}$. The input impedance reduced by the characteristic impedance Z_c is given by:

$$Z = j \tan(k - j\alpha)\ell. \tag{9.99}$$

Resonance frequencies are unchanged by damping and all input impedance maxima are equal to $Z_{\max} = 1/\tanh \alpha\ell$, while minima are $Z_{\min} = \tanh \alpha\ell$. The modal expansion (9.66) remains valid. It is possible to generalize the previous study of square signals, including the graphical method for building the solution. Exact calculations, which generalize the approach of Sect. 9.3.3, are tedious [35]. A significant simplification is obtained when the input impedance at zero frequency is assumed to be zero (instead of $Z_{\min}$). Then the static regime remains $p = 0$. For the instability threshold, it is not useful to make the calculation because the formula $A = Y_1$ given by the one-mode approximation remains valid, as well as Eq. (9.69). This is actually valid whatever the frequency dependence of the damping α is. When the blowing pressure increases the threshold of period doubling can be found; however, for a significant damping this threshold is larger than that of beating reed for the oscillation regime. As a consequence the rather large losses in real cylindrical instruments explains why it is very difficult to produce a period doubling.

- Now we consider the behavior of the Raman model when the reed beats. In steady-state regime, because $Z(0) = 0$, the two states (i.e., open reed and closed reed) are opposite. We write them again: $\pm p_\infty$ and expand the square signal into (odd) harmonics. For each of them the corresponding flow rate is deduced from the admittance $1/Z_{\max}$; then the oscillating part is $\pm p_\infty/Z_{\max}$. A constant (dc) flow rate denoted u_0 has to be added. Using Eq. (9.30), if $\Delta p = \gamma - p_\infty$, we find the steady-state regime:

$$\begin{aligned} &u_0 + p_\infty/Z_{\max} = \zeta(1 - \Delta p)\sqrt{\Delta p} \ \text{ with } 0 < \Delta p < 1; \\ &u_0 - p_\infty/Z_{\max} = 0 \text{ with } 1 - \gamma - p_\infty < 0 \ \text{ or } \ \Delta p \le 2\gamma - 1. \end{aligned} \tag{9.100}$$

Hence:

$$2\beta_1(\gamma - \Delta p) = (1 - \Delta p)\sqrt{\Delta p}, \tag{9.101}$$

$$\text{with} \quad \beta_1 = \tanh \alpha\ell/\zeta \simeq \alpha\ell/\zeta. \tag{9.102}$$

We confirm that the loss parameter intervenes via the ratio α/ζ. The threshold of beating reed is given by $\Delta p = 2\gamma - 1$, therefore $\gamma = (1 + \beta_1^2)/2$. It is slightly modified by the losses if β_1 is small. Moreover by solving[33] Eq. (9.101), it can be shown that: *if γ is lower than* 1, there is always a unique solution, and it can be proved to be stable. But if *if γ is higher than* 1 when the mouth pressure is large, there are two possible cases:

- either $\beta_1 < \dfrac{1}{2}$: there are two solutions, one is stable, and the other one is unstable if γ is lower than the extinction threshold given by $\gamma_{\text{extinc}} \simeq \frac{1}{3}\left[1 + \frac{1}{\beta_1\sqrt{3}}\right]$, while there is no solution if $\gamma > \gamma_{\text{extinc}}$ (as expected this threshold tends to infinity when losses tend to 0).
- or $\beta_1 > \dfrac{1}{2}$: there is no solution.

Figure 9.19 shows the two cases: the first one corresponds to an inverse bifurcation at extinction, with hysteresis. For $\gamma > 1$, when forcing the breath, the pressure increases following the (stable) upper branch, then diminishes. Then the oscillating solution disappears abruptly and the static solution is retrieved. When the breath is diminished anew, the static solution is kept up to $\gamma = 1$, where there is a jump to the upper oscillating branch. The maximum pressure, or saturation pressure is obtained for $\gamma_{\text{sat}} \simeq \frac{1}{3}\left[1 + \frac{1}{\beta_1 3\sqrt{3}}\right]$. It is undoubtedly the most usual case.

The second case shows a direct bifurcation at extinction, which is a remarkable result: it is possible to play pianissimo at extinction also, by pinching strongly the reed! This technique is used by some instrumentalists, who reduce the reed opening and therefore the parameter ζ. Comparisons with experiment give excellent results [30], especially when nonlinear losses are taken into account at the various openings (see Chap. 8, Sect. 8.4.5), by using c_d as a fitting parameter. As a conclusion, the Raman model gives very interesting results, although the pressure signals are square signals.

9.4.7 *Miscellaneous Considerations About Clarinet-Like Instruments*

In the present chapter we did not treat the reality of the resonator geometry, with toneholes, changes in cross section, etc. As noted earlier, there is an average

[33] Equation (9.101) can be graphically solved, by seeking the intersection of the straight line corresponding to the left term with the function defined on the right-hand side and depicted in Fig. 9.9.

compensation of the action of the different elements resulting in a reduction of inharmonicity [32, 37]. When toneholes are open, one could think that the existence of cutoff frequency hampers the oscillations because the higher order peaks become low. The reduction of the compass is effective because it is difficult for the fundamental frequencies to be higher than the cutoff (from experience, players know that it is easy to obtain higher order regimes for the note with all holes closed, while it is more difficult for the other notes). But the dominant feature is that at low frequencies the effective length of the tube is shorter when opening the toneholes, thus the threshold diminishes and the oscillations become easier.

Another possibility for easing the oscillations is the use of the vocal tract: the two resonators are in series. If the player manages to have resonances of the vocal tract at medium frequencies, he can act on the tuning and tone color. Moreover he can reinforce the even harmonics of the sound, which do no longer correspond to impedance minima and can have an effect on the playing frequency (via the inharmonicity). This topic was recently investigated, and some aspects remain open. So a difficult question can be asked: what physical quantity can be regarded as a source, e.g., as imposed by the player? Up to now we assumed that it is the mouth pressure, assumed to be uniform. On this topic, we refer to the following references [26, 27, 52, 53, 63, 65, 97, 103, 120]. Another important subject is the role of the reed dynamics, that we have completely ignored up to now. We will include it in Sect. 9.5.

Finally we mention the problem of the measurement of the input impedance, considering the complicated geometry of the mouthpiece. The matching between a turbulent jet and an acoustic field is extremely complicated (see, e.g., [100]). Even when exciting the mouthpiece by an acoustic source at its output, the acoustic field is not planar, and cannot be characterized by a unique quantity such as the input impedance. Moreover the reed excite the mouthpiece on its side, therefore produces evanescent modes. The general solution chosen by several authors is to replace the mouthpiece by a cylindrical tube having the same volume, with a cross section are equal to that of the mouthpiece output. The first advantage is to be able to compare with plane-wave models of the input impedance. The second advantage is that near the first impedance maximum, the effect of the mouthpiece depends on its volume only, thus the results of the theoretical models of the nonlinear coupled system can be rather reliable. However, this is not true for the impedance minima, and more generally at higher frequencies, when the mouthpiece cannot be regarded as a lumped element. Notice that this difficulty can be anyway of minor importance when compared to the effect of the vocal tract. Remember that a one-dimensional model is a great simplification.

9.4.8 Conical Reed Instruments

The resonator of conical reed instruments such as the saxophone has been studied in Chap. 7. They are truncated cones, and have a mouthpiece similar to that of a

clarinet, but their resonators are very different from an acoustical point of view. Oboes and bassoons have a double reed with a nonlinear characteristic which slightly differs from that of single reeds (see Sect. 9.2.5.2), but what follows deals with both single and double reed instruments. Indeed it appears that the shape of the resonator plays a predominant role. As an illustration it is possible to buy a mouthpiece of sopranino saxophone type adapted to the bassoon, and it is noticeable that the sounds are rather similar to those normally obtained with a double reed [61]. For the lowest notes of a conical pipe, the first impedance peak is lower than the second. Furthermore the second peak corresponds more or less to the octave instead to the twelfth.

The resonance frequencies are approximately a complete series of harmonics (see Chap. 7). The Helmholtz motion (HM) is also for conical instruments an interesting approximation of the pressure signal (except near the oscillation threshold). We will see that the signal is a "rectangle signal," with a duration ratio of the two states equal to the length ratio of the missing cone (due to the truncation) and the truncated cone (see Fig. 9.20).

In comparison with cylindrical instruments, one supplementary parameter is needed, e.g., the apex angle, which makes the problem far more difficult. The approach without losses leading to two-state signals implies one more approximation: the length of the missing cone needs to be much smaller than the wavelength. This hypothesis is paradoxical for a rectangle signal which is rich in high harmonics!

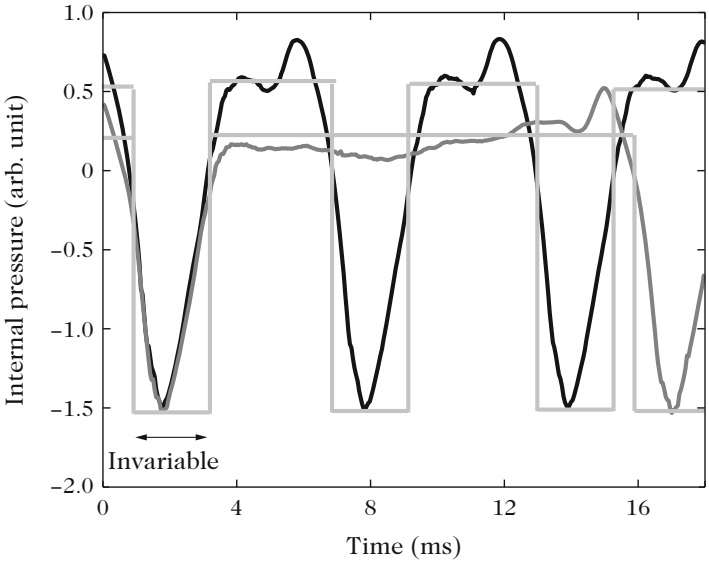

Fig. 9.20 Periodic signal of barytone saxophone, and the approximation by a rectangle signal. The signal is the internal pressure for two notes, which are the lowest and the highest of the first register. The state of negative pressure, which corresponds to a beating-reed, is common to the two notes

Moreover the "small oscillation" approach as well as the variable truncation method is not of much interest because the bifurcation at low mouth pressure is inverse. This remarks explain why many problems remain open.

9.4.8.1 Small Oscillation Solution (with Losses)

At the instability threshold of the static solution, it has been seen that oscillations can start (linearly) and are quasi sinusoidal. If the impedance of the second peak is higher than that of the first, the first oscillation threshold is that of the octave regime, not that of the fundamental one. This explains why it is difficult for beginners to play the fundamental regimes. Going further, we consider the nonlinearities in steady-state regime, using the harmonic balance for small oscillations in order to find the existence threshold of the oscillating solution [we refer to the explanation accompanying Eq. (9.83)]. Equations (9.74) and (9.75) have to be solved without hypothesis with respect to even and odd harmonics. The "small oscillation" solution is written as[34] [60]:

$$P_1^2 = \frac{Y_1 - A}{3C + \frac{2B^2}{Y_2 - A}} = \frac{(Y_1 - A)(Y_2 - A)}{3C(Y_2 - A) + 2B^2} \tag{9.103}$$

$$P_2 = \frac{BP_1^2}{Y_2 - A}. \tag{9.104}$$

For the clarinet, Y_2 is very large, $Y_2 > Y_1$, and the result (9.77) is obtained, as well as Eq. (9.85) for small oscillations.

We start the investigation with a case simpler than that of the lowest notes: the case of higher notes for which *the second peak is smaller than the first*, but has the same order of magnitude. Now Y_2 is larger than Y_1, but remains small: the second term of the denominator of Eq. (9.103) is the larger term (the term in C can be ignored). In order to find a solution, it is necessary for P_1^2 to be positive. Thus A needs to be either smaller than Y_1 or larger than Y_2 (here we assume that the two resonance frequencies are harmonic, therefore the two admittances are real for the playing frequency). Starting away from the oscillation threshold $A = Y_1$, the solution P_1^2 only exists if $A < Y_1$. The case is similar to the case of a clarinet for which C would be positive, implying an inverse bifurcation (see Fig. 9.14). Close to the threshold, the oscillating solution is unstable. The existence of a subcritical threshold can be shown. Above this threshold the oscillation becomes stable (an example is shown in Fig. 9.21). When the blowing pressure (like A) increases from 0, there is a jump at the threshold $A = Y_1$ to a finite value of the amplitude, while when the blowing pressure decreases, the player can reach the subcritical threshold, where he jumps back to the static regime.

[34] The series is truncated to harmonics 1 and 2 (and -1 and -2), and the harmonic 0 (dc component) is negligible because the input impedance at zero frequency is very small. For small amplitudes the influence of the higher harmonics is of higher order in P_1.

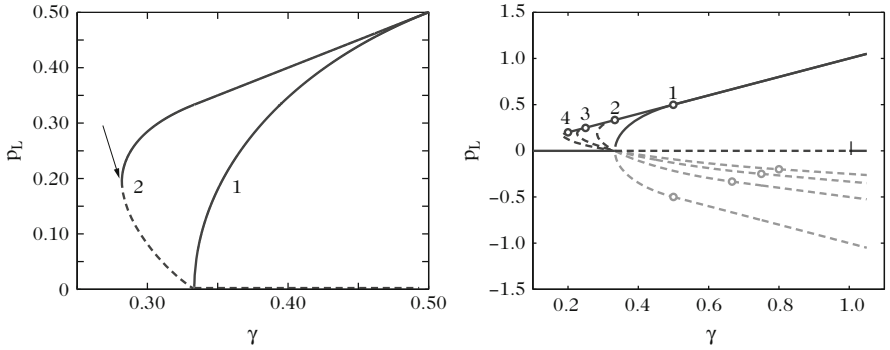

Fig. 9.21 Helmholtz motion for a cylindrical saxophone. The *right plot* shows for different values of β the values of the pressure during the long state p_L with respect to the mouth pressure γ. The increasing part corresponds to p_L^+, and the *decreasing part* corresponds to p_L^-. The stable HM is in *solid black line*, the unstable HM is in *dotted black line*, and the inverse HM is in *gray*. The integer N is related to β by $\beta = 1/(1+N)$. The *asterisk* indicates the beating thresholds. The *left plot* depicts a zoomed view for $N = 1$ and 2: the bifurcation is direct for $N = 1$ and inverse for $N = 2$. The *arrow* indicates the subcritical threshold at $\gamma = 0.28$

Therefore there is a hysteresis. It is not possible to play pianissimo, and it is easier to play with a low amplitude, when playing decrescendo than playing crescendo (if it is assumed that the player modifies the mouth pressure only). Figure 9.21 (left) shows an example of inverse bifurcation for a cylindrical saxophone, treated in the next sections.

In the case where the admittance Y_2 is smaller than the admittance Y_1, which is the general case for lower notes, the fundamental regime can exist with small oscillations only if $A < Y_2$, and it is still unstable (but the octave regime can exist and be stable), or if $A > Y_1$: however, for the latter case it can be shown that the regime is the inverse HM, discussed in the next section. The important feature is that the octave regime is favored. The previous discussion analyzed the phenomena occurring when there is a maximum input impedance at the double frequency, instead of a minimum as for the case of a clarinet.

9.4.8.2 "Cylindrical Saxophone", Statement of the Problem

Coming back to the lossless approximation, it is possible to go slightly further. On the one hand if losses are ignored, the two thresholds $A = Y_1$ or Y_2 are equal [see Eq. (9.103)], and information is lost; on the other hand, if a supplementary approximation is added, results about the amplitude can be found. Figure 9.20 shows that the internal sound of a saxophone can be loosely approximated by a rectangle signal, and this gives the idea to seek an analogy with the bowed string, which is studied in Chap. 11. For that purpose, it was seen in Chap. 7 that considering the natural frequencies, an approximation of the diverging cone is a cylinder of length

$\ell + x_1$ open at the two ends, called "cylindrical saxophone". x_1 is the distance of the input of the truncated cone to its apex, and it is assumed to be small compared to the wavelength [see Eq. (7.88), and Fig. 7.10]. So, when losses are ignored, the input admittance is written as:

$$Y = \frac{S_1}{\rho c}\left[\frac{1}{jkx_1} + \frac{1}{j\tan k\ell}\right] \quad \text{or} \tag{9.105}$$

$$Y \simeq \frac{S_1}{\rho c}\left[\frac{1}{j\tan kx_1} + \frac{1}{j\tan k\ell}\right]. \tag{9.106}$$

Formula (9.106) is analogous to the mechanical impedance of a string at the location of the bow (see the table of Sect. 1.6 of Chap. 1). The two ends of the string are in series, with the same velocity at the bow position. For the cylindrical saxophone, the two ends, of length ℓ and x_1, are in parallel, with the same pressure at their input, where the reed is located. As a first approximation, this equivalence between a conical tube and a cylindrical one remains valid for any length ℓ, and for any effective length when holes are open. In what follows, we make an analysis similar to the one we have made for the clarinet in Sect. 9.3.3. As far for the clarinet, we will not obtain much information about the spectrum, because we ignore the losses, as for the clarinet, and in addition we assume the length x_1 to be small compared to the wavelength (notice that this is wrong for higher harmonics). But many phenomena can be explained thanks to this simplified model,[35] that was proposed for the first time by Gokhshtein [59].[36]

Thus we seek a periodic solution of period $T = 2L/c$, where $L = \ell + x_1$. The pressure and the flow rate have the frequencies $f_n = nc/2L$ as *only possible components*, and they satisfy $\sin kL = 0$ (this can include the dc component). We will now investigate a particular solution, the Helmholtz motion. Beforehand we propose an analysis of the different possible solutions, for the interested reader.

[35] With this model, a clarinet is not analogous to a bowed string, because this should imply an infinite value for x_1. However, if a cylinder is excited at its middle, the two ends of the tubes play the same role, thus a clarinet is equivalent to a cylinder of double length, excited at its middle and having a half cross section. This can be checked by using Eq. (9.106) with $\ell = x_1$.

[36] Dalmont [31] showed that a step cone built with N cylindrical pipe segments of equal length x_1 and cross section $s_n = n(n+1)/2$ (where the integer n is the rank order of the cylindrical segment and s_n its cross-section area) has the same admittance [Eq. (9.106)] as a cylindrical saxophone of cross-section area $S_1 = s_1/2$ when $\ell = Nx_1$. Their realization is easier than that of a cylindrical saxophone, but is limited to the condition of integer ℓ/x_1. It is the reason why these instruments allow studying the Helmholtz motion in a precise way [90, 91]. It is noticeable that bamboo "saxophones" exist with a geometry approaching that of such step cones.

Different Possible Solutions

In order to study the different possible solutions, we rewrite Eq. (9.106) in the form:

$$U(\omega) \sin kx_1 \sin k\ell = P(\omega) \sin kL.$$

The inverse Fourier Transform of this expression is Eq. (4.65), if the analogy between stringed instruments and reed instruments is used. For frequencies f_n, equations $\sin kL = 0$ and $\sin k\ell = -(-1)^n \sin kx_1$ are valid. It is deduced that the corresponding components of the flow rate vanish, except if $\sin kx_1 = 0$, i.e., for $f_m = mc/2x_1$, where m is another integer. Now f_m can belong to frequencies f_n, thus $x_1/L = m/n$ (all integer values of m are not possible). This implies

- either the ratio $\beta = x_1/L$ is a rational number, and the flow rate can have non-zero components for frequencies $mc/2x_1$ such as $m = n\beta$. For instance if $\beta = 2/5$, the pairs $(m, n) = (2, 5),\ (4, 10)$, etc. are possible.
- or $m = n = 0$, and a priori the dc component of the flow rate does not vanish whether β is rational or not. If β is irrational, the dc component of the flow rate is the only non-zero component.

For the pressure, the component f_n vanishes if $\sin kx_1 = 0$: this can happen only if β is rational, or if $n = 0$. As a summary:

- β is irrational, and the pressure involves all harmonics f_n, except the continuous component; the flow rate is continuous (in particular when it vanishes at every time, i.e., when the reed beats!).
- β is rational, and the pressure has all harmonics f_n except harmonics f_m (they are called "missing harmonics") and among the harmonics f_n the flow rate has the harmonics f_m only. Then the flow rate is periodic with the period $2x_1/c$ or a submultiple which remains compatible with the period of the solution, $2c/L$ (if a signal is periodic with period T, it is also periodic with period pT, where p is any integer).

Therefore numerous solutions to our problem exist. A simple particular case is that where the solution has two states only. For instance the pressure has a negative value p_S during a time $T_S = \tilde{\beta}T$, and a positive value p_L during a time $T_L = (1 - \tilde{\beta})T$. The flow rate also has two states, because its values are related to those of the pressure through the nonlinear reed characteristics. If we subtract the dc component, the flow rate is proportional to the pressure, and its spectrum is proportional to the pressure spectrum. It has been seen that if β is irrational, the flow rate is continuous, with two equal states, similarly to the behavior of a clarinet. Conversely if β is rational, both the flow rate and the pressure have harmonics f_n except harmonics f_m; but the flow rate cannot

(continued)

have other harmonics than f_m, thus in this case it is continuous as well. A more straightforward proof of this result is the following: the mean pressure vanishes, thus $\tilde{\beta}p_S+(1-\tilde{\beta})p_L = 0$ (remind that the indices L and S correspond to long and short, respectively); on the other hand because the losses are ignored, the injected power needs to vanish, thus: $\tilde{\beta}p_S u_S+(1-\tilde{\beta})p_L u_L = 0$ and $u_S = u_L$. We still need to find the possible values of $\tilde{\beta}$, for a stable or unstable solution. If β is irrational, any value is possible, but if β is rational, there is a limitation because the harmonics f_m are absent of the spectrum: we need to choose a value of $\tilde{\beta}$ which suppresses these frequencies in the spectrum. This topic has been investigated by several authors [28, 119].

9.4.8.3 The Particular Case of the Helmholtz Motion

A particular solution was discovered by Helmholtz. It is called "Helmholtz motion" (HM), which describes the motion of a bowed string that players normally seek. In this case the division $\tilde{\beta} = T_s/T$ of the period is equal to the division $\beta = x_1/L$ of the length of the instrument, either a bowed string or a cylindrical saxophone. This case is shown in Fig. 9.20. Because the flow rate is constant, the two states of the pressure satisfy

$$F(p_L) = F(p_S); \tag{9.107}$$

$$\beta p_S + (1-\beta)p_L = 0. \tag{9.108}$$

We choose the function given by Eq. (9.31). When the reed does not beat, we have

$$F^2(p) = F_0^2 + A_2 p + B_2 p^2 + C_2 p^3, \text{ where } F_0 = \zeta(1-\gamma)\sqrt{\gamma}; \tag{9.109}$$

$$A_2 = \zeta^2(1-\gamma)(3\gamma-1); \quad B_2 = \zeta^2(3\gamma-2); \quad C_2 = -\zeta^2. \tag{9.110}$$

(it can be noticed that $B_2^2 = \zeta^4 + 3A_2C_2$). In the useful range of mouth pressure γ A_2 is either positive or negative, and B_2 and C_2 are negative. The flow rate being constant, we find

$$A_2(p_L - p_S) + B_2(p_L^2 - p_S^2) + C_2(p_L^3 - p_S^3) = 0. \tag{9.111}$$

The solution $p_L = p_S$ is trivial: it is the static regime, because Eq. (9.108) implies $p_L = p_S = 0$. The final result for the oscillating solutions is the following[37]:

$$p_L^{\pm} = \frac{2\beta}{1+3\chi^2}\left((2-3\gamma)\chi \pm \sqrt{\chi^2+(1-\gamma)(3\gamma-1)}\right) \tag{9.114}$$

$$p_S^{\pm} = -\frac{2(1-\beta)}{1+3\chi^2}\left((2-3\gamma)\chi \pm \sqrt{\chi^2+(1-\gamma)(3\gamma-1)}\right) \tag{9.115}$$

$$\text{where} \quad \chi = \frac{T_L - T_S}{T_L + T_S} = \frac{p_S + p_L}{p_S - p_L} = 1 - 2\beta. \tag{9.116}$$

The parameter ζ does not intervene: it intervenes in the value of the flow rate only. Thus there are two different oscillating solutions: one with a pressure p_L, which increases with the blowing pressure γ (sign $+$), the other one with a decreasing pressure (exponent $-$). An important value of γ is what it is called the subcritical threshold γ_{sc} for which the two values $p_L^{\pm}$ are equal, as well as the values $p_S^{\pm}$ (the argument of the square root vanishes):

$$\gamma_{sc} = \frac{2}{3}\left[1 - \sqrt{1-3\beta+3\beta^2}\right] \simeq \beta\left(1 - \frac{\beta}{4} + O(\beta^2)\right). \tag{9.117}$$

These results are valid when the reed does not beat. When it beats, the flow rate needs to vanish for two different values of the pressure, therefore one is γ and the other one is lower than $\gamma - 1$. Using (9.108), and the signs $+$ and $-$ for the increasing and decreasing functions of p_L, we obtain

$$\text{if } p_L^{+} = \gamma,\ p_s^{+} = -(1-\beta)\gamma/\beta; \text{ this implies: } \gamma > \beta \tag{9.118}$$

$$\text{if } p_s^{-} = \gamma, p_L^{-} = -\beta\gamma/(1-\beta); \text{ this implies: } \gamma > 1-\beta. \tag{9.119}$$

Figure 9.21 shows the solutions p_L for different values of β. Some comments can be added

[37] Starting from (9.111) for $p_L \neq p_S$, the solutions satisfy

$$A_2 + B_2(p_L + p_S) + C_2\left[\frac{3}{4}(p_L+p_S)^2 + \frac{1}{4}(p_L - p_S)^2\right] = 0. \tag{9.112}$$

This equation is solved for the unknown $\sigma = p_L + p_S$, then, because $p_L = -\beta\sigma/\chi$, it is found:

$$p_L^{\pm} = -\frac{2\beta}{C_2}\frac{1}{1+3\chi^2}\left(-B_2\chi \pm \sqrt{\chi^2(B_2^2 - 3A_2C_2) - A_2C_2}\right). \tag{9.113}$$

For the polynomial function (9.55), the expression is exactly the same, if the subscript 2 is suppressed in the coefficients, and the above result can be easily used in both cases.

- For the clarinet, χ vanishes, and the result becomes very simple [Eq. (9.62) is found].
- For conical instruments, β is small and the subcritical threshold (9.117) is very close to the beating reed threshold β: such instruments are expected to function mainly with a beating reed.
- This is true for positive values of p_L: the solution is the standard HM, analogous to the usual solution for bowed strings, and an inverse bifurcation prevails. The result of the previous section is confirmed.
- For negative values of p_L, the HM is "inverse." It seems to be produced with a direct bifurcation, but this issue is very delicate, because the losses differentiate the thresholds (Y_1 and Y_2 are different). The problem is rather simple if Y_2 is larger than Y_1, but the difficulty increases when the number of impedance peaks having an amplitude larger than that of the first peak increases. The analysis of a system with two peaks was done [33] for the different regimes (standard, inverse and octave; the latter case appears when the second peak is larger than the first). A more detailed study of the general case with N peaks (for small values of β) remains to be performed.
- A signal close to the inverted HM was obtained by experiment for saxophone-like instruments, but was not observed for bowed strings. The mouth pressure was strong, probably for pressure beyond the saturation threshold of the standard HM.
- The stability was studied for the case $\beta = 1/3$ [91]: the ab initio solution [Eq. (4.65)] can be used, by considering a small deviation from the sought solution, but difficulties can occur when two stable regimes are very close together. When $1/\beta$ is an integer, another method is the Floquet method, which generalizes what we did in Sect. 9.3.3.5, but the recurrence relationships become longer.[38]
- The bifurcation point of the static regime is obtained for $p_L = p_S = 0$. This implies $A_2 = 0$, i.e., $\gamma = 1$ or $1/3$. The value 1 for γ corresponds to a closed reed, after Eqs. (9.118) and (9.119), and the bifurcation occurs at $\gamma = 1/3$ independently of β. The interpretation is easy: when the equations are derived assuming small oscillations (see the previous section), the solution is quasi sinusoidal at the threshold limit, and the equation for the first harmonic (9.77) applies in all cases. Therefore the threshold is $A = 0$ when losses are ignored. Notice that the first harmonic approximation cannot distinguish the two HMs, because it does not provide the sign of P_1. In order to distinguish the two regimes, we have to calculate more harmonics, and this is necessary also for the distinction between square and rectangle signals.

[38]The period needs to be split into $1/\beta$ points, and high order matrices need to be studied for the position of eigenvalues with respect to unity. This issue was investigated in numerous articles about bowed strings [122].

9.4.8.4 Considerations About the Spectrum of Conical Instruments

The question of the relation between the conical shape and the sound spectrum remains largely open, in particular for the radiated sound. The simplification of the signal shape shown in Fig. 9.20 obviously yields the suppression of higher frequencies in the spectrum. However, for a clarinet we have seen that the simplified square signal yields relevant results for the signal amplitudes, the oscillation regimes, and the amplitude of the first odd harmonics far from the oscillations threshold. This simplification corresponds to a model with losses independent of frequency, or lossless. For a conical instrument, a supplementary approximation was needed. The hypothesis that it is equivalent to a cylindrical saxophone is only valid over a limited frequency range, because the length of the missing cone, denoted x_1, is assumed to be small compared to the wavelength[39] We have seen that the pressure signal when the reed is beating is common to the different notes, and we can suppose that:

- Characteristic frequencies common to different notes exist in the spectrum, including higher frequencies, and a consequence is the apparition of formants or anti-formants;
- For the lowest ones, the common frequencies are the same as those of a cylindrical saxophone

Internal Spectrum

Let us consider first the spectrum of the internal pressure at low frequencies. We can imagine without rigorous proof that the maximum of this spectrum is linked to that of the input impedance. The latter can be determined by using Eq. (7.105), which describes the envelope curve of the impedance peaks of a truncated cone. The envelope is proportional for all notes to the following function:

$$\frac{1}{1+\frac{1}{k^2x_1^2}}\frac{1}{\sqrt{kx_1}}.$$

A simple calculation gives a rough estimation for the position of this maximum: $kx_1 = \sqrt{3}$. A formant can be found around the corresponding frequency. For instance, for a soprano saxophone, it is 670 Hz. For the lowest notes of an instrument, there are few low harmonics (1 and 2) in the spectrum because of the shape of the input impedance curve.

- At higher frequency, we examine first the case of a cylindrical saxophone. The first characteristics of the spectrum is necessarily the absence of a certain

[39]Thanks to the choice of the mouthpiece dimensions and instrument input, this limit can be put off rather high, see Chap. 7. For instance, let us assume that the limit is around $kx_1 = 1$.

category of harmonics, similarly to the absence of even harmonics for the clarinet. When the ratio β ($= x_1/L$) is the inverse of an integer, the harmonics m/β should be absent. Because the fundamental of the first register is $c/2L$, this corresponds to frequencies $mc/2x_1$, which are the natural frequencies of a pipe of length x_1. As they do not depend on the played note, an anti-formant is expected at these frequencies, which are such that $kx_1 = m\pi$. The anti-formant can exists also if β is irrational, but they are less pronounced because there are no harmonics at exactly these frequencies.

- What happens for a conical instrument? Obviously if the quantity kx_1 is of order of π or larger, the use of a cylindrical saxophone model becomes meaningless. Nevertheless it is possible to find frequencies which are independent of the notes and for which the input impedance is minimum (and other frequencies for which the input impedance is maximum). We start from Eq. (9.105), and ignore the losses. As we have seen, an excellent approximation for the frequency of the first maximum at the mouthpiece input is $c/2(\ell + x_1)$. Hence $k(\ell + x_1) = \pi$. We know that it is not exactly the playing frequency, because the latter depends on the excitation level, but we assume that it is valid. The harmonics of this frequency are not necessarily resonance frequencies, because they do not satisfy the condition $kx_1 \ll 1$. However, the harmonic n satisfies

$$k(\ell + x_1) = n\pi \quad \text{thus} \quad \cot k\ell = \cot(n\pi - kx_1) = -\cot kx_1. \tag{9.120}$$

In other words, for a given frequency which exists in the spectrum, the input admittance of the truncated cone (and therefore the admittance at the input of the mouthpiece) does not depend on the fingering, i.e., on the played note. These admittances exhibit extrema which are common to the different notes, as shown in Fig. 9.22. Hence in the spectrum of the internal pressure formants and anti-formants are expected. They are the elements common to the different notes that we mentioned above. They can be calculated for a given shape of the mouthpiece, but here we do not discuss this matter further. The first anti-formant is slightly higher than that of a cylindrical saxophone ($kx_1 = \pi$). But these formants and anti-formants are less accentuated than those of a cylindrical saxophone, because losses make their presence less obvious.

External Spectrum

The previous analysis was focusing on the internal spectrum. What happens for the radiated pressure? For the lowest frequencies the previous reasoning can be extended by straightforward use of the shape of the input impedance curve. The scarcity of the lowest frequencies in the spectrum of the internal pressure is accentuated by the fact that the radiated pressure is the time derivative of the output flow rate. This is clearly observed, e.g., in the spectrogram of bassoon (see Fig. 7.26 of Chap. 7).

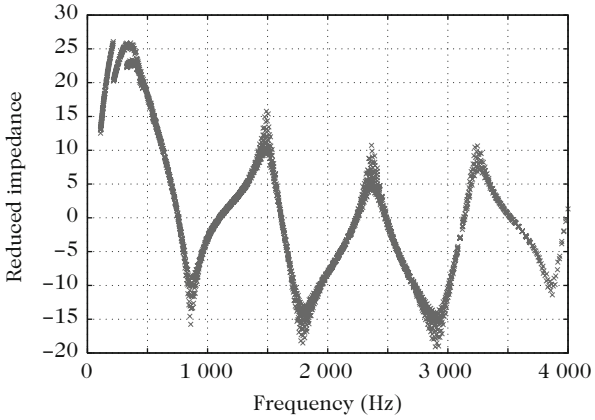

Fig. 9.22 Input impedance for 100 values of ℓ linearly distributed on one octave. The visco-thermal losses are taken into account. The points indicate the impedance modulus for the fundamental frequency and its harmonics for the notes corresponding to each length value. Above 500 Hz, extrema common to the different notes are clearly observed. Minima are found around 800, 1800, 2900 Hz. The dimensions are those of a tenor saxophone with a mouthpiece. The toneholes are ignored (the change of note is obtained thanks to a modification of ℓ). Courtesy of S. Karkar

Unfortunately for the higher frequencies we do not have much insight. Formants and anti-formants exist, but they are less pronounced and their position differs from that observed in the spectrum of the internal pressure. We saw that for a cylindrical instrument the issue of the relative amplitude of the even and odd harmonics is subtle. We imagine that this subtlety is similar for a cylindrical saxophone for the main harmonics versus the missing ones. The problem becomes even more intricate for a conical instrument.[40]

What is clear is that the level difference between formants and anti-formants is much smaller than for the internal pressure, as for the difference between even and odd harmonics of the clarinet.[41] Nevertheless, contrary to some possible hypotheses, the position of the formants is not directly linked to the length x_1 of the missing cone or to the mouthpiece shape.

The previous analysis shows that if the length x_1 of the missing cone is reduced, and then if for a given length, the apex angle is increased, the first characteristic frequencies increase. Observing the increase of the taper from the first saxophones of Adolphe Sax to modern saxophones, it is possible to explain this increase by the aim to enrich the timbre [74], as probably requested by jazz music. In comparison to a violin, this would correspond to a play closer to the bridge. It is well known

[40]Remember that this discussion ignores the existence of toneholes, which strongly complicate the sound analysis above the cutoff frequency (see Chap. 14). Moreover the reed dynamic also is ignored.

[41]This is due to the difference between the input impedance and the pressure transfer function: the first function of the frequency has poles and zeros, while the second has poles only.

that the timbre is richer in harmonics because the first missing harmonic becomes higher (similarly to what happens when playing a guitar close to the bridge).

Finally we mention the study by Benade and Lutgen [13], who measured the external spectrum averaged in a room and showed for the highest frequencies the existence of a frequency above which the amplitude of the pressure spectrum decreases as f^3: this frequency would be linked to the cutoff frequency of the toneholes lattice. Moreover they showed that minima exist in the spectrum of a given note, and that this is related to the reed beating. To our mind many issues require further studies in this matter.

9.5 Behavior of the 3-Equation Model with Reed Dynamics (Non-beating Reed)

9.5.1 Introduction

Synthetic sounds show that what instrumentalists call "squeaks" for single reed instruments are sounds with a frequency close to that of the (first) reed resonance. A beginner has to learn how to avoid them, by intuitively controlling the reed damping with his lower lip. The 3-equation model (9.26)–(9.28) can explain the relevance of this intuition. Two parameters need to be added to the study of Sects. 9.3 and 9.4: the damping factor and natural frequency of the reed, because the reed is assumed to be a single-degree-of-freedom oscillator. At the same time it is possible to study what happens when the playing frequency is close to the reed natural frequency. It is the case for reed instrument for notes belonging to the high part of the compass. It is also the case for reed organ pipes for which the reed resonance determines the playing frequency and the resonator role is limited to a coloring of the sound: these pipes are tuned by modifying a tuning spring. It can be said that the corresponding regime is the "reed regime," as opposed to the "resonator regime": this opposition was largely explored by Bouasse [17]. The case of lip-reed instruments is an intermediate case because the natural frequency of the reed (i.e., of the lips) needs to be very close to that of the resonator, yielding a strong coupling.

In order to solve the three dimensionless equations (9.26)–(9.28), the assumption of square signals is no more suitable, because the reed resonance modifies the spectrum. Notwithstanding some approximations remain possible. We start by focusing our attention on the instability threshold of the static regime, by using the characteristic equation (see Sect. 9.4.2) and supposing that the reed does not beat, because the amplitudes are extremely small near the threshold. To this end we base our study on the work by Wilson and Beavers [121], noted as WB, which is an important milestone in the research on reed instruments.[42] We first consider an

[42]What is the most important for the determination of the pitch? Is it the reed or the resonator? Historically it was one of the most important subjects of musical acoustics. We can cite Weber

inward-striking reed, later an outward-striking one. The latter was not considered up to now because they cannot function for frequencies which are very low compared to the reed natural frequency.

9.5.2 Oscillation Threshold for an Inward-Striking Reed

The previous presentation needs to be completed. Actually, two effects of the reed need to be distinguished: (1) the reed dynamics, and (2) the volume flow rate created by the reed displacement, which modifies the equation of the resonator [see Eq. (9.18)]. The distinction between these two effects is rather subtle, as this will be explained in the present section. The historical development can be summarized as follows:

Effect of the Reed Displacement

Helmholtz [68] and many authors tried to understand the effect of the flow rate in order to compare instruments such as clarinets with instruments such organ reed pipes. For the first type, the parameter defined as the ratio of the pipe resonance frequency to the reed resonance frequency is small, and the reed has a small influence on the playing frequency. Conversely for the latter type, the same ratio is large, and the playing frequency is close to the reed resonance frequency. For this study, a linear theory is used, assuming that the playing frequency is the resonance frequency of a composite resonator, i.e., the air column coupled to the reed. The reed dynamics is ignored, and therefore the reed acts as a simple spring. This leads to a simple transcendental equation, which describes the transition of the playing frequency from the pipe resonance to the reed resonance, when the pipe resonance frequency increases up to the reed resonance frequency.

Effect of the Reed Dynamics

How is it possible to proof that, when the reed dynamics is ignored, the playing frequency is the resonance of the composite resonator? Actually, this is true at the threshold of oscillation, as shown by the characteristic equation (9.78) which has been written in Sect. 9.4.2. It involves the input admittance of the composite resonator. It is obtained by linearizing the nonlinear equation of the excitor, and

[118], Helmholtz [68], and Bouasse [17], who performed a thorough literature review. He discussed all works of his time with many experimental results, which remain to be studied in detail. Works on valves with weak coupling of two resonators can also be cited [49, 108] (for us one of the resonators would be the vocal tract).

yields the value of both the operating (or playing) frequency, and the mouth pressure. For the nonlinear model proposed in this chapter, the latter is found to be equal to the third of the closure pressure p_M, whatever the ratio pipe-resonance frequency/reed-resonance frequency.[43]

One century after Helmholtz, Wilson, and Beavers were the first authors to propose a model based on the Bernoulli equation. They tried to take the reed dynamics into account, considering a single-degree-of-freedom oscillator. However, they ignored the effect of the reed flow. The solving is based anew on the derivation of the characteristic equation, which is much more complicated than when ignoring the reed dynamics. Concerning the dependence of the playing frequency with respect to the ratio pipe frequency/reed frequency, it seems to be similar to that found for the other effect (no reed dynamics, but the reed flow is considered). However, the deviation from the pipe resonance frequency is much smaller than that found for the reed flow effect. Moreover, when taken into account both effects, the effect of the reed flow appears to be dominant (this has been explained in [101]). Conversely the effect of the reed dynamics on the mouth-pressure threshold can be dominant, and is strongly influenced by the quality factor of the reed. For a strongly damped reed (for instance the clarinet reed, which is strongly damped by the player lip), the pressure threshold is close to $p_M/3$. However, for a slightly damped reed, the pressure threshold is largely lowered, and this explains why squeaks are obtained with a clarinet when the reed is insufficiently damped by the lip.

The present section considers first the two effects together.

9.5.2.1 Characteristic Equation, Real Frequency Solution for the Thresholds

We start from the three equations (9.26)–(9.28), by slightly modifying them. The two first equations can be written in the frequency domain[44]:

$$U = YP + j\omega X \Delta\ell/c \tag{9.121}$$

$$X = DP \quad \text{where } D(\omega) = \left[1 + \frac{j\omega q_r}{\omega_r} - \frac{\omega^2}{\omega_r^2}\right]^{-1}. \tag{9.122}$$

As WB did [121], we derive the characteristic equation, but we wish also to investigate the effect of the reed displacement flow rate, which is proportional to

[43] Notice that these results are valid if the threshold of oscillation is equal to the threshold of instability of the static regime, i.e., if the bifurcation is direct. This is the case for a clarinet or an organ reed pipe.

[44] Remind the notations: U is the volume flow rate, P is the pressure at the resonator inlet, X the reed displacement, Y the admittance at the resonator inlet. γ is the mouth pressure, ζ is the reed parameter. All quantities are dimensionless (see Sect. 9.2.5.3). $\Delta\ell$ is the length associated to the reed flow rate, ω_r the reed angular frequency, and q_r^{-1} its quality factor.

$\Delta\ell$, and was ignored by these authors. We linearize Eq. (9.28) around the static regime ($p = x = 0$), assuming again the zero frequency impedance to be zero:

$$u = \zeta\sqrt{\gamma}(1-\gamma)\left[1 + \frac{x}{1-\gamma} - \frac{p}{2\gamma}\right]. \tag{9.123}$$

Writing this equation in the frequency domain and limiting it to a single harmonic, using the two linear equations (9.121) and (9.122), and finally dividing the two sides of the equation by P_1, we find the characteristic equation:

$$Y + Dj\omega\frac{\Delta\ell}{c} = \zeta\sqrt{\gamma}\left[D - \frac{1-\gamma}{2\gamma}\right]. \tag{9.124}$$

This equation generalizes the relation $Y = A$ that we obtained in Sect. 9.4.2: this can be checked by writing $\Delta\ell = 0$. and $D = 1$. We determine the thresholds by solving this equation for a real frequency ω. We assumed that we are around a static, non-beating regime and have linearized the nonlinear equation: the quantities x and p being small, the non-beating reed condition for the static regime is simply[45] as $\gamma < 1$. Thus results such with $\gamma > 1$ are not relevant, even if in certain cases the following analysis can lead to such values.

9.5.2.2 Results of Wilson and Beavers for a Cylinder

We present hereafter the experimental result of WB and compare them with numerical solutions of Eq. (9.124) (see [101]). The latter slightly differs from those of WB, especially because we take into account the reed displacement flow rate. Then analytical approximate results are provided.

- The results shown in Fig. 9.23 correspond to a weak damping of the reed (of type metallic organ reed, $q_r = 0.008$). The abscissa is the product $k_r\ell$. For a given reed frequency (here $f_r = 700\,\text{Hz}$), it is proportional to the length. Thus these curves are obtained when the tube length varies, e.g., with a slide. For a given length, several solutions, which correspond to different tube modes, are possible. Only the oscillation frequency with the lowest pressure threshold is indicated. The reed parameters were measured using different techniques. The thresholds were measured by increasing the blowing pressure until a sound is produced (in this study the bifurcation is assumed to be direct).

  It can be observed that the threshold frequencies are always lower than the natural frequencies of both the reed and the resonator. The latter are given by decreasing hyperbolas (in dotted lines) by $\cot k\ell = 0$, or $k\ell = (2n-1)\pi/2$,

[45] It would be tedious to go beyond this value for solving the complete equation (9.30): indeed if for $p = 0$, the function $F(p)$ is regarded as a function of γ, its derivative is not continuous in $\gamma = 1$. Moreover we know that the model slightly disagrees with experiment.

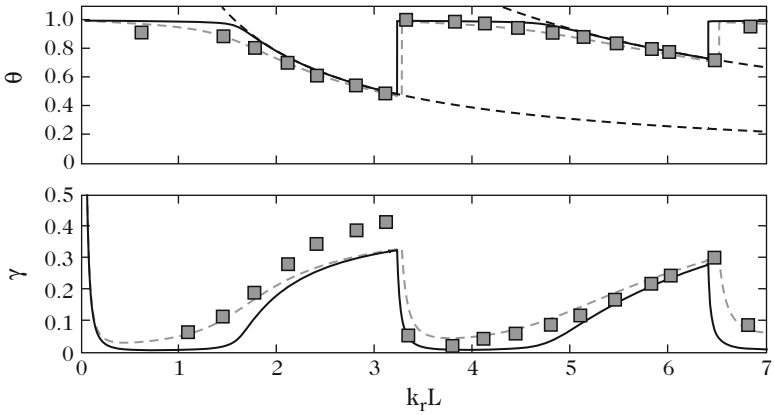

Fig. 9.23 Thresholds of frequency θ and of mouth pressure γ for a weakly damped reed. $q_r = 0.008$; $\zeta = 0.1$; $f_r = 700$ Hz ; $r = 6.4$ mm. *Solid line*: theoretical results [101] without reed displacement flow rate, corresponding to the calculation by Wilson and Beavers [121]; *dashed line*: theoretical results with the reed displacement flow rate ($\Delta\ell = 5$ mm); *dotted line*: hyperbolas of the natural frequencies of the resonator. The *squares* are the experimental results by WB

i.e., $\theta = \omega/\omega_r = (k_r\ell)^{-1}(2n-1)\pi/2$. When the length increases initially the frequencies of the first regime are obtained, then those of the second one, followed by the third one, etc. The pressure thresholds differ drastically much from the value predicted by the model without losses and reed dynamics, $\gamma = 1/3$. They can reach values smaller than $1/20$, because the reed greatly favors the oscillation when ω/ω_r is close to unity. But when $k_r\ell$ approaches the values $n\pi$ from below, the functioning is very similar to the functioning without reed dynamics, i.e., the playing frequency corresponds to a tube resonance, with a pressure threshold close to $1/3$. Then suddenly the solution corresponding to the following regime appears, because its threshold is much lower, and the playing frequency is close to the reed natural frequency. Consequently for a long tube the reed favors either "squeaks" when $k_r\ell$ is close to $n\pi$, or approaches acoustic resonance frequencies when $k_r\ell$ is far from these values.

- Now let us look at Fig. 9.24, for which the reed damping is strong, $q_r = 0.4$ (the reed is of clarinet-type). The variation of the playing frequencies is qualitatively similar to that for a weak damping but squeaks cannot be obtained, because the pressure thresholds would be very high. These thresholds are much closer to the thresholds that we have calculated without reed dynamics [Eq. (9.69)]. And the thresholds of the higher order regimes become higher than those of the first regime. This allows keeping the first acoustic regime for any length, and prevents the production of the other regimes. Because the reed is more damped than in the previous case, its role is weaker in the variation of the pressure thresholds and the resonator acoustic losses play a much greater role.[46]

[46]Notice that it is easy for a clarinet to obtain squeaks by driving the mouthpiece in the mouth in order to suppress the damping by the lip.

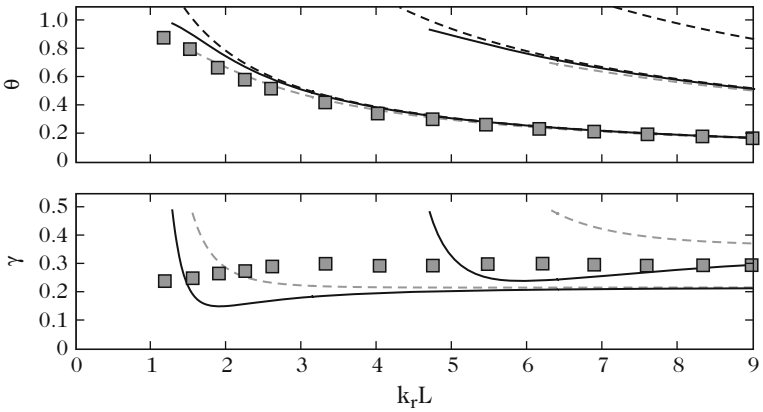

Fig. 9.24 Thresholds of frequency θ and of mouth pressure γ for a strongly damped reed. $q_r = 0.4$; $\zeta = 0.13$; $f_r = 750\,\text{Hz}$; $r = 6.4\,\text{mm}$. *Solid line*: theoretical results [101] without reed flow rate, corresponding to the calculation by Wilson and Beavers [121]; *dashed line*: theoretical results with reed flow rate ($\Delta\ell = 12\,\text{mm}$); *dotted line*: hyperbolas of the natural frequencies of the resonator. The *squares* are the experimental results by WB

9.5.2.3 Analysis of Threshold Frequencies

For the analysis we simplify the problem by ignoring (for the moment) both the reed displacement flow rate and the acoustic losses in the resonator. The admittance Y is purely imaginary. For a cylinder of length ℓ, $\Im m(Y) = -\cot k\ell$. For a resonator of arbitrary shape, we reduce the admittance to one mode, of subscript n, and even to one "single" mode, of positive frequency (see Chap. 2). This implies that we search for a frequency that is not too far from the natural frequency of the resonator. We rewrite Eq. (9.66) in the following form (see Chap. 2):

$$Y \simeq 2jF_n^{-1}(\omega - \omega_n^+) \text{ where } \omega_n^+ = \omega_n + j\omega_n/(2Q_n), \text{ thus} \quad (9.125)$$

$$\Im m(Y) \simeq 2F_n^{-1}(\omega - \omega_n) \quad (9.126)$$

(remind that for a cylinder, $2F_n^{-1} = \ell/c$). If $\Re e(Y) = 0$ and $\Delta\ell = 0$, the separation of the real and imaginary parts of the characteristic equation yields

$$\frac{1-\gamma}{2\gamma} = \Re e(D) = \frac{1}{\eta}. \quad (9.127)$$

$$\Im m(Y) = \Im m(D)\zeta\sqrt{\gamma} = -\frac{\zeta\sqrt{\gamma}\theta q_r}{\eta(1-\theta^2)}, \quad (9.128)$$

where:

$$\theta = \frac{\omega}{\omega_r} \text{ and } \eta = \frac{1}{\Re e(D)} = 1 - \theta^2 + \frac{q_r^2\theta^2}{1-\theta^2}. \quad (9.129)$$

The parameters ζ, q_r, ω_r, and those of the resonator are fixed, thus two unknowns remain for the characterization of the threshold: the threshold frequency θ and the mouth pressure γ (for the sake of simplicity, the subscript th has been omitted). The calculation seems to be tedious, but some results are surprisingly simple and informative. We first retrieve the results obtained without reed dynamic ($\theta = 0$): because in such a case $\eta = 1$, $\gamma = 1/3$ and $\Im m(Y) = 0$. Then Eq. (9.127) yields

$$\gamma = \frac{\eta}{2+\eta}. \tag{9.130}$$

This can be brought in Eq. (9.128), therefore, for a cylinder, the following result is obtained

$$-\Im m(Y) = \cot k\ell = \cot k_r \ell\theta = \zeta F(\theta) \tag{9.131}$$

$$\text{where } F(\theta) = q_r\theta\left[(1-\theta^2)^2 + q_r^2\theta^2\right]^{-1/2}\left[(3-\theta^2)(1-\theta^2) + q_r^2\theta^2\right]^{-1/2}.$$

Equation (9.131) has only one unknown, ω, or $\theta = k\ell/k_r\ell$ when $k_r\ell$ is fixed. Up to $\theta = 0.8$, the function $F(\theta)$ has a nearly linear variation with respect to $q_r\theta$, thus it is proportional to q_r. A numerical calculation shows that the increase is monotonous from 0 to $1/q_r$ when θ varies from 0 to 1 (see Fig. 9.25). Thus for two different values of q_r, the curves intersect very close to $\theta = 1$. Because $F(\theta)$ is positive, the cotangent function is always positive and the solutions are always below the hyperbolas $\cot k\ell = 0$, whose solutions are $\theta = (k_r\ell)^{-1}(2n-1)\pi/2$ (see Figs. 9.23 and 9.24). For a one-mode resonator, a similar result can be obtained: following Eq. (9.125), the solutions are smaller than the natural frequencies of the resonator:

$$\omega = \theta\omega_r = \omega_n - \frac{1}{2}\zeta F_n F(\theta). \tag{9.132}$$

The previous explanation is not a rigorous proof because the unknown ω is included in $F(\theta)$, but it is undoubtedly correct when ζ is not too large.[47]

- *For the case of a strongly damped reed*, the quantity $\zeta F(\theta)$ is rather large except near $\theta = 1$, where there is no solution. Thus the threshold frequencies are rather far from the resonator natural frequencies, roots of $\cot k\ell = 0$ (i.e., $k\ell = (2n-1)\pi/2$): it should be remembered that a weak relative difference can be important from the musical point of view, because one semitone corresponds to 6 % in the frequency. In order to calculate the threshold frequencies with a good accuracy, it is possible to use perturbations, bringing into the second member of Eq. (9.132),

[47] We know that the results with $\gamma > 1$ are not relevant, because they correspond to a complete closure of the mouthpiece. According to Eq. (9.127), this corresponds to $\eta < 0$ and therefore to $\theta > 1$. With this theory we cannot know determine whether the playing frequency can exceed the reed resonance or not.

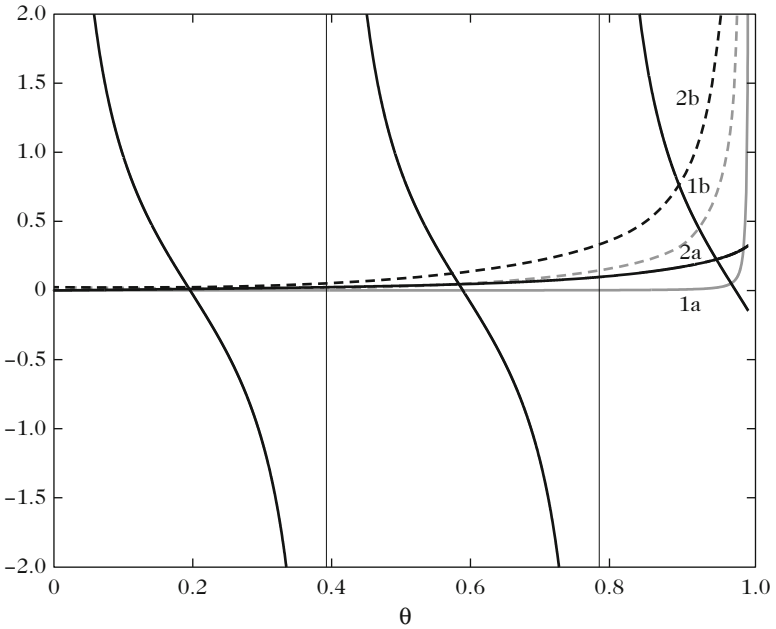

Fig. 9.25 Comparison of the function $\cot k_r \ell\theta$ for $k_r\ell = 8$ (*thin line*) and the function $\zeta F(\theta)$ for the two cases shown in Figs. 9.23 (*solid line 1a*) and 9.24 (*solid line 2a*). It is observed that the playing frequencies are smaller than the natural frequencies of the tube which cancel the cotangent function $F'(\theta)$, [Eq. (9.138)]. The latter represents the effect of the reed displacement flow rate, which is predominant near the reed resonance for both cases

the values of k we found with $\theta = k/k_r$. The variation of frequency due to damping can be written in the form of a length correction, equal to:

$$\Delta\ell = \zeta F(\theta)/k = \zeta F(\theta)/(\theta k_r).$$

Then, because in this case θ is small compared to unity, the square roots involved in $F(\theta)$ can be simplified by ignoring the terms in $q_r\theta$, giving:

$$\Delta\ell = \frac{q_r\zeta}{k_r(1-\theta_n^2)^{3/2}(3-\theta_n^2)^{1/2}}, \tag{9.133}$$

where $\theta_n = (2n-1)\pi/(2k_r\ell)$. Hence this length correction is positive. It is proportional to the reed damping and inversely proportional to the reed frequency. This was expected, because the correction needs to vanish when the latter tends to infinity. For a sufficiently high reed frequency, the denominator simplifies to $k_r\sqrt{3}$.

- *The case of a weakly damped reed* is not very different regarding frequencies: however, the quantity $\zeta F(\theta)$, which is ζ/q_r for $\theta = 1$, can be very large near

this value of θ, thus the frequencies are far from the tube natural frequencies. The quasi horizontal portion of the frequency curve starting from the values $k_r\ell = n\pi$ is longer than in the case of a strong damping. This seems to be obvious because when there is no damping the reed dynamic plays a more important role, and the threshold frequencies are more distant from the tube natural frequencies. However, for small values of the solutions θ, they are closer to the tube frequencies than for a strongly damped reed.

9.5.2.4 Threshold Pressures

For the threshold pressure, the main result is shown in Fig. 9.23: its variation is rather strong with the tube length or the reed natural frequency (parameter $k_r\ell$). When the playing frequency approaches the tube frequencies, the quantity η becomes close to unity, corresponding to a threshold pressure close to $1/3$ [in fact its value is slightly higher, because of the tube losses, see Eq. (9.69)].

The minima of threshold pressure can be easily determined because γ is a monotonously increasing function of η. The study of the function $\eta(\theta)$ [Eq. (9.129)] shows that it has one minimum, for $\theta_c^2 = 1 - q_r$. Its value is $\eta_{\min} = q_r(2 - q_r)$, and, using Eq. (9.130) the minimum of γ is

$$\gamma_{\min} = \frac{q_r(2 - q_r)}{2 + q_r(2 - q_r)}. \tag{9.134}$$

For a weak damping q_r, this expression simplifies in $\gamma_{\min} \simeq q_r(1 - 3q_r/2)$. For a strong damping, the minima $\gamma_{\min}$ are higher. However, we did not take into account the tube losses, and this expression cannot explain why the second minimum is higher than the first (see Fig. 9.24). Therefore this analysis should be refined further, because such a difference can be responsible for the jump to the second register (twelfth register), even without register hole, and consequently is important from a musical point of view.

The search for the value of $(k_r\ell)_{\min}$ at which there is a minimum of threshold pressure can be done using Eq. (9.132). The first order approximation $\theta \simeq 1 - q_r/2$ yields

$$F(\theta) = \frac{1 - 3q_r/4}{2\sqrt{q_r}}, \text{ and } \omega_n = \omega_r\left[1 - \frac{q_r}{2}\right] + \frac{\zeta F_n}{4\sqrt{q_r}}\left[1 - \frac{3q_r}{4}\right]. \tag{9.135}$$

For a cylinder:

$$k_r\ell = (2n - 1)\frac{\pi}{2}\left[1 + \frac{q_r}{2}\right] - \frac{\zeta}{2\sqrt{q_r}}\left[1 - \frac{q_r}{4}\right]. \tag{9.136}$$

For a strong damping, the second term remains small and the order of magnitude is given by $(k_r\ell)_{\min} = (2n-1)\pi/2$; when the damping decreases, the values of $(k_r\ell)_{\min}$ decrease significantly.[48]

What is the influence of resonator losses, that we have ignored up to now? A general idea can guide us: if reactive phenomena have a great influence on the frequencies, it is not the case of dissipative phenomena. However, the latter have an influence on the threshold pressure and need to be considered. A detailed calculation can be found in [101], and gives the following result:

$$\gamma_{\min} = \gamma_0 \left[1 + 2Y_{mn}\sqrt{\gamma_0}/\zeta\right]. \tag{9.137}$$

γ_0 is the value when tube losses are ignored [Eq. (9.134)], and $Y_{mn} = 1/Z_{Mn}$ [see Eq. (9.66)] is the minimum admittance of the tube, equal to $\alpha\ell$ for a cylinder (where α is the loss coefficient of the tube). As expected it appears that the minimum increases when the length increases, and that it is larger for the second register than for the first one.

9.5.2.5 Effect of the Reed Displacement Flow Rate

Figures 9.23 and 9.24 show that near the reed resonance, the effect of the reed displacement flow rate on the threshold frequencies is more important than that of damping. A complete calculation is difficult, therefore we limit the study to the threshold frequencies by ignoring the reed dynamic, in order to compare the two effects separately. Equation (9.124) shows that the reed displacement flow intervenes as a simple (reactive) modification of the input admittance of the resonator. If $q_r = 0$, the left member of (9.124) is imaginary and determines the frequencies, while the right member is real and imposes the pressure. Equation (9.131) leads to the definition of a new function, $F'(\theta)$:

$$-\Im m(Y) = k\Delta\ell\frac{1}{1-\theta^2} = F'(\theta) \quad \text{where} \quad F'(\theta) = k_r\Delta\ell\frac{\theta}{1-\theta^2}. \tag{9.138}$$

The quantity $k_r\Delta\ell$ is small.[49] For small values of θ, the right members of Eqs. (9.138) and (9.131) have the same order of magnitude. However, close to the

[48] *Above the values* $(k_r\ell)_{\min}$, Fig. 9.24 shows also the growth of the three branches of the curve $\gamma(k_r\ell)$. The second branch growths slower than the first, and the third growths slower than the second, because the frequencies are less and less remote from the reed resonance (θ does not take small values for the branches corresponding to higher regimes). *Below the values* $(k_r\ell)_{\min}$, the growth is very fast, because between θ_c and $\theta = 1$, γ increases from $\gamma_{\min}$ to a value close to 1 (infinite η).

[49] The order of magnitude of $\Delta\ell$ can be estimated to 1 cm, by measuring the playing frequencies when they are close to the resonance frequencies of the tube [32]. From the data of Figs. 9.23 and 9.24, the following values are obtained, respectively: $k_r\Delta\ell = 0.06$ and 0.16.

reed resonance ($\theta = 1$), the reed displacement flow term becomes much larger than the reed dynamics one. This is shown in Fig. 9.25. Indeed the function $\theta/(1-\theta^2)$ is increasing from 0 to infinity when θ increases from 0 to 1 (it resembles the function $F(\theta)$, but the latter is limited to a finite value, $1/q_r$).

In order to solve Eq. (9.138) in the case of a one-mode resonator, Eq. (9.126) is used

$$\theta = \theta_n - \frac{1}{2}\frac{\theta F_n \Delta\ell}{c(1-\theta^2)} \quad \text{where} \quad \theta_n = \frac{\omega_n}{\omega_r}. \tag{9.139}$$

For a cylinder, in the limit of small θ, the reed displacement flow effect is reduced to a simple length correction, as explained when defining $\Delta\ell$ [see Eq. (9.17)]. Indeed the result is $f = \dfrac{(2n-1)c}{4(\ell+\Delta\ell)}$. Obviously this can be improved by a perturbation calculation [75]. Nevertheless the problem is more complicated close to the reed resonance: if θ tends to unity, $\Im m(Y)$ tends to infinity, and we approach the anti-resonances of the tube. For certain lengths of the tube, when $k_r\ell$ corresponds to a tube anti-resonance, the playing frequency is the reed natural frequency. If θ is close to unity, the solution can be sought in the form $\theta = 1-\varepsilon$, writing $\theta_n = 1-\varepsilon_n$, and this leads to a quadratic equation in ε:

$$2\varepsilon(\varepsilon - \varepsilon_n) = \beta(1 + O(\varepsilon)),$$

where $\beta = \frac{1}{2}F_n\Delta\ell/c$ is small (it is equal to $\Delta\ell/\ell$ for a cylinder). Therefore:

$$\varepsilon = \frac{\varepsilon_n}{2}\left[1 + \sqrt{1 + \frac{2\beta}{\varepsilon_n^2}}\right]. \tag{9.140}$$

The square root comes typically from mode coupling. This explains why, as soon as we are interested in more complicated problems, it is extremely difficult to find analytical solutions. The principle of this study should be emphasized: we sought the playing frequencies at the threshold by calculating the frequencies for which the imaginary part of the passive resonator admittance vanishes. The passive resonator consists of the tube and the reed, while the effect of the flow coming from the mouth is totally ignored. Historically this approach was used by many authors (see, e.g., [83]) and give often interesting results, because the reed displacement flow has an effect preponderant over the reed dynamic. The theoretical curves of the playing frequencies can be fitted with experimental results, and a reasonable value of the reed displacement flow rate is obtained. This allows predicting threshold frequencies, but the measurement of the threshold pressure remains difficult.

9.5.3 Oscillation Threshold for an Outward-Striking Reed

9.5.3.1 Characteristic Equation

We now investigate an outward-striking reed, which is the elementary model for lip reeds. There is a major difference with respect to the previous case: the closure pressure is negative, therefore the mouth pressure is always far from this pressure. Using a 3-equation model, we will show that the playing frequency is higher than that of the reed: a functioning in square signals is not possible, and we need to take into account the reed dynamic (in order to get square signals, it would be mandatory to inhale).

Using Eqs. (9.37)–(9.39), we obtain the characteristic equation, which is the counterpart of (9.124):

$$Y + Dj\omega\frac{\Delta\ell}{c} = \zeta\sqrt{\gamma}\left[-D - \frac{1+\gamma}{2\gamma}\right]. \tag{9.141}$$

We ignore the reed displacement flow rate, although its potential importance was not studied yet, and we ignore the losses in the tube. As a result:

$$\gamma = -\frac{\eta}{2+\eta}; \tag{9.142}$$

$$\Im m(Y) = \frac{\zeta\sqrt{\gamma}\theta q_r}{\eta(1-\theta^2)}. \tag{9.143}$$

9.5.3.2 Threshold Frequencies

Because of the sign of the second member of (9.143), the quantity $\eta(1-\theta^2)$ is always positive, and the playing frequencies are always higher than the natural frequencies of the tube (see Fig. 9.26). They are also higher than those of the reed, because positive γ implies negative η. Then, by bringing Eq. (9.142) into Eq. (9.143), we obtain an equation similar to Eq. (9.131):

$$\Im m(Y) = \zeta G(\theta) \tag{9.144}$$

$$\text{where } G(\theta) = q_r\theta\left[(1-\theta^2)^2 + q_r^2\theta^2\right]^{-1/2}\left[-(3-\theta^2)(1-\theta^2) - q_r^2\theta^2\right]^{-1/2}.$$

This implies

$$(3-\theta^2)(1-\theta^2) + q_r^2\theta^2 < 0. \tag{9.145}$$

This inequality is satisfied between the two roots θ_1 and θ_2 of a second order equation. As q_r is sufficiently small: $\theta_1 \simeq 1 + q_r^2/4$ and $\theta_2 \simeq \sqrt{3}(1 - q_r^2/4)$.

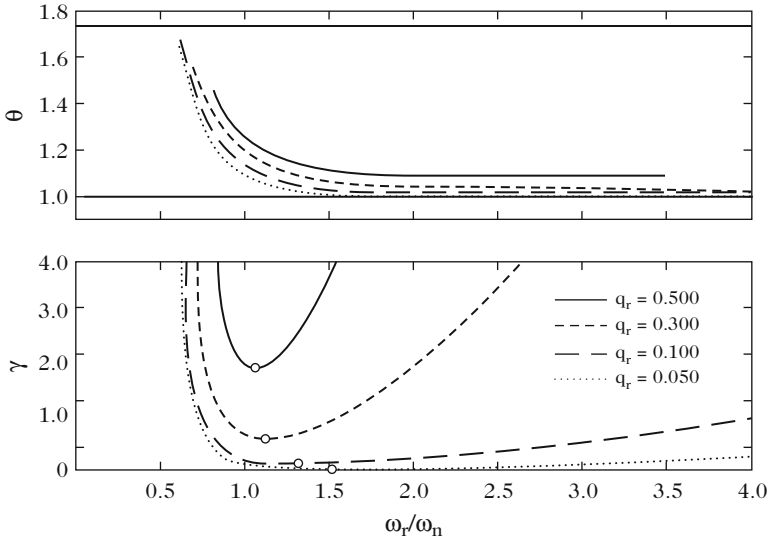

Fig. 9.26 Frequency and mouth-pressure thresholds for an outward-striking reed for different values of the reed damping

For inward-striking reeds, the value $\theta = 1$ can be reached from below. Here it cannot be reached, but θ can be rather close to unity. For the two extreme values, the tube would function at anti-resonances, but we will see that they cannot be reached. We do not write the equivalent of Sect. 9.5.2.5, but because the threshold frequency is higher than the reed frequency, the reed displacement flow produces again a cumulative effect with that of the reed dynamic. Indeed the reed flow term in Eq. (9.138) remains unchanged, but with $\theta > 1$. It increases the shift of threshold frequencies compared to the reed frequency or to the tube natural frequencies.

9.5.3.3 Threshold Pressure

Because $\theta > 1$, the quantity $\eta + 2$ needs to be positive [see Eq. (9.145)]. Thus η lies between -2 and 0. For the two limit values θ_1 and θ_2, for which $\eta = -2$, the threshold γ is infinite; therefore it is not possible, in practice, to play close to these values. For a fixed reed frequency, the interval which can be reached by changing the resonator length is significantly smaller than $\sqrt{3}$ (one sixth). Experimentally an interval of one third was found [29]. This enlightens the interest for brass instruments to have a reed with variable characteristics, that the player adapts to the tube length. This behavior greatly differs from that of an inward-striking reed, for which θ can vary from 0 to 1! The minima of γ can be calculated similarly to what was done in Sect. 9.5.2.4: according to Eq. (9.142), they correspond to maxima of η, thus to $\theta_c'^2 = 1 + q_r$, i.e., $\theta_c' \simeq 1 + q_r/2$, and they are:

$$\gamma_{\min} = \frac{q_r(2+q_r)}{2+q_r(2+q_r)}. \tag{9.146}$$

For a weak damping, this becomes $\gamma \simeq q_r(1-q_r/2)$, and is found to be slightly higher than for an inward-striking reed with the same parameters. Because the value $\theta_c'^2 = 1 + q_r/2$ is quite close to θ_1, we observe that for a cylinder the curves of threshold pressure with respect to the parameter $k_r\ell$ display a strong asymmetry relative to the minimum (see Fig. 9.26). This result is in agreement with those of [29].

9.5.4 Modal Approach of the Dynamical System

In what follows we consider the analysis of the linearized system in terms of modes. An approximation of the characteristic equation (9.124) or (9.141) is obtained by expanding the input impedance in a modal series, similar to (9.66), and by truncating the series to the first mode of the resonator, as we did in Sect. 9.3.4. Considering the expression of $D(\omega)$, we obtain an equation of the fourth order in $s = j\omega$, which has real coefficients. This implies that if s is a solution, its conjugate s^* is a solution as well. Thus the four solutions are: s_1, s_1^*, s_2, s_2^*.

The characteristic equation is a polynomial, and $p(t)$ is the sum of exponentials of type $\exp(st)$. If the real part of both s_1 and s_2 are negative, the exponentials are decreasing, and the static solution $P_1 = 0$ is stable. It becomes unstable when one of the two real parts become positive. In other words if one real part is positive and the other vanishes, we get an instability threshold of the static regime. If the two real parts become positive, we have the sum of two increasing exponentials with different frequencies, which correspond to the imaginary parts of s_1 and s_2. It should be remembered that we do not know anything about the existence of oscillating solutions, because the nonlinear terms were suppressed, and obviously we do not know anything about their stability!

An approximation of the fourth order equation is obtained by ignoring the negative frequencies. This results in a quadratic equation. For the function $D(\omega)$ defined by Eq. (9.122), a treatment similar to that we did for the function $Y(\omega)$ [see Eq. (9.125)] can be done, with the following result:

$$D^{-1}(\omega) \simeq -\frac{2}{\omega_r}(\omega - \omega_r^+) \;\text{ where } \omega_r^+ = \omega_r + j\omega_r q_r/2. \tag{9.147}$$

For an inward-striking reed, the characteristic equation (9.124) becomes

$$(\omega - \omega_r^+)(\omega - \tilde{\omega}_n^+) = \frac{\omega_r F_n}{4}\left[j\zeta\sqrt{\gamma} + \frac{\omega\Delta\ell}{c}\right]$$
$$\text{with}\quad \tilde{\omega}_n^+ = \omega_n^+ + j\frac{F_n}{4}\zeta\frac{1-\gamma}{\sqrt{\gamma}}. \tag{9.148}$$

It exhibits two modes coupled by the flow from the mouth and the reed displacement flow. However, the mode of the tube itself is modified by the mouth flow, with an increase of the losses (as γ is lower than unity): this effect corresponds to the resistance due to the flow if the reed is prevented from vibrating around its average position, which is determined by the blowing pressure ($x = 0$). Therefore these two modes are passive (the imaginary parts of ω_r^+ and $\tilde{\omega}_n^+$ are positive). This approximation of the characteristic equation assumes that the playing frequency and the frequencies of both the tube and the reed do not differ much. The sum of the roots of this equation is

$$\omega_1 + \omega_2 = \omega_r^+ + \tilde{\omega}_n^+ .$$

Thus if one root, for example, ω_1, is real, the other root will have a positive imaginary part because the two modes are passive. In other words, when one of the exponentials which is decreasing becomes increasing, the other one is always decreasing. The thresholds we studied in Sect. 9.5.2.1 are *instability thresholds of the static regime*.[50] Similarly to what was done in Chap. 6 about piano strings (Sect. 6.3.2), it would be possible to discuss approximate solutions. A similar analysis can easily be done for an outward-striking reed.

9.5.5 Discussion of the Results

In the present section the role of the reed resonance has been examined together with the use of the damping for the control of the regimes for a cylindrical tube. For certain lengths of tubes, the effect of damping can be very important. This explains why it is not possible to have toneholes very close to the mouthpiece on a clarinet, because the tuning and the timbre would depend too much on the reed. The present section has been limited to the instability threshold of the static regime, for a cylindrical tube or a single-mode resonator. Implicitly the bifurcation has been assumed to be direct, while this is wrong in many cases, such as that of conical tubes. Consequently our study has drastic limitations. In addition the reduction of the reed vibration to a single mode is a supplementary limitation at higher frequencies, especially for brass instruments. No results have been obtained concerning the spectrum: the reader can refer to [110] or [54] (for results of the harmonic balance). Indeed the theoretical approach becomes much more difficult at higher frequencies, because the tube resonances become weaker and many other

[50] This does not demonstrate that considering an infinity of modes for the resonator this result would remain valid, but it is a reasonable hypothesis. Moreover we do not forget that the bifurcation can become inverse when a second mode is added to the resonator model, as it was seen for conical reed instruments, and maybe also if a second mode is added to the reed model (a reed with two modes seems to be necessary to model some behaviors of the excitor of brass instruments, see Fig. 9.3).

phenomena intervene: for instance the higher modes of the reed or the vocal tract can become important, and the radiation becomes more complicated, as it will be seen in the fourth part. However, thanks to this complexity, the playing of the higher notes is more flexible for the instrumentalist.

In the present section the addition of the two parameters of the reed dynamics implies complicated consequences on the effect of the main parameters on the playing frequency, the sound level or the spectrum. One aspect is the effect of inharmonicity of the excitation pressure (see Sect. 9.4.5), but few theoretical results has been published (see also [75]). Recently some advanced experimental studies has been published for reed instruments [4, 14, 19, 61, 62] and for brass instruments [42, 51].

The previous study gives us some insight on the free reeds (either without resonator, such as that of the accordion and harmonica, or weakly coupled to a resonator, such as organ reeds [48, 49, 84, 95, 108]). For these instruments, the playing frequencies are expected to be linked mainly to the reed resonance, and indeed the organ makers tune the reed tubes by moving the tuning spring (who plays the role of the lower lip of the clarinettists). Nevertheless they can choose a resonator with a resonance close to that of the reed. For a free reed, the damping is weak, and it can be accepted that the radiation impedance plays the role of a very short tube, and we expect that the thresholds correspond to very small values of $k_r\ell$ (see Fig. 9.23). Obviously this view is schematic, and this subject deserves longer developments.

Concerning brass instruments, it has been seen in Chap. 7 that the absence of toneholes implies the existence of a great number of significant modes for the resonator. The study of the regimes is a complex task, especially if two modes of the reed are taken into account. However, general ideas were already given by Benade [10]. The harmonicity of the impedance peaks 2, 3, 4, etc. allows playing notes without change in pitch related to the excitation level. The frequency of these notes corresponds to an impedance peak, and the harmonics to other peaks (for instance, consider peak 2, and peaks 4, 6, 8, etc. which are almost harmonically related). Moreover it is possible to play "pedal" sounds, whose harmonics correspond to a peak, except the fundamental. The theoretical study of the existence and stability of these regimes requires long computation, which is tedious but possible today.

Finally a general conclusion can be drawn concerning the influence of losses of every kind on the playing frequencies. Ignoring the losses leads to a first assessment of the frequencies, and with this approximation, the nonlinear excitation has no effect on the playing frequencies. This justifies the basic, fruitful approach (since Bernoulli): the playing frequencies were assumed to be the natural frequencies of the linear resonator. However, we have seen that for the examination of the transition between the "resonator regime" and the "reed regime," the reed damping needs to be considered and the parameters of the linearized excitation play a role [see Eq. (9.131)].

References

1. Adachi, S., Sato, M.: Trumpet sound simulation using a two-dimensional lip vibration model. J. Acoust. Soc. Am. **99**(2), 1200–1209 (1996)
2. Allwright, D.: Harmonic balance and Hopf bifurcation. Math. Proc. Camb. Philos. Soc. **82**, 453–467 (1977)
3. Almeida, A., Vergez, C., Caussé, R.: Quasistatic nonlinear characteristics of double-reed instruments. J. Acoust. Soc. Am. **121**(1), 536–546 (2007)
4. Almeida, A., George, D., Smith, J., Wolfe, J.: The clarinet: how blowing pressure, lip force, lip position and reed "hardness" affect pitch, sound level, and spectrum. J. Acoust. Soc. Am. **134**, 2247–2255 (2014)
5. Avanzini, F., Walstijn, M.V.: Modelling the mechanical response of the reed-mouthpiece-lip system of a clarinet. part i. a one-dimensional distributed model. Acta Acust. United Acust. **90**, 537–547 (2004)
   Acta Acustica united with Acustica
6. Backus, J.: Vibrations of the reed and the air column in the clarinet. J. Acoust. Soc. Am. **6**, 806–809 (1961)
7. Backus, J.: Small-vibration theory of the clarinet. J. Acoust. Soc. Am. **35**(3), 305–313 (1963)
8. Barjau, A., Agulló, J.: Calculation of the starting transients of a double-reed conical woodwind. Acustica **69**, 204–210 (1989)
9. Barjau, A., Gibiat, V.: Study of woodwind-like systems through nonlinear differential equations. Part II. Real geometry. J. Acoust. Soc. Am. **102**, 3032–3037 (1997)
10. Benade, A.H.: Fundamentals of Musical Acoustics. Oxford University Press, London (1976)
11. Benade, A.H., Gans, D.J.: Sound production in wind instruments. Ann. N. Y. Acad. Sci. **155**, 247–263 (1968)
12. Benade, A.H., Kouzoupis, S.N.: The clarinet spectrum: theory and experiment. J. Acoust. Soc. Am. **83**(1), 292–304 (1988)
13. Benade, A.H., Lutgen, S.J.: The saxophone spectrum. J. Acoust. Soc. Am. **83**(5), 1900–1907 (1988)
14. Bergeot, B., Almeida, A., Gazengel, B., Vergez, C., Ferrand, D.: Response of an artificially blown clarinet to different blowing pressure profiles. J. Acoust. Soc. Am. **135**, 479–490 (2014)
15. Bernoulli, D.: Physical, mechanical and analytical researches on sound and on the tones of differently constructed organ pipes (in French). Mem. Acad. R. Sci. **1764**, 431–485 (1762)
16. Bilbao, S., Torin, A., Chatziioannou, V.: Numerical modeling of collisions in musical instruments. Acta Acust. United Acust. **101**, 155–173 (2015)
17. Bouasse, H.: Wind instruments. In: Metallic and Membranous Reeds, Reed and Flue Pipes, Organ, Instruments with Horn Mouthpiece (in French), vol. 1, 2nd edn. Librairie Scientifique et Technique, Paris (1986)
18. Boutillon, X.: Analytical investigation of the flattening effect - the reactive power balance rule. J. Acoust. Soc. Am. **90**(2), 754–63 (1991)
19. Boutin, H., Fletcher, N., Smith, J., Wolfe, J.: Relationships between pressure, flow, lip motion, and upstream and downstream impedances for the trombone. J. Acoust. Soc. Am. **137**, 1195–1209 (2015)
20. Brod, K.: The clarinet as a bifurcation system: an application to the iterated map method(in German). Acustica **72**, 72–78 (1990)
21. Bromage, S., Campbell, D.M., Gilbert, J., Stevenson, S.: Experimental investigation of the open area of the brass player's vibrating lips. In: Forum Acusticum Budapest 2005, Budapest, Hungary, pp. 729–734 (2005)
22. Bromage, S., Campbell, D.M., Chick, J., Gilbert, J., Stevenson, S.: Motion of the brass player's lips during extreme loud playing. In: 8ème Congrès Français d'Acoustique, Tours, France, pp. 721–724 (2006)

23. Bromage, S., Campbell, D., Gilbert, J.: Open areas of vibrating lips in trombone playing. Acta Acust. United Acust. **96**, 603–613 (2010)
24. Campbell, M.: Brass instruments as we know them today. Acta Acust. United Acust. **90**, 600–610 (2004)
25. Castellengo, M.: Multiple sounds in wind instruments (in French). Report, IRCAM (1983)
26. Chen, J., Smith, J., Wolfe, J.: Pitch bending and glissandi on the clarinet: roles of the vocal tract and partial tone hole closure. J. Acoust. Soc. Am. **126**(3), 1511–1520 (2009)
27. Clinch, P.G., Troup, G.J., Harris, L.: The importance of vocal tract resonance in clarinet and saxophone performance, a preliminary account. Acustica **50**, 280–284 (1982)
28. Cremer, L.: The Physics of the Violin (Orig. "Physik der Geige"). MIT (orig.: Hirzel, 1981), Cambridge, MA (1984)
29. Cullen, J.S., Gilbert, J., Campbell, M.: Brass instruments: linear stability analysis and experiments with an artificial mouth. Acustica Acta Acustica **86**(4), 704–724 (2000)
30. Dalmont, J.P., Frappé, C.: Oscillation and extinction thresholds of the clarinet: comparison of analytical results and experiments. J. Acoust. Soc. Am. **122**(2), 1173–1179 (2007)
31. Dalmont, J.P., Kergomard, J.: Lattices of sound tubes with harmonically related eigenfrequencies. Acta Acustica **2**, 421–430 (1994)
32. Dalmont, J.P., Gazengel, B., Gilbert, J., Kergomard, J.: Some aspects of tuning and clean intonation in reed instruments. Appl. Acoust. **46**, 19–60 (1995)
33. Dalmont, J.P., Gilbert, J., Kergomard, J.: Reed instruments, from small to large amplitude periodic oscillations and the Helmholtz motion analogy. Acustica **86**, 671–684 (2000)
34. Dalmont, J.P., Gilbert, J., Ollivier, S.: Nonlinear characteristics of single-reed instruments: quasistatic volume flow and reed opening measurements. J. Acoust. Soc. Am. **114**(4), 2253–2262 (2003)
35. Dalmont, J.P., Gilbert, J., Kergomard, J., Ollivier, S.: An analytical prediction of the oscillation and extinction thresholds of a clarinet. J. Acoust. Soc. Am. **118**(5), 3294–3305 (2005)
36. Debut, V.: Two studies of a clarinet-like instrument: analysis of natural frequencies of the resonator and calculation of self-sustained oscillations by modal expansion (in French). Ph.D. thesis, Université Aix-Marseille II (2004)
37. Debut, V., Kergomard, J., Laloë, F.: Analysis and optimisation of the tuning of the twelfths for a clarinet resonator. Appl. Acoust. **66**, 365–409 (2005)
38. Doc, J., Vergez, C.: Oscillation regimes produced by an alto saxophone: influence of the control parameters and the bore inharmonicity. J. Acoust. Soc. Am. **137**, 1756–1765 (2015)
39. Doc, J., Vergez, C., Missoum, S.: A minimal model of a single-reed instrument producing quasi-periodic sounds. Acta Acust. United Acust. **100**, 543–554 (2014)
40. Ducasse, E.: Modeling and time domain simulation of wind instruments with single reed in playing situation (in French). Ph.D. thesis, Université du Maine, Le Mans (2001)
41. Elliott, S.J., Bowsher, J.M.: Regeneration in brass wind instruments. J. Sound Vib. **83**(2), 181–217 (1982)
42. Eveno, P., Petiot, J., Gilbert, J., Kieffer, B., Caussé, R.: The relationship between bore resonance frequencies and playing frequencies in trumpets. Acta Acust. United Acust. **100**, 362–374 (2014)
43. Fabre, B., Gilbert, J., Hirschberg, A., Pelorson, V.: Aeroacoustics of musical instruments. Annu. Rev. Fluid Mech. **44**, 1–25 (2012)
44. Facchinetti, M.L., Boutillon, X., Constantinescu, A.: Numerical and experimental modal analysis of the reed and the pipe of a clarinet. J. Acoust. Soc. Am. **113**(5), 2874–2883 (2003)
45. Farner, S.: Harmbal. Computer program in c (2005). Available at http://www.lma.cnrs-mrs.fr/logiciels/harmbal/
46. Farner, S., Vergez, C., Kergomard, J., Lizee, A.: Contribution to harmonic balance calculations of self-sustained periodic oscillations with focus on single-reed instruments. J. Acoust. Soc. Am. **119**(3), 1794–1804 (2006)

47. Ferrand, D., Vergez, C.: Blowing machine for wind musical instrument: toward a real-time control of the blowing pressure. In: IEEE 2008 Mediterranean Conference on Control Automation, vols. 1–4, pp. 556–561 (2008)
48. Fletcher, N.H.: Excitation mechanisms in woodwind and brass instruments. Acustica **43**, 63–72 (1979). Erratum: **50**, 155–159 (1982)
49. Fletcher, N.H.: Autonomous vibration of simple pressure-controlled valves in gas flow. J. Acoust. Soc. Am. **93**(4), 2172–2180 (1993)
50. Fletcher, N.H., Rossing, T.D.: The Physics of Musical Instruments. Springer, New-York (1991)
51. Freour, V., Lopes, N., Hélie, T., Caussé, R., Scavone, G.: In-vitro and numerical investigations of the influence of a vocal-tract resonance on lip auto-oscillations in trombone performance. Acta Acust. United Acust. **101**, 256–269 (2015)
52. Fritz, C.: Influence of musician's vocal tract on clarinet playing (in French). Ph.D. thesis, Université de Paris 6 (2004)
53. Fritz, C., Wolfe, J.: How do clarinet players adjust the resonances of their vocal tracts for different playing effects? J. Acoust. Soc. Am. **118**(5), 3306–3315 (2005)
54. Fritz, C., Farner, S., Kergomard, J.: Some aspects of the harmonic balance method applied to the clarinet. Appl. Acoust. **65**, 1155–1180 (2004)
55. Gibiat, V., Castellengo, M.: Period doubling occurrences in wind instrument musical performances. Acustica **86**, 746–754 (2000)
56. Gilbert, J.: Instruments with single reed: extension of the harmonic balance method, role of the resonance inharmonicity, measurement of the input quantities (in French). Ph.D. thesis, Université du Maine (1991)
57. Gilbert, J., Kergomard, J., Ngoya, E.: Calculation of the steady-state oscillation of a clarinet using the harmonic balance method. J. Acoust. Soc. Am. **86**, 35–41 (1989)
58. Gilbert, J., Ponthus, S., Petiot, J.F.: Artificial buzzing lips and brass instruments: experimental results. J. Acoust. Soc. Am. **104**, 1627–1632 (1998)
59. Gokhshtein, A.: Self-vibration of finite amplitude in a tube with a reed. Sov. Phys. Dokl. **24**, 739–741 (1979)
60. Grand, N., Gilbert, J., Laloë, F.: Oscillation threshold of woodwind instruments. Acustica **83**, 137–151 (1997)
61. Grothe, T.: Experimental investigation of bassoon acoustics. Ph.D. thesis, Technische Universität Dresden (2013)
62. Grothe, T., Baumgart, J.: Assessment of bassoon tuning quality from measurements under playing conditions. Acta Acust. United Acust. **101**, 238–246 (2015)
63. Guillemain, P.: Some roles of the vocal tract in clarinet breath attacks: natural sounds analysis and model-based synthesis. J. Acoust. Soc. Am. **121**(4), 2396–2406 (2007)
64. Guillemain, P., Kergomard, J., Voinier, T.: Real-time synthesis of wind instruments using nonlinear physical models. J. Acoust. Soc. Am. **105**(1), 444–455 (2005)
65. Guillemain, P., Vergez, C., Farcy, A.: An instrumented saxophone mouthpiece and its use to understand how an experienced musician plays. Acta Acust. United Acust. **96**, 622–634 (2012)
66. Guimezanes, T.: Experimental and numerical study of the clarinet reed (in French). Ph.D. thesis, Université du Maine, Le Mans (2008)
67. Heinrich, J.M., Kergomard, J.: The bassoon, history, acoustics, reed (in French). Report, Bulletin du Groupe d'Acoustique Musicale né 82–83 (1976)
68. Helmholtz, H.V.: App. VII, In the theory of pipes. In: On The Sensations Of Tone, 2nd english edn., p. 576. Dover, New York (1954)
69. Hirschberg, A.: Aero-acoustics of wind instruments. In: Mechanics of Musical Instruments. CISM Courses and Lectures, vol. 355, pp. 291–369. Springer, Wien, New York (1995)
70. Idogawa, T., Kobata, T., Komuro, K., Masakazu, I.: Nonlinear vibrations in the air column of a clarinet artificially blown. J. Acoust. Soc. Am. **93**(1), 540–551 (1993)
71. Iooss, G., Joseph, D.: Elementary Stability and Bifurcation Theory. Undergraduate Texts in Mathematics. Springer, Berlin (1980)

72. Karkar, S., Cochelin, B., Vergez, C.: A high-order, purely frequency based harmonic balance formulation for continuation of periodic solutions: the case of non-polynomial nonlinearities. J. Sound Vib. **332**, 968–977 (2013)
73. Kergomard, J.: Elementary considerations on reed-instrument oscillations. In: Weinreich, A.H.J.K.G. (ed.) Mechanics of Musical Instruments, CISM Courses and Lectures, vol. 335, pp. 229–290. Springer, Wien (1995)
74. Kergomard, J.: An acoustic revolution: the saxophone (in French). In: Colloque Acoustique et instruments anciens, Cité de la musique, Paris, pp. 237–254 (1998)
75. Kergomard J., Gilbert, J.: Analysis of some aspects of the role of the reed of a cylindrical wind instrument (in French). In: Actes du 5ème congrès Français d'acoustique, pp. 294–297 (2000)
76. Kergomard, J., Ollivier, S., Gilbert, J.: Calculation of the spectrum of the self-sustained oscillators using a variable truncation method: application to cylindrical reed instruments. Acustica **86**, 685–703 (2000)
77. Kergomard, J., Dalmont, J., Gilbert, J., Guillemain, P.: Period doubling on cylindrical reed instruments. In: 7th CFA-30th DAGA, pp. 113–114 (2004)
78. Maganza, C., Caussé, R., Laloë, F.: Bifurcations, period doubling and chaos in clarinetlike systems. Europhys. Lett. **1**, 295–302 (1986)
79. McIntyre, M.E., Schumacher, R.T., Woodhouse, J.: On the oscillations of musical instruments. J. Acoust. Soc. Am. **74**(5), 1325–1345 (1983)
80. Mersenne, M.: Harmonie Universelle, vol. 1636, Edition facsimilé. CNRS (1963)
81. Meynial, X.: Micro-interval systems for wind instruments with toneholes - oscillation of a single reed coupled with a resonator of simple shape (in French). Ph.D. thesis, Université du Maine (1987)
82. Meynial, X., Kergomard, J.: Micro-interval systems for wind instruments with toneholes (in French). J. Acoustique **1**, 255–270 (1988)
83. Miklos, A., Angster, J., Pitsch, S., Rossing, T.: Interaction of reed and resonator by sound generation in a reed organ pipe. J. Acoust. Soc. Am. **119**(5), 3121–3129 (2006)
84. Millot, L., Baumann, C.: A proposal for a minimal model of free reeds. Acta Acust. United Acust. **93**, 122–144 (2007)
85. Mira, C.: Nonlinear Controlled Systems (in French). Hermès, Paris (1990)
86. Nederveen, C.J.: Acoustical Aspects of Woodwind Instruments. Northern Illinois University Press, IL. New edition, 1998 (1969)
87. Nederveen, C., Dalmont, J.: Mode locking effects on the playing frequency for fork fingerings on the clarinet. J. Acoust. Soc. Am. **131**, 689–697 (2012)
88. Newton, M., Campbell, M., Gilbert, J.: Mechanical response measurements of real and artificial brass players lips. J. Acoust. Soc. Am. **123**, EL14–EL20 (2007)
89. Ollivier, S.: Study of wind instruments with single reed (in French). Ph.D. thesis, Université du Maine (2002)
90. Ollivier, S., Dalmont, J.P., Kergomard, J.: Idealized models of reed woodwinds. Part I: analogy with the bowed string. Acta Acust. United Acust. **90**(6), 1192–1203 (2004)
91. Ollivier, S., Kergomard, J., Dalmont, J.P.: Idealized models of reed woodwinds. Part II: on the stability of "two-step" oscillations. Acta Acust. United Acust. **91**(1), 166–179 (2005)
92. Picart, P., Leval, J., Piquet, F., Boileau, J., Guimezanes, T., Dalmont, J.: Study of the mechanical behaviour of a clarinet reed under forced and auto-oscillations with digital Fresnel holography. Strain **46**, 89–100 (2010)
93. Rayleigh, L.: The Theory of Sound, vol. 2. Dover, New York (1877). Second edition, 1945 Re-issue
94. Ricaud, B., Guillemain, P., Kergomard, J., Silva, F., Vergez, C.: Behavior of reed woodwind instruments around the oscillation threshold. Acta Acust. United Acust. **95**, 733–743 (2009)
95. Ricot, D., Caussé, R., Misdariis, N.: Aerodynamic excitation and sound production of blown-closed free reeds without acoustic coupling: the example of the accordion reed. J. Acoust. Soc. Am. **117**(4), 2279–2290 (2005)

96. Sattinger, D.: Topics in Stability and Bifurcation Theory. Lecture Notes in Mathematics. Springer, Berlin (1973)
97. Scavone, G.P., Lefebvre, A., da Silva, A.R.: Measurement of vocal-tract influence during saxophone performance. J. Acoust. Soc. Am. **123**(4), 2391–2400 (2008)
98. Schumacher, R.T.: Self-sustained oscillations of the clarinet: an integral approach. Acustica **40**, 298–309 (1978)
99. Schumacher, R.T.: Ab initio calculations of the oscillations of a clarinet. Acustica **48**(2), 71–85 (1981)
100. Silva, A.D., Scavone, G., van Walstijn, M.: Numerical simulations of fluid-structure interactions in single-reed mouthpieces. J. Acoust. Soc. Am. **122**, 1798–1809 (2007)
101. Silva, F., Kergomard, J., Vergez, C., Gilbert, J.: Interaction of reed and acoustic resonator in clarinetlike systems. J. Acoust. Soc. Am. **124**(5), 3284–3295 (2008)
102. Silva, F., Vergez, C., Guillemain, P., Kergomard, J., Debut, V.: Moreesc: a framework for the simulation and analysis of sound production in reed and brass instruments. Acta Acust. United Acust. **100**, 126–138 (2014)
103. Sommerfeldt, S.D., Strong, W.J.: Simulation of a player-clarinet system. J. Acoust. Soc. Am. **83**(5), 1908–1918 (1988)
104. Taillard, P., Kergomard, J.: An analytical prediction of the bifurcation scheme of a clarinet-like instrument: effects of resonator losses. Acta Acust. United Acust. **101**, 279–291 (2015)
105. Taillard, P., Kergomard, J., Laloë, F.: Iterated maps for clarinet-like systems. Nonlinear Dyn. **62**, 253–271 (2010)
106. Taillard, P., Laloë, F., Gross, M., Dalmont, J., Kergomard, J.: Statistical estimation of mechanical parameters of clarinet reeds using experimental and numerical approaches. Acta Acust. United Acust. **100**, 555–573 (2014)
107. Takahashi, K., Kodama, H., Nakajima, A., Tachibana, T.: Numerical study on multi-stable oscillations of woodwind single-reed instruments. Acta Acust. United Acust. **95**, 1123–1139 (2009)
108. Tarnopolsky, A.Z., Fletcher, N.H., Lai, J.C.S.: Oscillating reed valves—an experimental study. J. Acoust. Soc. Am. **108**(1), 400–406 (2000)
109. Team, N.U.: Music acoustics 'robot clarinet' (2008). http://www.phys.unsw.edu.au/jw/clarinetrobot.html
110. Thompson, S.C.: The effect of the reed resonance on woodwind tone production. J. Acoust. Soc. Am. **66**(5), 1299–1307 (1979)
111. Valette, C., Cuesta, C.: Mechanics of the Vibrating String (in French). Hermès, Paris (1993)
112. van Walstijn, M., Avanzini, F.: Modelling the mechanical response of the reed-mouthpiece-lip system of a clarinet. Part II: a lumped model approximation. Acta Acust. United Acust. **93**, 435–446 (2007)
113. Vergez, C., Lizée, A.: A frequency-domain approach of harmonic balance solutions stability. In: Forum Acusticum, Budapest, pp. 539–543 (2005)
114. Vergez, C., Rodet, X.: Experiments with an artificial mouth for trumpet. In: ISMA'98 Proceedings, pp. 153–158. Leavenworth, Washington (1998)
115. Vergez, C., Rodet, X.: Air flow related improvements for basic physical models of brass instruments. In: Proceedings of ICMC'2000, Berlin, pp. 62–65 (2000)
116. Vergez, C., Rodet, X.: Trumpet and trumpet player: physical modeling in a musical context. In: Proceedings of the International Congress of Acoustics (ICA), Rome, p. CDROM IV (2001)
117. Vergez, C., Almeida, A., Caussé, R., Rodet, X.: Toward a simple physical model of double-reed musical instruments: influence of aero-dynamical losses in the embouchure on the coupling between the reed and the bore of the resonator. Acta Acust. United Acust. **89**(6), 964–973 (2003)
118. Weber, W.: Theorie der Zungenpfeifen. Annalen der Physik und Chemie, hrsg. von J.C. Poggendorf **93**, 193–246 (1829)
119. Weinreich, G., Caussé, R.: Elementary stability considerations for bowed-string motion. J. Acoust. Soc. Am. **89**(2), 887–895 (1991)

120. Wilson, T.: The measured upstream impedance for clarinet performance and its role in sound production. Ph.D. thesis, University of Washington (1996)
121. Wilson, T.A., Beavers, G.S.: Operating modes of the clarinet. J. Acoust. Soc. Am. **56**(2), 653–658 (1974)
122. Woodhouse, J.: Idealised models of a bowed string. Acustica **79**, 233–250 (1993)
123. Woodhouse, J., Schumacher, R., Garoff, S.: Reconstruction of bowing point friction force in a bowed string. J. Acoust. Soc. Am. **108**(1), 357–68 (2000)
124. Worman, W.: Self-sustained nonlinear oscillations of medium amplitude in clarinet like-systems. Ph.D. thesis, Case Western Reserve University Cleveland (1971)